

DESIGN, QUANTIFICATION, AND
DEMONSTRATION OF LARGE SCALE PHOSPHORUS
REMOVAL STRUCTURES IN OKLAHOMA

By

JAMES MICHAEL BOWEN

Bachelor of Science in Environmental Science

Oklahoma State University

Stillwater, Oklahoma

2013

Submitted to the Faculty of the
Graduate College of the
Oklahoma State University
in partial fulfillment of
the requirements for
the Degree of
MASTER OF SCIENCE
July, 2015

DESIGN, QUANTIFICATION, AND
DEMONSTRATION OF LARGE SCALE PHOSPHORUS
REMOVAL STRUCTURES IN OKLAHOMA

Thesis Approved:

Dr. Chad Penn

Thesis Adviser

Dr. Glenn Brown

Dr. Garey Fox

Dr. Jason Warren

Name: JAMES MICHAEL BOWEN

Date of Degree: JULY, 2015

Title of Study: DESIGN, QUANTIFICATION, AND DEMONSTRATION OF LARGE SCALE PHOSPHORUS REMOVAL STRUCTURES IN OKLAHOMA

Major Field: PLANT AND SOIL SCIENCES

Abstract: Phosphorus (P) lost from agricultural and urban soils can enter waterways causing eutrophication resulting in reduced water quality. Conventional best management practices (BMPs) are effective at reducing particulate P loss, but do little to stop dissolved P which is 100% bioavailable. The use of landscape filters filled with materials that have a high affinity for P, i.e. P sorbing materials (PSMs), has been shown to reduce transport of dissolved P. These studies examined the process of using a previously developed model to design a P removal structure to meet removal goals. Specifically, we designed, constructed, and monitored a P removal structure on a poultry farm using the model, compared the model predictions for P removal to measured P removal, and also integrated the design process, including the model, into the Phosphorus Removal Online Guidance (PhROG) design software. The poultry farm structure has removed 57.5% of the P load during the first 21 months of operation which exceeds the goal of 45% cumulative removal for 1 y. The discrepancy in removal is due to an over estimation of the annual P load. The model predictions based on the current P loading are in agreement with the measured removal. The results from this structure were also used in validation of the model. The measured discrete P removal curve from a total of 14 sets of observations, including laboratory flow-through, a pilot-scale structure, and other field structure experiments, were found to be not significantly different from the model predictions. The validation of the model was critical since it is the foundation of the PhROG design software. In order to aid the user, a handbook that details the inputs required and how they affect structure design was created. This software is the culmination of years of research into the design and construction of these structures that aims to make the design process approachable and easy for the layperson. P removal structures are a viable BMP to reduce transport of dissolved P and can be designed to meet removal goals safely and effectively.

TABLE OF CONTENTS

| Chapter | Page |
|--|------|
| I. INTRODUCTION..... | 1 |
| Literature review..... | 3 |
| Eutrophication..... | 3 |
| Sources of P transported to surface waters..... | 3 |
| Forms of P transported in runoff..... | 5 |
| Methods for reducing non-point P transport (Containment)..... | 5 |
| Conservation tillage..... | 5 |
| Buffer zones..... | 6 |
| Removing P from the site (Remediation)..... | 7 |
| Phytoremediation..... | 7 |
| P sorbing materials..... | 8 |
| Amendments to manure..... | 9 |
| Amendments to soil..... | 10 |
| P removal structure..... | 11 |
| Site requirements and basic components of a P removal structure..... | 11 |
| Examples of P removal structures..... | 13 |
| Need for methods to design P removal structures..... | 18 |
| Individual flow-through model..... | 19 |
| Universal flow-through model..... | 22 |
| Design software..... | 23 |
| Objectives..... | 24 |
| References..... | 25 |
| II. PHOSPHORUS REMOVAL STRUCTURES: A MANAGEMENT OPTION FOR LEGACY PHOSPHORUS..... | 34 |
| Abstract..... | 34 |
| Introduction..... | 35 |
| Assessment of site location..... | 38 |
| Site data collection required for structure design..... | 40 |
| Sizing the P removal structure..... | 41 |
| Required mass of PSM..... | 41 |
| Orientation of the PSMs..... | 45 |
| Site preparation for construction of the structure..... | 48 |

| | |
|--|-----|
| Construction and installation of the structure | 48 |
| Structure monitoring and data analysis | 50 |
| Performance of the P removal structure..... | 51 |
| Effluent safety..... | 56 |
| Summary..... | 57 |
| Widespread implementation and future research..... | 57 |
| References..... | 60 |
| | |
| III. VALIDATION OF THE UNIVERSAL FLOW-THROUGH PHOSPHORUS SORPTION MODEL..... | 63 |
| | |
| Abstract..... | 63 |
| Introduction..... | 65 |
| Materials and methods | 68 |
| Chemical characterization of PSMs..... | 68 |
| Physical Characterization of PSMs..... | 69 |
| Solution analysis of effluent | 69 |
| Validation scenarios..... | 70 |
| Controlled setting..... | 70 |
| Laboratory flow-through testing of PSMs | 70 |
| Pond filter structure..... | 71 |
| Field structures..... | 71 |
| Golf course structure..... | 71 |
| Poultry farm structure | 72 |
| Data analysis and modelling..... | 73 |
| Statistical analysis..... | 77 |
| Results and discussion | 77 |
| Overall design curve estimation..... | 77 |
| Example validation scenarios | 81 |
| Laboratory flow-through..... | 81 |
| Pond filter structure..... | 84 |
| Golf course structure..... | 86 |
| Effluent safety..... | 88 |
| Conclusion | 91 |
| References..... | 93 |
| | |
| IV. HANDBOOK FOR THE PHOSPHORUS REMOVAL ONLINE GUIDANCE (PHROG) DESIGN SOFTWARE | 97 |
| | |
| Abstract..... | 97 |
| Introduction..... | 99 |
| Design Curve | 101 |
| Sizing a filter using the design curve..... | 102 |
| Estimating the equation for a design curve..... | 104 |

| | |
|---|-----|
| Impact of material physical characteristics on P removal structure design and performance | 106 |
| Characterization of PSMs | 108 |
| Methods of physical characterization | 108 |
| Methods of chemical characterization | 111 |
| Ca materials | 112 |
| Fe and Al materials | 113 |
| Site requirements for a phosphorus removal structure | 114 |
| Site characterization..... | 115 |
| Peak flow rate and annual flow volume..... | 115 |
| Estimation of dissolved P concentrations | 117 |
| Hydraulic head and area for structure..... | 118 |
| Proper drainage of P removal structures..... | 120 |
| Required site inputs and specifications into the software..... | 122 |
| Design structure vs. predicting performance of an existing structure | 122 |
| Two broad styles for P removal structures: bed vs. ditch structure..... | 122 |
| Specific inputs for structure design..... | 123 |
| Chemical and physical characteristics of PSM to be used..... | 123 |
| Site characteristics and constraints | 125 |
| Additional factors for predicting existing structures | 129 |
| Optional inputs: total and particulate P removal..... | 130 |
| General output from software | 131 |
| Case studies..... | 133 |
| Maryland ditch design..... | 133 |
| Existing Maryland ditch..... | 146 |
| Vermont tile drainage | 148 |
| Surface and blind inlets..... | 155 |
| Existing blind inlet..... | 156 |
| Bioretention cell..... | 160 |
| Existing bioretention cell | 165 |
| Conclusion | 167 |
| References..... | 169 |

LIST OF TABLES

| Table | Page |
|--|------|
| <p>2.1: Required mass, area, and depth of several phosphorus sorbing materials (PSMs) for removing the indicated percent of the year 1 P load (22 kg) and treat the peak flow rate of 2.8 m³ min⁻¹ (1.6 ft³ s⁻¹) on a poultry farm located in Eastern Oklahoma. Calculations made based on respective design curves (figure 2.3) and material and site characteristics. Lifetime indicates the number of years in which the theoretical structure would be able to remove P at this site under current conditions.</p> | 47 |
| <p>2.2: Summary of the conditions and performance of the poultry farm phosphorus (P) removal structure during the first 21 mo of monitoring.</p> | 51 |
| <p>3.1: Results from paired t-tests used to compare the predicted and measured values for the y-intercept and slope of the discrete P removal curves, the maximum phosphorus (P) loading when the material is spent, and the maximum cumulative P removal (mg kg⁻¹ and %). The actual data was collected from laboratory flow-through experiments, a pilot-scale filter, and two field structures that were not used in creation of the model. n=14, α=0.05.</p> | 77 |
| <p>3.2: Model-predicted and measured slope and intercept of the exponential phosphorus (P) removal curve (equation 3.1) for each validation scenario, along with the resulting maximum P loading (mg P kg⁻¹; equation 3.5) at which the material will no longer sorb P. The maximum cumulative P removal is shown as both mg P kg⁻¹ of material and a percentage (equations 3.3 and 3.4).</p> | 79 |
| <p>3.3: Influent and effluent water analysis from a subset of 18 random outflow and inflow sample pairs from the poultry farm P removal structure, conducted for safety assessment. All the samples were tested for Na, Ca, Mg, K, S, P, Fe, Zn, Cu, Mn, Al, Ni, B, As, Cd, Cr, Ba, Pb, and Co using inductively coupled plasma atomic emission spectroscopy (ICP-AES). Each pair was compared with the difference between the effluent concentration and influent concentration being reported below as release with the minimum and maximum release shown. Negative values for release indicate a reduction in concentration and are listed as sorption events. Positive values indicate an increase in concentration after passing through the filter and are listed as release events. EPA drinking water standards, both primary and secondary, is shown for comparison.</p> | 89 |

| Table | Page |
|--|------|
| 4.1: The Runoff Coefficient for a variety of soil types, vegetation, and topographies are shown (Jarrett, 1997). | 117 |
| 4.2: Selected channel types are shown with their Manning's roughness coefficient (Jarrett, 1997)..... | 129 |

LIST OF FIGURES

| Figure | Page |
|--|------|
| 1.1: Data from a flow-through experiment of an acid mine drainage residual (AMDR) at a retention time of 0.28 min and a phosphorus (P) concentration of 1 mg L ⁻¹ are shown with the discrete P removal plotted versus the cumulative P added. The exponential regression equation and r-squared are shown. | 19 |
| 2.1: Justification for the cost and construction of a phosphorus (P) removal structure (left), and example of a P removal structure in Maryland designed to treat runoff water from a poultry farm as the water drains from a retention pond into a ditch through the filtration material (steel slag; right). | 37 |
| 2.2: Aerial view of the site described in this paper in which the phosphorus (P) removal structure was constructed (left), and contour map showing (in red) the structure location and berms used to converge water into the structure (right)..... | 39 |
| 2.3: Example (upper) of a phosphorus (P) removal curve as determined by a flow-through P sorption experiment conducted on a P sorbing material, and (lower) side cutaway diagram of the P removal structure constructed on a poultry farm..... | 42 |
| 2.4: The frame of the phosphorus (P) removal structure from the perspective of looking from the downhill (drainage) side toward the uphill (inflow) side (top left), side view (top right), structure partly filled with slag showing the attached inflow perforated pipes (bottom left), and the complete structure from the perspective of looking from the inflow toward the drainage side (bottom right). Note the H flume for monitoring flow rates. | 49 |
| 2.5: Predicted vs measured discrete dissolved phosphorus (P) removal for the poultry farm P removal structure described in this case study. Individual points are the measured discrete P removal from 36 runoff events. The equation and R ² are shown for the exponential regression of the measured data points depicted as a dashed line. The solid line is the model predicted design curve shown with its equation (full curve shown in inset). *Significant at the 0.05 level..... | 52 |

| | |
|--|-----|
| 2.6: Predicted vs measured cumulative dissolved phosphorus (P) removal for the poultry farm P removal structure described in this case study. Individual points are the measured cumulative P removal plotted as mg P removed kg ⁻¹ PSM (upper) and as a percentage (lower). The equation and R ² are shown for the exponential regression of the measured data points depicted as a dashed line (lower). The solid line is the cumulative removal predicted using the universal flow-through model (upper and lower). *Significant at the 0.05 level..... | 53 |
| 3.1: Predicted and measured values for phosphorus (P) removal by an acid mine drainage residual (AMDR), as a function of P loading, under laboratory flow-through conditions using a P concentration of 1 mg L ⁻¹ and a retention time (RT) of 0.71 min. (a) discrete P removal, (b) cumulative P removal expressed as a %, and (c) cumulative P removal expressed as mg kg ⁻¹ PSM. †Significant at the 0.1 level. | 82 |
| 3.2: Predicted and measured values for phosphorus (P) removal by treated steel slag, as a function of P loading, in a pilot scale flow-through pond filter with a P concentration of 0.5 mg L ⁻¹ and a retention time (RT) of 10 min. (a) discrete P removal, (b) cumulative P removal expressed as a %, and (c) cumulative P removal expressed as mg kg ⁻¹ PSM..... | 85 |
| 3.3: Predicted and measured values for phosphorus (P) removal by steel slag (>6.35 mm), as a function of P loading, for a field scale P removal structure located on a golf course. Flow-weighted inflow dissolved P concentration was 0.69 mg L ⁻¹ and a weighted retention time (RT) of 10 min. (a) discrete P removal, (b) cumulative P removal expressed as a %, and (c) cumulative P removal expressed as mg kg ⁻¹ PSM..... | 87 |
| 4.1: Data from a flow through of a treated EAF steel slag at a retention time of 0.71 min and a P concentration of 1 mg L ⁻¹ are shown with the discrete P removal percentage plotted versus the mg of cumulative P added per kg of material. The equation and r-squared are shown for an exponential regression. | 101 |
| 4.2: The discrete P removal curve of a treated EAF steel slag at a retention time of 0.71 min and a P concentration of 1 mg L ⁻¹ was integrated resulting in the cumulative P removal curve shown here. The cumulative P removal as a percentage is plotted versus the cumulative P additions in mg kg ⁻¹ of slag. The equation and r-squared are shown for an exponential regression..... | 102 |
| 4.3: The flow-through set up is shown with the Mariotte bottle holding the P solution which supplies the cell containing the P sorbing material of known mass. The flow rate is maintained by a peristaltic pump which draws the solution through the cell. Diagram source: DeSutter et al. 2006..... | 105 |
| 4.4: A cutaway side view of a P removal structure that shows the water flow through the P sorbing material (PSM) layer (a), downward into the subsurface drainage layer (b). | 107 |
| 4.5: A sample particle size distribution curve for a material is shown with the particle size in mm shown versus the percent of particles finer than that diameter. | 110 |

| Figure | Page |
|--|------|
| 4.6: A proposed site for P removal structure is shown (upper) with the maximum allowable area for the structure enclosed by a dashed line. The hydraulic head, the elevation difference from inlet to outlet, is shown at the site (upper) and in a cutaway diagram (lower)..... | 119 |
| 4.7: A drainage ditch fed by a tile drained agricultural field in Ohio is shown with top width, bottom width, and depth marked. | 120 |
| 4.8: The subsurface drainage layer of a P removal structure was exposed prior to the addition of steel slag. The drainage layer used 10 cm diameter perforated PVC pipes. | 121 |
| 4.9: The “Design Structure” tab and “Existing Structure” tab from the PhROG software are shown. Only one of these two will be visible at a time, but both are shown to highlight the different inputs..... | 122 |
| 4.10: A screenshot of the PhROG software is shown with the corresponding tabs for designing or quantifying a bed or ditch structure. | 123 |
| 4.11: The “Estimate Design Curve” and “Material Physical Characteristics” tabs of the PhROG software are shown highlighted. These tabs are used to input the chemical and physical characteristics of the PSM. | 124 |
| 4.12: A diagram of a P removal structure is shown located in a ditch that drains agricultural fields. The ditch dimensions, top width, bottom, width, and depth, are marked with arrows..... | 134 |
| 4.13: Two of the input tabs of the PhROG software are shown with values that correspond to the Maryland Swift ditch example. The site and ditch characteristics, namely loading and dimensions, are highlighted in red. | 135 |
| 4.14: Two of the input tabs of the PhROG software are shown with values that correspond to the Maryland Swift ditch example. The removal goals and flow constraints are highlighted in red. | 136 |
| 4.15: Two of the input tabs of the PhROG software are shown with values that correspond to the Maryland Swift ditch example. The section with subsurface drainage inputs is highlighted in red..... | 136 |
| 4.16: A screenshot of the PhROG software is shown with the chemical characteristics inputs highlighted in red. | 137 |
| 4.17: A screenshot of the PhROG software showing the desired structure retention time highlighted in red. | 138 |

| Figure | Page |
|--|------|
| 4.18: A screenshot of the PhROG software showing the material physical characteristics highlighted in red. | 138 |
| 4.19: A screenshot of the interface of the PhROG software with the Go button highlighted in red. | 139 |
| 4.20: A screenshot of a ditch structure design output produced using the PhROG software. | 139 |
| 4.21: An example output from the PhROG software that highlights the goals and the estimated lifetime to meet minimum flow rate and retention time variable. | 140 |
| 4.22: An example output of the PhROG software that shows the removal performance of the ditch structure design highlighted in red. | 141 |
| 4.23: An example output for a ditch structure designed using PhROG software. | 142 |
| 4.24: An example output from PhROG software for a ditch structure that uses sieved steel slag as a PSM. | 143 |
| 4.25: An example output from the PhROG software for a ditch structure that uses steel slag as a PSM. | 144 |
| 4.26: An example output from the PhROG software for a ditch structure designed using treated steel slag. | 145 |
| 4.27: This screenshot of the PhROG software shows the input tabs for the characteristics of an existing ditch structure. | 146 |
| 4.28: The PhROG software output shown estimates the performance of an existing ditch structure. | 147 |
| 4.29: An example P removal structure design that uses a subsurface bed to treat a tile drain is shown. | 148 |
| 4.30: The site characteristics and bed design constraints are shown for an example structure in a tile drained field. | 149 |
| 4.31: An example design for a P removal structure that uses fine limestone to treat tile drain effluent. | 150 |
| 4.32: An example design for a P removal structure using a fine limestone material to remove 70% of the P load in tile drain effluent. | 151 |

| Figure | Page |
|--|------|
| 4.33: The PhROG design output for a subsurface bed structure using a fine limestone material is shown. This design will remove 70% of the cumulative dissolved P load for 5 y..... | 152 |
| 4.34: An example structure design that uses wollastonite to remove 35% of the annual load for 1 yr..... | 153 |
| 4.35: The example output from PhROG for a subsurface bed treating tile drainage using wollastonite material..... | 154 |
| 4.36: A blind inlet is pictured that is partially exposed to show the drainage layer and media..... | 155 |
| 4.37: A screenshot from the PhROG software showing inputs used to quantify an existing bed structure..... | 156 |
| 4.38: A screenshot of the PhROG software showing the chemical and physical characteristics of a sieved limestone being used in a blind inlet..... | 157 |
| 4.39: The PhROG output quantifying the performance of a blind inlet is shown. ... | 157 |
| 4.40: The chemical and physical characteristics are shown for a steel slag used in a blind inlet..... | 158 |
| 4.41: The PhROG output quantifying the P removal performance of a blind inlet is shown..... | 158 |
| 4.42: The PhROG input screen is shown with the characteristics of a limestone sand PSM..... | 159 |
| 4.43: The PhROG output for an existing blind inlet that utilizes a limestone sand is shown..... | 159 |
| 4.44: A cut away side view of a bioretention cell is shown with the inlet, outlet, and media layer labelled. The media layer is buried beneath a small layer of soil that is pictured as the thin brown layer..... | 160 |
| 4.45: A completed bioretention cell is pictured in the foreground with a surface layer of rock with several small bushes planted in it..... | 161 |
| 4.46: The PhROG input screen is shown with the various sections highlighted in red. This is an example design of a bioretention cell..... | 162 |

| Figure | Page |
|--|------|
| 4.47: The PhROG output screen is shown with the different sections highlighted in red. This design is for a bioretention cell that will remove 50% of the annual P load for 20 y and is drained by 2 in pipes..... | 163 |
| 4.48: The PhROG output screen is shown with the different sections highlighted in red. This design is for a bioretention cell that will remove 50% of the annual P load for 25 y and is drained by a 4 in pipe. | 164 |
| 4.49: The PhROG output screen is shown with the different sections highlighted in red. This design is for a bioretention cell that will remove 50% of the annual P load for 25 y and is drained by a 6 in pipe. | 165 |
| 4.50: The PhROG software input screen for an existing bioretention cell that utilized a 5% fly ash 95% sand mixture is shown with various tabs highlighted..... | 166 |
| 4.51: The output from PhROG from quantifying the performance of an existing bioretention cell is shown with the flow results and lifetime of the filter highlighted. | 167 |

CHAPTER I

INTRODUCTION

The United States Environmental Protection Agency's (USEPA) 303d impaired waterway list has nutrients listed as the cause of 7,755 impairments (USEPA, 2011). Excessive nutrients in waterways lead to algal blooms and subsequent reductions in dissolved oxygen during their degradation (Dodds, 2002). Due to atmospheric sources of nitrogen (N), phosphorus (P) is usually the most limiting nutrient in freshwater, so even small additions can lead to eutrophication (Schindler et al., 2008). While point sources of P, such as waste water treatment plants, are easy to identify and monitor, diffuse nonpoint sources, such as agricultural fields and urban runoff, are harder to identify and remediate (Carpenter et al., 1998). Sites that are built up with excessive P release small amounts of dissolved P over the course of years or decades until soil levels are reduced to a safe level, providing a "legacy" of P due to prior mismanagement (Sharpley et al., 2013). Nutrient management coupled with proper handling of manure disposal can help prevent buildup of P, but this will do nothing for sites that already have a legacy P problem. In order to deal with legacy P, over application of P must cease along with containment of the P. Eutrophication is only a threat if the P can be transported to a surface water body, thus reducing transport is critical on high P soils. Reduction of P transport begins with preventing soil detachment which can be achieved with any best management practice (BMP) that works to reduce erosion, such as conservation tillage. Next, transport must be reduced which can be accomplished in two ways; physical and chemical. Vegetative buffers and grass waterways help reduce sediment loss from a site by reducing water velocity thereby reducing the capacity of the

water to suspend soil particles. Chemical reduction of P can be achieved by adding amendments to soil and manure that have an affinity for P which prevents P from being in solution.

Unfortunately these options do nothing to fix the underlying problem. Remediation of the excessive P can be achieved by phytoremediation and P removal structures, which target P in different ways. Phytoremediation works by “mining” the soil with plants which are eventually removed along any P it contains, from the watershed. This is effective in truly remediating the problem at a site, but due to the large amount of P present and the limited ability of plants to uptake P, this process can take years or decades (Delorme et al., 2000; Kratochvil et al., 2006). While the plants are mining the soil there is a constant release of dissolved P from the site which is 100% bioavailable. Conventional BMPs for P loss focus on particulate P loss, so they are aimed at reducing erosion with little capacity to reduce dissolved P losses. A P removal structure has been shown to reduce dissolved P transport by using filter media with an affinity for P that can be removed when spent (Penn et al., 2007). These structures are able to immediately reduce the dissolved P loss from a site, but do not address the underlying problem of the P source; thus, P removal structure should be used in conjunction with phytoremediation and nutrient management.

P removal structures are the only BMP that can address dissolved P losses from a site, but they have not been adopted as a widespread practice. In order for P removal structures to be accepted as a BMP there is a need for a system and method to design them for each specific site and particular set of removal goals. The foundational work for such design was carried out in a variety of studies where pilot structures were constructed and sorption materials were evaluated resulting in a universal model that estimates the removal ability of a P sorption material (PSM) (Penn and Bryant, 2006; Penn et al., 2007; Stoner et al., 2012). This paper focuses on the need and development of software that utilizes the universal model to help users design a P removal structure or to quantify removal of an existing structure.

Literature Review

Eutrophication

Eutrophication results from excess nutrient additions, primarily N and P, that increase the growth of primary producers (Allaby, 2010; Smith, 1969). Primary producers interfere with drinking water treatment facilities, can release toxins, and exert an increased oxygen demand when they decompose decreasing dissolved oxygen which can lead to fish kills (Carpenter et al., 1998). Natural sources of N and P include dissolution from geologic formations, desorption from sediments, legume N fixation, mineralization of organic matter, and some atmospheric deposition. However, the amount of N deposition can be ten times the amount of P deposited (Jassby et al., 1994; Tisdale et al., 1993; Zhai et al., 2009). A 37 year study in Ontario, Canada assessed the impact of different ratios of N and P on eutrophication and changes in the composition of phytoplankton present (Schindler et al., 2008). P and N were added annually to the lake starting in 1969 with consistent P additions and the amount of N reducing each year until 1990 when no more N additions were made (Schindler et al., 2008). The eutrophic condition of the lake persisted after N applications ceased due in part to an increased presence of N fixing cyanobacteria who took advantage of the excess P (Schindler et al., 2008). Due to the atmospheric source of N, P will be more limiting than N in an aquatic environment and will drive eutrophication.

Sources of P transported surface waters

Nitrogen is found in the soil solution as nitrate (NO_3^-) or ammonium (NH_4^+), and are held in the soil using non-specific adsorption which is relatively weak and reversible (Bohn et al., 2001). Phosphorus present in the soil solution is phosphate in different stages of protonation (PO_4^{3-} , HPO_4^{2-} , or $H_2PO_4^-$) and is held via ligand exchange which is relatively strong and irreversible when compared with non-specific adsorption (Bohn et al., 2001). The greater

mobility of N in comparison to P reduces the lag time between management changes and a reduced output in runoff from a site unlike P which can continue to be a problem for many years after management changes are made (Meals et al., 2010; Sharpley et al., 2013).

P fertilizer recommendations in Oklahoma are based on a sufficiency recommendation that sets a soil test value as 100% sufficiency where no increase in yield is expected with additional P additions (Zhang and Raun, 2006). If P is applied in excess of this sufficiency, it starts to accumulate in the soil over time and will become a source of dissolved P. Routine soil testing and proper application methods and rates of fertilizer, including golf course, agricultural and urban areas, will help prevent a site from becoming built up with excess P (Withers et al., 2005).

Past mismanagement of P in agricultural or urban areas leads to P in excess of sufficiency levels which will slowly be lost from the site as dissolved P in runoff for years to come creating a “legacy” of P (Sharpley et al., 2013). The amount of dissolved P that is released has been correlated with the degree of P saturation in the soil, a measure that compares the amount of amorphous Fe and Al to P present in the soil (Gburek et al., 2005). The time required to reduce the soil test P to reasonable levels will vary with mineralogy of the site and cropping systems, but will take years or decades to reach acceptable levels (Kratovich et al., 2006; Penn et al., 2005; van der Salm et al., 2009). While studying P drawdown in North Carolina, soils were built up with annual P applications over the course of 8 years and then monitored for soil test P for the next 26 years with limited yield data of the corn and soybeans (McCollum, 1991). McCollum found a slow decline of P even with crop removal of P that took 14 to 16 years after final P application for a soil initially testing 100 g P m^{-3} to reach levels that would reduce yield (1991). A study in Maryland had similar results with none of their treatments reducing elevated P levels to the agronomic optimum and, given the trends, would not do so for several years or possibly decades (Kratovich et al., 2006).

Forms of P transported in runoff

P found in runoff can be defined operationally according to filtration, with P that passes a 0.45 μm filter being dissolved and retained being particulate, and sample preparation, with digestion representing total values (Haygarth and Sharpley, 2000). Both inorganic and organic P can be found both in dissolved forms and attached to particles (Gburek et al., 2005). The dissolved forms of P include phosphate which is bioavailable and complexes which may or may not be bioavailable. The P associated with particles is not bioavailable, but may be released into solution depending on solution conditions such as pH or P concentration (Essington, 2004; Withers and Jarvie, 2008).

Methods for reducing non-point P transport (Containment)

Conservation tillage

Due to the erosion risk associated with conventional tillage systems and the relative insolubility of P, one of the easiest methods to reduce particulate P loss from a site is to change to conservation tillage. Conservation tillage refers to any tillage method that reduces disturbance of the surface compared to conventional tillage, leaving plant residue on the surface (Brady and Weil, 2008). A study was conducted to investigate the water quality impacts of conservation tillage by monitoring nutrient and sediment loss from fields in seven watersheds located in western Oklahoma, northwestern Texas, and southern Kansas from 1977-1990 (Sharpley and Smith, 1994). As expected, the sediment loss from sites that employ conventional tillage were higher than conservation tillage by 95-96% with reductions in total P of 84-88% upon changing to conservation tillage, but there was an increase in dissolved P lost in runoff ranging from 58-308% with a maximum of 3.1 mg L^{-1} (Sharpley and Smith, 1994). The increases in dissolved P concentrations in runoff can be attributed to decreased sediment loss under conservation tillage which may help buffer the runoff dissolved P concentration, increased concentration of P in the

upper layer of soil due to lack of incorporation of fertilizer, and the decreased amount of runoff in a conservation tillage. Although decreased runoff in conservation tillage systems may promote increased P concentrations, but loading of P may remain similar when compared to a conventional system (Logan, 1982). The reductions in erosion make conservation tillage an attractive system to adopt since this will reduce particulate P transport, but the possibility of increased dissolved P in runoff may necessitate implementation of additional best management practices to reduce the threat of nutrient loss and subsequent eutrophication of receiving bodies of water.

Buffer zones

Vegetated buffer strips along riparian areas and at the edge of agricultural fields help slow water velocity allowing for sediment to fall out of suspension, reducing loss of the sediment and any nutrients attached to it (Brady and Weil, 2008). Since the areas are vegetated, there is also an opportunity for infiltration allowing the plants to uptake nutrients present in the runoff helping reduce the amount that is lost from the site (Brady and Weil, 2008). The ability of a buffer strip to reduce sediment and nutrient transport was assessed on a site with a 7 year old riparian buffer that was subjected to an amendment used to simulate agricultural runoff which was a mixture of N fertilizer, P fertilizer, and topsoil resulting in a known concentration of inorganic and organic N and P (Mankin et al., 2007). The buffer strips reduced total solids concentration by an average of 97.9% and total P concentrations by an average of 42.9%, but dissolved P was only reduced by an average of 16% (Mankin et al., 2007). This low reduction is not an anomaly among buffer strips. A review of 11 studies examining dissolved P reductions due to buffer strips showed removal efficiency that ranged from -83% to +95% showing the variable nature of this BMP when it comes to dissolved P (Dorioz et al., 2006). The values of removal were roughly 20% to 30%, but remobilization of P in these strips during winter and after they become saturated with P is a concern (Dorioz et al., 2006). A study was conducted using 2 m soil

blocks filled with different soil types which were subjected to a simulated rainfall event using a synthetic mixture containing P and chloride as a tracer for 2 hrs followed by 4 hrs of deionized water (Darch et al., 2015). Runoff samples were collected from the surface and subsurface and then analyzed for total and dissolved P. The retention of dissolved P was 20% and -61% for the clay and loam textures, respectively (Darch et al., 2015). Dissolved P reductions by buffer strips are a function of the ability of the strip to reduce runoff volume and the soil's P sorption which varies with initial soil levels and mineralogy (Fox and Penn, 2013; Penn et al., 2005; Vadas et al., 2005). Fox and Penn produced a model using data from 10 vegetated buffer strip studies that could predict total P removal using the reduction in runoff and sediment due to the strips (2013). By removing observations that had high initial soil P concentrations, the R^2 of the linear model was improved from 0.68 to 0.92 and the intercept decreased. The reduction in the intercept moved it closer to a 1:1 prediction line. This change is indicative of the influence of soil P level on the effectiveness of dissolved P removal in buffer strips. Buffer strips are very effective at reducing total P and can reduce dissolved P in certain conditions. These strips do not remove P from the site and can possibly become saturated with P providing a source to nearby surface waters.

Removing P from the site (Remediation)

Phytoremediation

Removal of biomass from a site for purposes such as crop harvest or bagging lawn clippings, will remove any nutrients present within that plant matter. Thus, biomass removal conducted on a site with excess soil P can help reduce the P source contributing to runoff and leaching. A long term study in Maryland established plots at four locations with four annual applications of three sources of P at 0, 100, 200, 300, and 400 kg total P ha⁻¹ y⁻¹ leading to five distinct levels of P in the soil that were then subjected to different cropping systems to assess drawdown of P in the soil (Kratovich et al., 2006). The study looked at forage and grain systems

for 2001-2004 and their ability to reduce soil P levels which were only significantly reduced at 7 of the 40 comparisons of different application rates and cropping systems (Kratovich et al., 2006). The forage systems caused a greater P reduction than the grains which is not surprising given the greater percentage of total biomass that is removed in a forage versus a grain system, such as the corn which produced a grain mass of 8.5 t ha⁻¹ and a shoot mass of 19.4 t ha⁻¹. The P removal for the corn harvested as a silage and a grain would be 95 kg of P ha⁻¹ and 19.1 kg of P ha⁻¹, respectively or nearly 5 times as much (Delorme et al., 2000).

A greenhouse study conducted by Gotcher et al. (2014) examined P removal by establishing crabgrass followed by complete harvest to reduce excess P present in the soil. Crabgrass was grown and then harvested seven times over two years using three different soil types at four distinct initial soil P levels (Gotcher et al., 2014). There was a reduction in P levels in the all of the soils for every initial soil P level after the second year, but the percent reduction was most prominent in the soils with lower initial P concentrations varying from 46-66% for the soil with no additional P. On the other hand, soils that initially had the highest soil P levels were only reduced by 10-22% after crabgrass harvests. The amount of time required to reduce the soil P concentrations to acceptable levels using biomass removal will vary with the crop grown and the soil type at that site, but the reductions observed in these studies suggest that it is not a fast process, although it would be effective in conjunction with other best management practices to help P transport reduce risk.

P sorbing materials

Certain materials are known to have a high affinity for P and have been used previously to reduce the solubility of P in soil, manure, and water (Moore and Miller, 1994; Penn and Bryant, 2006; Penn et al., 2007; Warren et al., 2008). These P sorbing materials (PSMs) utilize two of the most common P sorption mechanisms present in soil, precipitation and ligand

exchange, to remove P from solution (Sims and Pierzynski, 2005). Some materials can remove P from solution by providing dissolved Ca and increasing the solution pH which provides reactant and chemical potential for the precipitation of Ca phosphates, such as hydroxyapatite (Claveau-Mallet et al., 2011). Other PSMs rely on ligand exchange of P onto Fe or Al minerals present, which are commonly found in acid mine drainage residuals (AMDRs), bauxite residuals, and water treatment residuals (WTRs) (Arai and Sparks, 2001; Boisvert et al., 1997; Klimeski et al., 2014; Penn et al., 2011; Stoner et al., 2012). There are a variety of sources for PSMs, including natural materials like gypsum, manufactured products, and industrial by-products, such as steel slag, AMDRs, or WTRs, which have the advantage of being relatively inexpensive (Lyngsie et al., 2015; Stoner et al., 2012; Watts and Torbert, 2009).

Amendments to manure

Amending manure with materials that can reduce P solubility prior to land application can reduce the amount of P lost from the site (Brennan et al., 2011; Haggard et al., 2005; Moore et al., 1999; Smith et al., 2001; Warren et al., 2008). Smith et al completed a field trial in Arkansas that used liquid swine manure that was either untreated or treated with two rates of Al sulfate (alum) and Al chloride; a high rate that corresponded to a 1:1 molar ratio of Al to total P and a low rate that was half as much (Smith et al., 2001). The initial dissolved P of the manure was approximately 130 mg P L⁻¹ with both amendments lowering that to approximately 30 and 1 mg P L⁻¹ for the low and high rates, respectively. The plots that received alum treated manure reduced dissolved P in runoff by 33% for the low rate and 84% for the high rate compared to the untreated manure plots, and Al chloride showing reductions of 45% and 84% (Smith et al., 2001). The P lost from a site that received manure applications will be a function of particulate loss and the solubility of P, so amendments, such as alum, that reduce P solubility in manure will reduce loss.

Amendments to soil

The same amendments used with manure can be added directly to a soil to help reduce the amount of P lost from a site by decreasing P solubility. Bauxite residuals from Al mining contain Fe, Al, and Ca which make them a prime candidate for binding P. Two different neutralization methods were used in making bauxite residuals which were then mixed with water and soils taken from areas of Louisiana with a long history of manure applications (Udeigwe et al., 2009). After 48 hours of shaking, samples were tested for water soluble P which was 58-95% less in bauxite amended treatments versus the control showing the ability of the residuals to bind P (Udeigwe et al., 2009).

Field studies have shown that certain soil amendments can reduce water soluble P losses in runoff, but the reduction varies with material and time. An initial soil incubation study was used to determine appropriate rates for a field study that used alum, water treatment residuals, gypsum, and fly ash amendments to three different dairy farms in Pennsylvania to assess their ability to reduce P loss in runoff from areas with heavy animal traffic (Penn and Bryant, 2006). Runoff was initiated using rainfall simulation prior to amendment application (time 0) and at 7 and 28 days after amendment application; while amendments significantly reduced dissolved P loss at 7 days after application for two of the three sites, the results were temporary as 28 days after application there was no significant difference for all three sites (Penn and Bryant, 2006). Similar reductions in P sorption over time were observed in several studies testing amendment applications.

Al based water treatment residuals were applied to buffer strips in England and then irrigated with 0.45 mg P L^{-1} to induce runoff one day after application and then nine more times over the course of 42 weeks to assess their ability to reduce dissolved P loss from the site (Habibiandehkordi et al., 2014). The first runoff event (one day after application) resulted in

reductions in P of 57-65%, but the reductions were only 9-15.9% at 42 weeks after application (Habibiandehkordi et al., 2014). In a study completed in Alabama, gypsum applied to buffer strips also reduced dissolved P loss 32-40% compared to 18% with a buffer strip alone in a runoff event simulated directly after manure application (Watts and Torbert, 2009). Following a second runoff event 4 weeks after application there was no reduction for any treatment compared to the control plot that had no buffer strip and there was even an increase in the plot with the highest gypsum rate (Watts and Torbert, 2009). Studies that have investigated manure and soil amendments have shown decreases in dissolved P loss, but these losses reduce with time. Essentially, the decrease in P solubility appears to be temporary as the P solubility becomes re-equilibrated based on the soil chemical conditions and mineralogy. It is important to keep in mind that with such methods, P is not removed from the system.

P removal structure

While land application of PSMs to a soil with high P may reduce the amount of P lost from the site, the effect will be short lived (Habibiandehkordi et al., 2014; Penn and Bryant, 2006; Watts and Torbert, 2009). In order to correct the nutrient imbalance, P must be removed from the site through phytoremediation; however, large amounts of P will be lost from during this slow process. One remedy for reducing dissolved P losses during this period of phytoremediation is to trap the dissolved P before it reached a surface water body. A filter utilizing PSM media placed in areas with excessive dissolved P could intercept P in the drainage waters (Penn et al., 2007).

Site requirements and basic components of a P removal structure

Not all sites are viable for P removal structures and each site will require a uniquely designed filter to accommodate removal goals, desired lifetime of material, and the specific hydrology of that site. For a site to be a candidate for a structure it must meet three criteria: elevated dissolved P concentrations in the water to be treated, hydrologic connectivity to a

surface water body, and a potential interaction point where flow converges (Penn et al., 2014a). Due to the relatively short contact time between the PSM and the solution, there must be sufficient chemical potential in the form of dissolved P concentration, that will drive the equilibrium to less dissolved P and more solid P as either precipitated Ca phosphate or P bound to Fe and Al minerals. When dissolved P concentration is low, there is less chemical potential and therefore less sorption according to Le Chatelier's principle (the equilibrium law) (Atkins and de Paula, 2010). The dissolved P concentration required for most PSMs to function effectively in a filter is around 0.2 mg P L^{-1} , but some PSMs are able to remove P at lower concentrations (Penn et al., 2014a).

The source of dissolved P must be hydrologically connected to a surface water body in order for a P removal structure to be a viable option to reduce dissolved P transport (Penn et al., 2014a). If the flow at a site does not contribute to a surface water body, then other BMPs would be a better choice since runoff would simply need to be slowed until it can infiltrate. Structures should be placed strategically between large sources of dissolved P and the receiving water bodies.

Due to differences in flow, landscape, and P concentrations at a site, P removal structures will often vary greatly from one another in shape, but all include four main characteristics: the structure should be filled with a solid material having an affinity for P (a PSM), the PSM should be contained within an area that receives runoff with an elevated concentration of dissolved P, water has to be able to flow through the PSM, and the PSM must be able to be removed after it is spent (Penn et al., 2014a). These characteristics allow for a great deal of variability and creativity when designing a P removal structure. Two of the more common types of structures are bed and ditch filters. Bed filters rely on the flow of water through a bed of PSM which can be any shape or size. The size and function of bed filters vary from a 7.2 m^2 steel box treating runoff to a $28,830 \text{ m}^2$ series of beds at a waste water treatment plant (Penn et al., 2012; Shilton et al., 2006).

While most of the bed filters are exposed, they can also be buried, such as backfill for a tile drain or trenches filled with a PSM designed to treat subsurface flow (Bryant et al., 2012; McDowell et al., 2008). A bioretention cell, surface inlet, or blind inlet that uses a PSM in their media layer is a bed filter as well (Chavez et al., 2015; Feyereisen et al., 2015). A ditch filter is essentially just a bed filter that is built in a ditch. Ditch filters can range from small enclosed boxes built within a ditch to 100 ft sections of a ditch filled with over 100 ton of material (Bryant et al., 2012; Penn et al., 2007). Due to the broad description, a P removal structure can vary wildly in design.

Examples of P Removal Structures

Maryland AMDR Ditch Structure

P removal structures built in ditches are common, particularly in eastern Maryland, due to the convergence of runoff and the hydraulic head available due to the depth of the ditch. A filter was constructed in Maryland on a research farm with a 25 year history of poultry production and litter applications that resulted in excessive P levels of the soil (Penn et al., 2007). The runoff from the site had dissolved P concentrations ranging from 6-16 mg of P L⁻¹ resulting in an annual P load greater than 25 kg ha⁻¹ which would be delivered into the Chesapeake Bay, a water body with a history of eutrophication problems (Kemp et al., 2005; Penn et al., 2007). The filter consisted of an aluminum box measuring 2 m in length by 33 cm wide that confined 200 kg of AMDR (Penn et al., 2007). Ditch flow was forced to enter the structure by means of a flume that was also used to measure flow entering the structure. The structure was designed to handle 5.71 L s⁻¹, a value only exceeded 20% of the time in this ditch. Due to this design, the structure was only able to treat 9% of the flow associated with a tropical storm that produced runoff with 16 mg of P L⁻¹ (Penn et al., 2007). The structure was designed for 50% removal for 1 yr, but the design was based on a single point isotherm that have been shown to over predict P sorption (Stoner et al.,

2012). The structure was able to remove 0.54 kg of P, as well as reduce As, Cu, and Zn by 63%, 99%, and 94%, respectively.

Maryland Gypsum Ditch Structure

A P removal structure was built in a ditch that drains approximately 17 ha of a research farm in Maryland that was filled with 110 Mg of gypsum and 5 Mg of sand confined using a weir (Bryant et al., 2012). A 10 cm layer of the PSM was placed in the bottom of the ditch and covered with a sand layer used to surround the subsurface drainage that consisted of 6, 10 cm diameter pipes. That was covered with the final layer of PSM which was 35 cm deep. Due to the large mass of PSM used, the material was confined within the ditch using a weir that helped contain the material and permitted water to bypass the filter during high flow. Overall, the structure was able to reduce the P load by 22% removing 20 kg of dissolved P of the 92.9 kg that entered the ditch. Due to the lower hydraulic conductivity of the gypsum, 4 L s^{-1} , only 7% of the flow during storm events passed through the structure which resulted in an overall 9.2% P removal. The hydraulic conductivity of the structure decreased over the course of monitoring, from 4 L s^{-1} to $<1 \text{ L s}^{-1}$, requiring tilling of the surface of the structure.

Golf Course Structure

A P removal structure constructed on an Oklahoma golf course consisted of a steel box that was 2.4 m wide by 3 m long by 0.2 m deep and filled with steel slag resulting in a bed of material (Penn et al., 2012). The 63 ha watershed consisted of undeveloped area, residential, and a golf course that drains into a bar ditch drained into Stillwater Creek. Two ISCO 6712 (Teledyne Isco Inc., Lincoln, NE) automatic samplers were housed on site to collect runoff samples and monitor flow using an ISCO 730 flow module connected to an insert in the drainage pipe (Penn et al., 2012). The flow through the structure was a combination of runoff produced from irrigation and rainfall events that had a flow-weighted P concentration of 0.44 and 0.59 mg L^{-1} , respectively

(Penn et al., 2012). The structure size was limited by the area available in the ditch, but the design still allowed for 2,712 kg of steel slag which had a lifetime of 15.8 mo. The structure removed 25% of the P load during the first 5 mo. Water quality testing of outflow samples, i.e. treated water, showed no addition of heavy metals and similar alkalinity values for inflow and outflow samples (Penn et al., 2012).

Indiana Blind Inlets

Blind inlets are used to help reduce nutrient and sediment loss in tile-drained fields by filtering runoff through backfilled soil and a buried gravel or sand layer (Feyereisen et al., 2015). A 3.5 and 4 ha tile drained field in Indiana were fit with a tile riser and a blind inlet that could be switched between using a gate valve. The blind inlets consisted of a 4.25 by 4.25 by 1 m hole that had a 3 by 3 m septic tile placed on top of 10 cm of gravel and then buried in 60 cm of limestone and 30 cm of soil. From 2006 to 2013, these fields were monitored using ISCO 6712 automatic samplers to assess the ability of blind inlets to reduce P and sediment loss compared to the tile riser (Feyereisen et al., 2015). There were a total of 37 events that had flow from both the tile riser and the blind inlet. On average over the course of the experiment, the blind inlets were able to reduce the total P, dissolved P, and sediment by 56.67%, 60%, and 59.22%, respectively during the growing season (1 April to 15 Nov). The inlets are built according to existing standards, so designing these structures to meet specific removal goals is not possible (USDA-NRCS, 2010).

New Zealand Waste Water Treatment Plant

In 1993, a steel slag bed was added to the waste water treatment plant in Waiuku Auckland, New Zealand. The town of approximately 6,000 people produced an average daily flow of 2,000 m³ that had an average total P concentration of 8.2 and 8.6 mg L⁻¹ for 1993-1994 and 2002-2003, respectively (Shilton et al., 2006). The series of 10 beds are 29.6 by 97.4 by 0.5 m in size with a total area of 28,830 m². Each bed is filled with melter steel slag from a local steel

mill, New Zealand Steel, that ranged in size from 10 to 20 mm. Assuming an average daily flow, the retention time of this series of slag beds is 3 days, much greater than any of the P removal structures discussed here. The influent and effluent were tested every two weeks for 11 yr with daily testing during 1993-1994 and 2002-2003. During the course of monitoring the structure removed 22.4 tonnes of total P with 19.7 tonnes of that removal occurring within the first 5 yr of operation (Shilton et al., 2006). During the last year of monitoring the average effluent, 8.9 mg L⁻¹, was higher than the influent, 8.6 mg L⁻¹. The P removal dropped off drastically after the first 5 yr of operation with 88% of the removal occurring during this period. The scale is much larger for this structure than others discussed here, but they share the same basic characteristics.

Bioretention Cells

Ten bioretention cells (BRC) were constructed in Grove and Stillwater, Oklahoma to demonstrate their ability to reduce runoff from storms and P loss from the sites (Chavez et al., 2015). BRCs are able to reduce runoff quantity and improve water quality through the natural processes of the soil and plants present, which include physical filtration, sorption, and sedimentation (PGDER, 1993). These structures were built in drainage areas ranging in size from 0.045 to 0.77 ha that included paved areas, turf, and roofs. Structures were sized to handle 13 mm of runoff via ponding and an additional 13 mm in the pore space of the filter media (Chavez et al., 2015). The subsurface drainage layer consisted of 51 mm pipes that were covered with filter fabric to prevent clogging. The filter media used in the bottom layer was a mixture of 5% class C fly ash 95% clean sand (less than 5% fines) (Chavez et al., 2015). The media layer was covered with a 0.3 m layer of soil, but due to the low hydraulic conductivity of the soil used sand plugs were installed. Approximately 25% of the surface layer of each BRC was a sand plug that allowed for increased infiltration into the media layer. A variety of vegetation was established in the BRCs to maintain the aesthetic quality and aid in the function of the structure. Since these structures were designed to hold a specific amount of runoff, the mass of media was determined

by pore volume, which resulted in rather large masses with the mass of four structures ranging from 97 to 266 Mg. This large mass results in long lifetimes, some in excess of 50 yr.

Slag Trench

In order to assess the removal potential of a trench structure, twelve 5.2 by 1.2 m trenches were dug on turfgrass plots and then 6 were backfilled with EAF steel slag and 6 with river gravel (Wang et al., 2014). The trenches were designed to prevent subsurface flow in or out of the trench, so all water treated was runoff. Each trench contained approximately 1,008 kg of slag in four plastic containers that enabled easy replacement of the slag. The trench was placed in the middle of the plot allowing for an upper area contributing runoff and a lower area excluded from treatment that allowed testing of the runoff (Wang et al., 2014). Outflow samples were collected using ISCO automatic samplers with runoff flow rate measured using a 2.5 cm Parshall flume and an ISCO 710 ultrasonic module. Half of the plots received one application of triple superphosphate equivalent to 49 kg P ha⁻¹ in order to assess the its impact on dissolved P concentration in runoff. Runoff produced on the plots was due to both natural and irrigation events. The fertilized plots consistently produced higher levels of dissolved P which declined throughout the study. The range of P concentration in runoff produced from the fertilized and unfertilized plots was 1.0 to 13.1 mg L⁻¹ and 0.6 to 1.8 mg L⁻¹, respectively (Wang et al., 2014). The slag trenches were able to reduce dissolved P 22.8% for the fertilized plots and 29.6% for the unfertilized plots compared to 0.33% and 0.34% reductions seen in the gravel plots.

New Zealand Tile Drain

Tile drained fields are vital for agriculture in areas with shallow water tables. The drains are backfilled with porous media to ensure adequate drainage. The tile drains of a 10 ha dairy farm near Karaka, South Auckland, New Zealand were backfilled using either a locally available gravel considered to be inert or a mixture of 90% melter slag and 10% basic steel slag (McDowell

et al., 2008). The site had received dairy effluent from 300 head of cattle for longer than 15 yr, but had not received any applications in the 3 yr prior to the start of this 2 yr study. During the course of this experiment there were 10 events that produced flow in the tile. The average dissolved P concentration was 0.09 mg L^{-1} in the steel slag drain and 0.33 mg L^{-1} in the control drain (McDowell et al., 2008). This removal was not associated with a significant increase in effluent pH, 7.2 for the control versus 7.3 for the slag, or an increase in heavy metals, with the exception of 0.01 mg L^{-1} for the first event. Since the size of the structure was determined by common practices in tile drain installation and not removal goals, the lifetime of the material had to be estimated using removal data. Samples taken from a different site that was equivalent in size and management practices were used to assess the lifetime of the material. The drains at the other site had been in place since 1994 which, when coupled with the 2 yr removal data at the main site, allowed lifetime estimation using a power function regression. By plotting the effluent concentration versus the age of the drain, the time when the slag is spent, i.e. effluent concentration is equal to the control, was determined to be 25.3 yr (McDowell et al., 2008).

Need for methods to design P removal structures

The majority of the P removal structures used in research have not been designed with a removal goal or lifetime in mind. The designs were dictated by size constraints, due to either the available space or budget, or were chosen to meet a certain maximum flow rate. Other structures, like BRC and blind inlets, have design standards in place that are a function of water infiltration. Since these research structures are monitored removal performance is known, but in order for these structures to be used as a BMP, performance has to be estimated. Performance predictions are vital to the design and maintenance of these structures. Being able to predict the removal and estimate the lifetime of the material are vital to decisions about the size and when to clean out these structures. Being able to accurately predict the performance of a structure or to design one

to meet a certain goal requires knowledge of the site's hydrology and the ability measure or predict P affinity of the PSM.

Previous research has utilized batch testing for estimating P sorption, but the method does not accurately simulate field conditions. Use of flow-through experiments has resulted in more accurate sorption estimates due to its more accurate simulation of field conditions. Given the large variety of PSMs available there is a need for predictions that can accurately estimate the P sorption of these materials. This prediction would be the first step in the design process for a P removal structure. Adoption of these structures as a BMP and possible cost-sharing necessitate a standardized design process to ensure that the structures are operational and actually removing P.

Individual flow-through model

While batch testing for P sorption is easier to perform than a flow-through experiment, it can over predict P sorption and does not accurately reflect actual conditions (Klimeski et al., 2012; Penn and McGrath, 2011; Stoner et al., 2012). Testing the ability of materials to remove P in a flow-through setting yields better due to a more accurate simulation of field conditions (Stoner et al., 2012). The discrete P removal (%) can be expressed using an exponential equation with the removal being a function of the cumulative P added (mg kg^{-1}) as shown in figure 1.1.

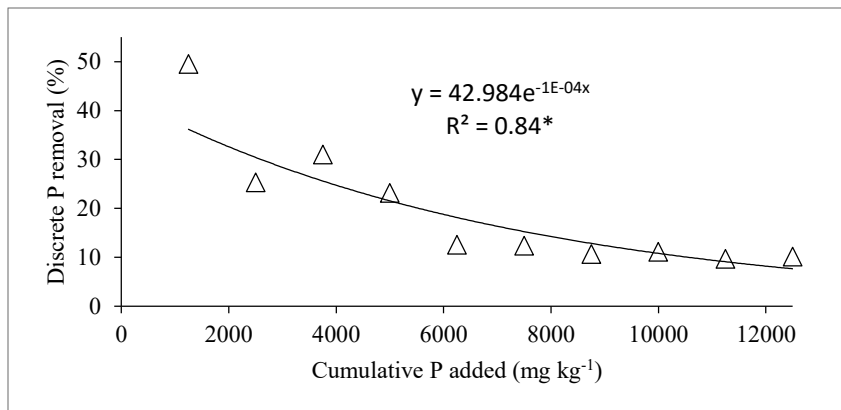


Figure 1.1. Data from a flow-through experiment of an acid mine drainage residual (AMDR) at a retention time of 0.28 min and a phosphorus (P) concentration of 1 mg L^{-1} are shown with the discrete P removal plotted versus the cumulative P added. The exponential regression equation and r-squared are shown.

The discrete removal curve relates the removal percentage to the mass of PSM, so it can be helpful in the design process. By integrating the discrete curve up to a particular loading and then dividing by that loading the cumulative P removal (%) can be estimated. Since the loading is a function of the P load entering the structure and the mass of PSM in the structure, the cumulative removal can be used to estimate the mass required to meet a removal goal. While this method is effective, it does require performing a flow-through experiment at an appropriate retention time and P concentration for the site. In order to predict discrete P removal curves, models were created by testing PSMs in laboratory or field scale experiments to gauge its ability to remove P. Penn and McGrath tested a steel slag utilizing flow-through experiments with retention times of 0.5, 3, 6, and 8 min and inflow P concentrations of 0.5, 1, 5, 10, and 15 mg of P L⁻¹ (Penn and McGrath, 2011). Discrete removal data from the flow-through experiments was plotted and then had an exponential regression performed with the equation taking the form of equation 1.1:

$$\text{Eq. 1.1 } \textit{Discrete P Removal (\%)} = be^{mx},$$

where b is the y-intercept, m is the slope, and x is the cumulative P added (mg kg⁻¹). Multiple linear regression (MLR) on the data produced two models which predict the slope and intercept of the discrete removal curve (Penn and McGrath, 2011). The models require input of the retention time and P concentration, as shown in equations 1.2a and b:

$$\text{Eq. 1.2a } \log(-m) = (\alpha RT) + (\beta P) + \chi$$

$$\text{Eq. 1.2b } \log(b) = (\delta RT) + (\varepsilon P) + \mu,$$

where m and b are the slope and intercept of the predicted discrete removal curve, i.e. design curve, and RT and P are the desired retention time and P concentration, respectively. The prediction coefficients, α , β , χ , δ , ε , and μ , vary with the material in question and its P affinity.

The resulting model from those experiments was used to estimate the P sorption of a pilot scale experiment conducted using 454 kg of steel slag, which fit relatively well with a slight over prediction of the cumulative P removal (Penn and McGrath, 2011). The fact that the model was developed testing samples of less than 5 g and was able to predict performance of a structure that used a mass 90,000 times greater than the preliminary laboratory flow through, suggests the benefit of using this particular approach of empirical modelling. After the success of the model in a pilot scale experiment, it was used in two field scale experiments that utilized steel slag from the same source as the slag used in development of the model (Penn et al., 2012; Wang, 2012). The previously described P removal structure located on an Oklahoma golf course was filled with steel slag and monitored until it was spent, followed by removal of the material; the actual removal was then compared to model predictions (Penn et al., 2012). The actual P removal of the structure was less than that predicted by the model due to differences between the chemical character of the slag used to create the model and the slag actually used in the P removal structure. Specifically, the slag used to create the model possessed higher pH, alkalinity, and total Ca (Penn and McGrath, 2011; Penn et al., 2012). A series of trench P removal structures using the same slag as the golf course structure were constructed on turfgrass plots and monitored for P removal over the course of 7 months (Wang, 2012). The model prediction for P removal of the trench structures over predicted removal in a similar fashion as the golf course structure. The actual P removal of the two structures was quite similar with the golf course structure removing 21.0% of dissolved P and the trenches removing 18.7% (Penn et al., 2012; Wang et al., 2014). As shown in equations 1.2a and b, the model only incorporated the P concentration and retention time, so any variations in the relevant chemical characteristics would lead to deviations between prediction and actual values as evidenced by the two previous studies. Models created for individual PSMs are not accurate if there is any variation in the material's chemical characteristics which limits their usefulness. The chemical characteristics of PSMs can vary over time even when produced at the same site.

Universal flow-through model

In order to create a model that is capable of being used for a variety of materials regardless of source, PSM characteristics need to be correlated with a material's ability to remove P. Stoner et al. (2012) characterized 12 PSMs, both chemically and physically, and tested their ability to sorb P in flow-through cells at retention times of 0.5, 3, 6, 8, and 10 min and P concentrations of 0.5, 1, 5, 10, and 15 mg P L⁻¹.

The ability to predict the discrete P removal curve (equation 1.1) for any material as a function of chemical characteristics of the PSM can be used to design a P removal structure; this predicted discrete P removal curve is known as the "design curve". The design curve can also be used to estimate the P removal of an existing structure. The chemical and physical characteristics of the PSMs were used to predict the slope and intercept of the design curve for the different P concentrations and retention times (equations 1.2a and b). Once non-significant chemical characteristics were removed, the resulting model was able to estimate the intercept and slope of the design curve using P concentration, retention time, and specific chemical and physical characteristics (Stoner et al., 2012). Mean particle size was the only physical characteristic of interest due to its effect on surface area of the particle and resulting reactivity. Due to the varying chemical characteristics of interest for the two main categories of sorption mechanisms, two separate models were necessary to accommodate the Ca group and the Fe and Al group. Chemical characteristics are first used to separate the PSMs into their respective group and then a slope and intercept is predicted for the design curve given a specific retention time and P concentration (Stoner et al., 2012). The retention time of water in the structure is only a factor for Ca materials that have a low pH and are poorly buffered, such as a gypsum (Stoner et al., 2012). Any PSM that uses Ca, Fe, or Al to sorb P can be entered into the model producing a design curve able to estimate the mass required to meet performance goals or quantify the removal of an existing structure.

Design software

Other BMPs that reduce the environmental impact of agriculture must be constructed according to standard designs, but there is no standardized design process available for P removal structures. Successfully designing a P removal structure requires striking a balance between the structure goals and constraints. The structure goals include the removal goal, desired lifetime of the structure, and the maximum flow rate the structure should be able to handle. The design is constrained by limitations at the site, such as available area and the hydraulic head which provides the driving force for water through the structure. The mass of PSM required to meet the removal goal and desired lifetime can be estimated using the universal flow-through model. Flow through the structure will depend on the orientation of the PSM and the subsurface drainage present in the structure. All of these factors must be considered in order to design a P removal structure that will meet performance goals. Given that every P removal structure design is the unique combination of site characteristics, performance goals, and the PSM, these calculations have to take each of these factors into consideration. Performing a series of these calculations to test the viability of different PSMs or goals for one site is time consuming and unlikely to be done by many structure designers.

Development of design software is needed to standardize the design process and make it more accessible. Without an easy means of designing structures with quantifiable removal there is no means of gauging their effectiveness accurately. Knowledge about the flow of water into and through the structure, both the PSM layer and the drainage layer, are vital to the removal performance of the design and must be included in the software. Water flow will be dictated by material characteristics and orientation, as well as the topography at the site. Since the model is the basis for removal prediction, the accuracy of its predictions must be validated before it is used as the basis of the software. Addressing these factors must be done in order to produce software that streamlines the P removal design process.

Objectives

The objectives of this study were to demonstrate the viability of P removal structures as a best management practice given certain, specific conditions, as well as provide guidance to producers in design, quantification, and construction of these structures. Validation of the universal flow-through model was also a key objective as it is the basis of design and quantification of these structures.

- 1) Construct and monitor a field scale P removal structure to demonstrate its viability as a best management practice to reduce dissolved P transport.
- 2) Validate the universal flow-through model using available flow-through data from P removal structures, pond filter experiments, and laboratory flow-through experiments coupled with characterization data from P sorbing materials used.
- 3) Create software that utilizes the universal flow-through model to help the user design P removal structures given certain inputs concerning the site and the P sorbing material in question, or to quantify the removal of existing structures.

REFERENCES

- Allaby T. (2010) *A Dictionary of Ecology*, 'Oxford University Press'.
- Arai Y., Sparks D. (2001) ATR–FTIR spectroscopic investigation on phosphate adsorption mechanisms at the ferrihydrite–water interface. *Journal of Colloid and Interface Science* 241:317-326.
- Atkins P., de Paula J. (2010) *Atkins' Physical Chemistry* OUP Oxford.
- Bohn H.L., McNeal B.L., O'Connor G.A. (2001) *Soil Chemistry*. 3rd ed. John Wiley & Sons, Inc., New York.
- Boisvert J.-P., To T.C., Berrak A., Jolicoeur C. (1997) Phosphate adsorption in flocculation processes of aluminium sulphate and poly-aluminium-silicate-sulphate. *Water Research* 31:1939-1946.
- Brady N.C., Weil R.R. (2008) *The Nature and Properties of Soils*. 14th ed. Prentice Hall, Upper Saddle River, New Jersey.
- Brennan R.B., Fenton O., Rodgers M., Healy M.G. (2011) Evaluation of chemical amendments to control phosphorus losses from dairy slurry. *Soil Use and Management* 27:238-246. DOI: 10.1111/j.1475-2743.2011.00326.x.

- Bryant R.B., Buda A.R., Kleinman P.J.A., Church C.D., Saporito L.S., Folmar G.J., Bose S., Allen A.L. (2012) Using Flue Gas Desulfurization Gypsum to Remove Dissolved Phosphorus from Agricultural Drainage Waters. *Journal of Environmental Quality* 41:664-671. DOI: 10.2134/jeq2011.0294.
- Carpenter S.R., Caraco N.F., Correll D.L., Howarth R.W., Sharpley A.N., Smith V.H. (1998) Nonpoint Pollution of Surface Waters with Phosphorus and Nitrogen. *Ecological Applications* 8:559-568. DOI: 10.2307/2641247.
- Chavez R., Brown G., Coffman R., Storm D. (2015) Design, Construction and Lessons Learned from Oklahoma Bioretention Cell Demonstration Project. *Applied Engineering in Agriculture* 31:63-71.
- Claveau-Mallet D., Wallace S., Comeau Y. (2011) Model of Phosphorus Precipitation and Crystal Formation in Electric Arc Furnace Steel Slag Filters. *Environmental Science & Technology* 46:1465-1470. DOI: 10.1021/es2024884.
- Darch T., Carswell A., Blackwell M.S.A., Hawkins J.M.B., Haygarth P.M., Chadwick D. (2015) Dissolved Phosphorus Retention in Buffer Strips: Influence of Slope and Soil Type. *Journal of Environmental Quality*. DOI: 10.2134/jeq2014.10.0440.
- Delorme T.A., Angle J.S., Coale F.J., Chaney R.L. (2000) Phytoremediation of Phosphorus-Enriched Soils. *International Journal of Phytoremediation* 2:173-181. DOI: 10.1080/15226510008500038.
- Dodds W.K. (2002) *Freshwater Ecology: Concepts and Environmental Applications* Academic Press, San Diego, California.

- Dorioz J.M., Wang D., Poulenard J., Trévisan D. (2006) The effect of grass buffer strips on phosphorus dynamics—A critical review and synthesis as a basis for application in agricultural landscapes in France. *Agriculture, Ecosystems & Environment* 117:4-21. DOI: <http://dx.doi.org/10.1016/j.agee.2006.03.029>.
- Essington M.E. (2004) *Soil and Water Chemistry: An Integrative Approach*. 1st ed. CRC Press, Boca Raton, Florida.
- Feyereisen G.W., Francesconi W., Smith D.R., Papiernik S.K., Krueger E.S., Wente C.D. (2015) Effect of Replacing Surface Inlets with Blind or Gravel Inlets on Sediment and Phosphorus Subsurface Drainage Losses. *Journal of Environmental Quality* 44:594-604. DOI: 10.2134/jeq2014.05.0219.
- Fox G., Penn C. (2013) Empirical model for quantifying total phosphorus reduction by vegetative filter strips. *Transactions of the ASABE* 56:1461-1469.
- Gburek W.J., Barberis E., Haygarth P.M., Kronvang B., Stamm C. (2005) Phosphorus Mobility in the Landscape, in: J. T. Sims and A. N. Sharpley (Eds.), *Phosphorus: Agriculture and the Environment*, American Society of Agronomy, Crop Science Society of America, and Soil Science Society of America. pp. 941-979.
- Gotcher M.J., Zhang H., Schroder J.L., Payton M.E. (2014) Phytoremediation of Soil Phosphorus with Crabgrass. *Agronomy Journal* 106:528-536.
- Habibiandehkordi R., Quinton J., SurrIDGE B.J. (2014) Long-term effects of drinking-water treatment residuals on dissolved phosphorus export from vegetated buffer strips. *Environmental Science and Pollution Research*:1-9. DOI: 10.1007/s11356-014-3802-y.

- Haggard B., Vadas P., Smith D., DeLaune P., Moore Jr P. (2005) Effect of poultry litter to water ratios on extractable phosphorus content and its relation to runoff phosphorus concentrations. *Biosystems engineering* 92:409-417.
- Haygarth P.M., Sharpley A.N. (2000) Terminology for phosphorus transfer. *Journal of Environmental Quality* 29:10.
- Jassby A.D., Reuter J.E., Axler R.P., Goldman C.R., Hackley S.H. (1994) Atmospheric deposition of nitrogen and phosphorus in the annual nutrient load of Lake Tahoe (California-Nevada). *Water Resources Research* 30:2207-2216.
- Kemp W., Boynton W., Adolf J., Boesch D., Boicourt W., Brush G., Cornwell J., Fisher T., Glibert P., Hagy J. (2005) Eutrophication of Chesapeake Bay: historical trends and ecological interactions. *Marine Ecology Progress Series* 303:1-29.
- Klimeski A., Uusitalo R., Turtola E. (2014) Screening of Ca-and Fe-rich materials for their applicability as phosphate-retaining filters. *Ecological Engineering* 68:143-154.
- Kratochvil R., Coale F., Momen B., Harrison Jr M., Pearce J., Schlosnagle S. (2006) Cropping systems for phytoremediation of phosphorus-enriched soils. *International journal of phytoremediation* 8:117-130.
- Logan T. (1982) Mechanisms for release of sediment-bound phosphate to water and the effects of agricultural land management on fluvial transport of particulate and dissolved phosphate. *Hydrobiologia* 91:519-530.
- Lyngsie G., Penn C.J., Pedersen H.L., Borggaard O.K., Hansen H.C. (2015) Modelling of phosphate retention by Ca-and Fe-rich filter materials under flow-through conditions. *Ecological Engineering* 75:93-102.

- Mankin K.R., Ngandu D.M., Barden C.J., Hutchinson S.L., Geyer W.A. (2007) Grass-Shrub Riparian Buffer Removal of Sediment, Phosphorus, and Nitrogen From Simulated Runoff1. JAWRA Journal of the American Water Resources Association 43:1108-1116. DOI: 10.1111/j.1752-1688.2007.00090.x.
- McCollum R. (1991) Buildup and decline in soil phosphorus: 30-year trends on a Typic Umprabuult. Agronomy Journal 83:77-85.
- McDowell R., Sharpley A., Bourke W. (2008) Treatment of drainage water with industrial by-products to prevent phosphorus loss from tile-drained land. Journal of environmental quality 37:1575-1582.
- Meals D.W., Dressing S.A., Davenport T.E. (2010) Lag time in water quality response to best management practices: A review. Journal of Environmental Quality 39:85-96.
- Moore P., Miller D. (1994) Decreasing phosphorus solubility in poultry litter with aluminum, calcium, and iron amendments. Journal of Environmental Quality 23:325-330.
- Moore P., Daniel T., Edwards D. (1999) Reducing phosphorus runoff and improving poultry production with alum. Poultry Science 78:692-698.
- Penn C., McGrath J., Bowen J., Wilson S. (2014a) Phosphorus removal structures: A management option for legacy phosphorus. Journal of Soil and Water Conservation 69:51A-56A.
- Penn C., Mullins G., Zelazny L., Warren J., McGrath J. (2004) Surface runoff losses of phosphorus from Virginia soils amended with turkey manure using phytase and high available phosphorus corn diets. Journal of environmental quality 33:1431-1439.

- Penn C.J., Bryant R.B. (2006) Application of phosphorus sorbing materials to streamside cattle loafing areas. *Journal of Soil and Water Conservation* 61:303-310.
- Penn C.J., Bryant R.B., Callahan M.P., McGrath J.M. (2011) Use of Industrial By-products to Sorb and Retain Phosphorus. *Communications in Soil Science and Plant Analysis* 42:633-644. DOI: 10.1080/00103624.2011.550374.
- Penn C.J., Bryant R.B., Kleinman P.J.A., Allen A.L. (2007) Removing dissolved phosphorus from drainage ditch water with phosphorus sorbing materials. *Journal of Soil and Water Conservation* 62:269-276.
- Penn C.J., McGrath J.M. (2011) Predicting Phosphorus Sorption onto Steel Slag Using a Flow-through approach with Application to a Pilot Scale System. *Journal of Water Resource and Protection* 03:235-244.
- Penn C.J., McGrath J.M., Rounds E., Fox G., Heeren D. (2012) Trapping Phosphorus in Runoff with a Phosphorus Removal Structure. *J. Environ. Qual.* 41:672-679. DOI: 10.2134/jeq2011.0045.
- Penn C.J., Mullins G.L., Zelazny L.W. (2005) Mineralogy in Relation to Phosphorus Sorption and Dissolved Phosphorus Losses in Runoff. *Soil Science Society of America Journal* 69:1532-1540. DOI: 10.1346/CCMN.1968.0160104.
- PGDER. (1993) Design manual for use of bioretention in stormwater management. Prince George's County (MD) Government, Department of Environmental Protection. Watershed Protection Branch, Landover, MD.

- Schindler D.W., Hecky R.E., Findlay D.L., Stainton M.P., Parker B.R., Paterson M.J., Beaty K.G., Lyng M., Kasian S.E. (2008) Eutrophication of lakes cannot be controlled by reducing nitrogen input: Results of a 37-year whole-ecosystem experiment. *Proceedings of the National Academy of Sciences of the United States of America* 105:11254-11258. DOI: 10.1073/pnas.0805108105.
- Sharpley A., Jarvie H.P., Buda A., May L., Spears B., Kleinman P. (2013) Phosphorus Legacy: Overcoming the Effects of Past Management Practices to Mitigate Future Water Quality Impairment. *J. Environ. Qual.* 42:1308-1326. DOI: 10.2134/jeq2013.03.0098.
- Sharpley A.N., Smith S. (1994) Wheat tillage and water quality in the Southern Plains. *Soil and Tillage Research* 30:33-48.
- Shilton A.N., Elmetri I., Drizo A., Pratt S., Haverkamp R.G., Bilby S.C. (2006) Phosphorus removal by an 'active' slag filter—a decade of full scale experience. *Water Research* 40:113-118. DOI: <http://dx.doi.org/10.1016/j.watres.2005.11.002>.
- Sims J.T., Pierzynski G.M. (2005) Chemistry of Phosphorus in Soils, in: M. A. Tabatabai and D. L. Sparks (Eds.), *Chemical Processes in Soils*, Soil Science Society of America. pp. 151-192.
- Smith D.R., Moore P.A., Griffis C.L., Daniel T.C., Edwards D.R., Boothe D.L. (2001) Effects of Alum and Aluminum Chloride on Phosphorus Runoff from Swine Manure. *Journal of Environmental Quality* 30:992-998. DOI: 10.2134/jeq2001.303992x.
- Smith F. (1969) *Eutrophication: Causes, Consequences, Correctives*. National Academy of Sciences, Washington, DC:631-645.
- Stoner D., Penn C., McGrath J., Warren J. (2012) Phosphorus Removal with By-Products in a Flow-Through Setting. *J. Environ. Qual.* 41:654-663. DOI: 10.2134/jeq2011.0049.

- Tisdale S.L., Nelson W.L., Beaton J.D., Havlin J.L. (1993) Soil Fertility and Fertilizers. 5th ed. Prentice Hall, Upper Saddle River, New Jersey.
- Udeigwe T.K., Wang J.J., Zhang H. (2009) Effectiveness of bauxite residues in immobilizing contaminants in manure-amended soils. *Soil science* 174:676-686.
- USDA-NRCS. (2010) Conservation practice standard: Underground outlet, National Resources Conservation Service.
- USEPA. (2011) National Summary of Impaired Waterways and TMDL Information, United States Environmental Protection Agency.
- Vadas P.A., Kleinman P.J.A., Sharpley A.N., Turner B.L. (2005) Relating Soil Phosphorus to Dissolved Phosphorus in Runoff: A Single Extraction Coefficient for Water Quality Modeling. *Journal of Environmental Quality* 34:572-80.
- van der Salm C., Chardon W.J., Koopmans G.F., van Middelkoop J.C., Ehlert P.A.I. (2009) Phytoextraction of Phosphorus-Enriched Grassland Soils. *Journal of Environmental Quality* 38:751-61.
- Wang Z. (2012) Phosphorus Reduction in Runoff Using a Steel Slag Trench Filter System, Oklahoma State University.
- Wang Z., Bell G.E., Penn C.J., Moss J.Q., Payton M.E. (2014) Phosphorus Reduction in Turfgrass Runoff Using a Steel Slag Trench Filter System. *Crop Science*.
- Warren J.G., Penn C.J., McGrath J.M., Sistani K. (2008) The impact of alum addition on organic P transformations in poultry litter and litter-amended soil. *Journal of environmental quality* 37:469-476.

- Watts D.B., Torbert H.A. (2009) Impact of gypsum applied to grass buffer strips on reducing soluble P in surface water runoff. *Journal of environmental quality* 38:1511-1517.
- Withers P.J.A., Abdalla C.W., Dodd A.R. (2005) Strategies for the Sustainable Management of Phosphorus, in: J. T. Sims and A. N. Sharpley (Eds.), *Phosphorus: Agriculture and the Environment*, American Society of Agronomy, Crop Science Society of America, and Soil Science Society of America. pp. 1069-1101.
- Withers P.J.A., Jarvie H.P. (2008) Delivery and cycling of phosphorus in rivers: A review. *Science of The Total Environment* 400:379-395. DOI: <http://dx.doi.org/10.1016/j.scitotenv.2008.08.002>.
- Zhai S., Yang L., Hu W. (2009) Observations of Atmospheric Nitrogen and Phosphorus Deposition During the Period of Algal Bloom Formation in Northern Lake Taihu, China. *Environmental Management* 44:542-551. DOI: 10.1007/s00267-009-9334-4.
- Zhang H., Raun B. (2006) *Oklahoma soil fertility handbook* Department of Plant and Soil Sciences, Oklahoma Agricultural Experiment Station, Oklahoma Cooperative Extension Service, Division of Agricultural Sciences and Natural Resources, Oklahoma State University.

CHAPTER II

PHOSPHORUS REMOVAL STRUCTURES: A MANAGEMENT OPTION FOR LEGACY PHOSPHORUS

Abstract

Reducing dissolved phosphorus (P) loss from soils can reduce the threat of eutrophication, but is not the focus of conventional best management practices (BMPs). Previous research has shown the use of landscape filters filled with materials that have a high affinity for P, i.e. a P removal structure, can reduce transport of dissolved P. The objectives of this study were to use the universal flow-through model to design a P removal structure on a poultry farm to remove 45% of the annual load, construct it, and monitor its removal performance. A treated electric arc furnace (EAF) steel slag was used as the filter media. Inflow and outflow water samples were collected via automatic sampler and tested for dissolved P with a subset tested for heavy metals. With the exception of sulfur, all elements in the tested outflow samples were below EPA drinking water standards. The structure removed 57.5% of the dissolved P in the first 21 mo of monitoring. While the percent removal goal was met, the mass of P removed was less than expected due to overestimation of the annual load of dissolved P produced at the site. The exponential regression of the discrete removal curve (% discrete P removal vs. cumulative P loading to structure) created with flow-weighted removal per event shows good agreement with model predictions. The ability of the model to predict P removal in a field structure help support the validity of the model and this design process.

Introduction

Phosphorus (P) loading is considered a primary contributor to surface water eutrophication (Daroub et al., 2009). Phosphorus moves from soil to surface water as dissolved or particulate P. Particulate P is typically not 100% bioavailable, having to enter solution (through dissolution or desorption) before being available for uptake. On the other hand, transported dissolved P is immediately 100% bioavailable to aquatic biota. In addition, dissolved P can be released over very long periods of time from high P source areas on the landscape even when practices are used to control particulate losses. Therefore, dissolved P is generally considered more problematic for water quality, both due to its immediate impact on the ecosystem and difficulties in controlling its movement.

The term “legacy P” is often used to refer to accumulated P that can serve as a long term source of P to surface waters. Terrestrial P legacies result from past management decisions that lead to high soil P concentrations (Sharpley et al., 2013). Soil P dynamics are such that once soil P concentrations are elevated it can take many years for them to decrease below levels of environmental concern. These high-testing soils are able to release dissolved P for many years, even after all P applications have ceased. Most examples of the slow recovery of terrestrial legacy P is for agricultural settings; however, it is important to note that legacy P can be found anywhere soil P has accumulated including horticultural, residential, and golf course settings. For example, Sharpley et al. (2009) showed that soil Mehlich-3 concentrations only decreased $4.6 \text{ mg kg}^{-1} \text{ yr}^{-1}$ (9.2 lbs ac^{-1}) after eliminating P applications while growing continuous corn. Multiple examples of long-term soil P draw down are provided by Sharpley et al. (2013). As long as soils remain high in soil P concentrations, they can act a source of P to surface waters if there is hydraulic connectivity.

Although current best management practices (BMPs) are effective at reducing the transport of particulate P or direct transfer of applied P, they tend to be mostly ineffective for dissolved P loss

from the terrestrial legacy P pools. This is due to the fact that most BMPs are focused on reducing erosion or placement of fertilizer P below the surface. For example, vegetated buffer strips are a viable BMP for trapping sediment (and therefore particulate P), but those accumulated sediments can potentially increase dissolved P release (Deng et al., 2011). Penn et al. (2012) monitored a 150 acre watershed dominated by a residential neighborhood and found that that there was little to no particulate P while dissolved P concentrations ranged from 0.3 to 1.5 mg L⁻¹ (0.3 to 1.5 ppm). Similarly, if subsurface flow to tile drainage or ditches is the dominant hydrologic process that transports P, then conventional BMPs will do little to reduce dissolved P losses in the short term (Vadas et al., 2007). Other BMPs such as manure transport programs, P draw down by crops, and nutrient management can reduce or prevent soil P from increasing, but as previously mentioned, such BMPs require appreciable time for soil P concentrations to decrease. During that time period, significant amounts of dissolved P can be lost. The temporal disconnect between water quality goals and the length of time that legacy terrestrial P remains a viable source, the difficulty in controlling dissolved P loss from soil, and the immediate bioavailability of dissolved P justify investment in a new BMP for reducing dissolved P transport to surface waters (figure 2.1). The P removal structure is a new BMP that can decrease dissolved P loading in the short term until terrestrial legacy P concentrations decrease below levels of environmental concern. Phosphorus removal structures contain P sorbing materials (PSMs) and can be placed in a location to intercept runoff or subsurface drainage with high dissolved P concentrations. As high P water flows through the PSMs, dissolved P is sorbed onto the materials (typically by ligand exchange or precipitation mechanisms), allowing low P water to continue to the outlet. An example of a P removal structure is shown in figure 2.1. While P removal structures vary in form and appearance they include three common elements: 1) the use of a “filter material” that has a high affinity for P; 2) containment of that material; and 3) the ability to remove that material and replace it after it becomes saturated with P (i.e. when it no longer removes P). Researchers throughout the world have examined various materials that may

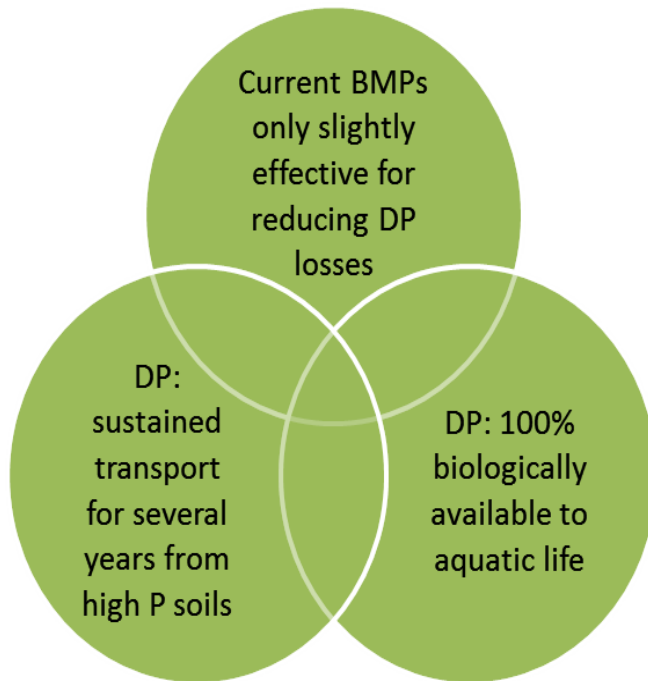


Figure 2.1. Justification for the cost and construction of a phosphorus (P) removal structure (left), and example of a P removal structure in Maryland designed to treat runoff water from a poultry farm as the water drains from a retention pond into a ditch through the filtration material (steel slag; right).

serve as a PSM in this fashion (Claveau-Mallet et al., 2011; Klimeski et al., 2012; Vohla et al., 2011; Lyngsie et al., 2013). While the operational theory of P removal structures is simple, proper design of a structure for specific site conditions and a given “lifetime” is more involved. Here, we provide a case study example of design and construction of a P removal structure for a poultry farm located in Eastern Oklahoma.

Assessment of Site Location

There are three site requirements for construction of a P removal structure:

- Elevated dissolved P concentrations in runoff. For most PSMs, it is generally not worthwhile to construct a P removal structure unless the dissolved P concentrations are greater than 0.2 mg L^{-1} (0.2 ppm). Most PSMs are unable to sorb appreciable amounts of P from low concentration water for prolonged periods due to the equilibrium law (Le Chatlier’s principle), although there are some PSMs capable of this.
- Hydraulic connectivity. In other words, the runoff or subsurface drainage produced at the site must have the potential to reach a surface water body.
- Flow convergence. The potential to channel the runoff water into a single point for treatment is necessary to build an effective filter. This is inherent to a site if there is a drainage ditch, culvert, subsurface drainage outlet, or similar convergence point. Otherwise, the flow must be manipulated so that it will converge into a single point for treatment.

The site used in this case study was a nine acre sub-watershed with several poultry houses (figure 2.2). Poultry litter spillage occurred near the entrance to the houses and the site was hydrologically connected to a nearby creek, located within the Illinois River Watershed. An elevation survey and visual observations during runoff events were used to determine the exact location of the structure (figure 2.2). Starting in September, 2012, grab samples of

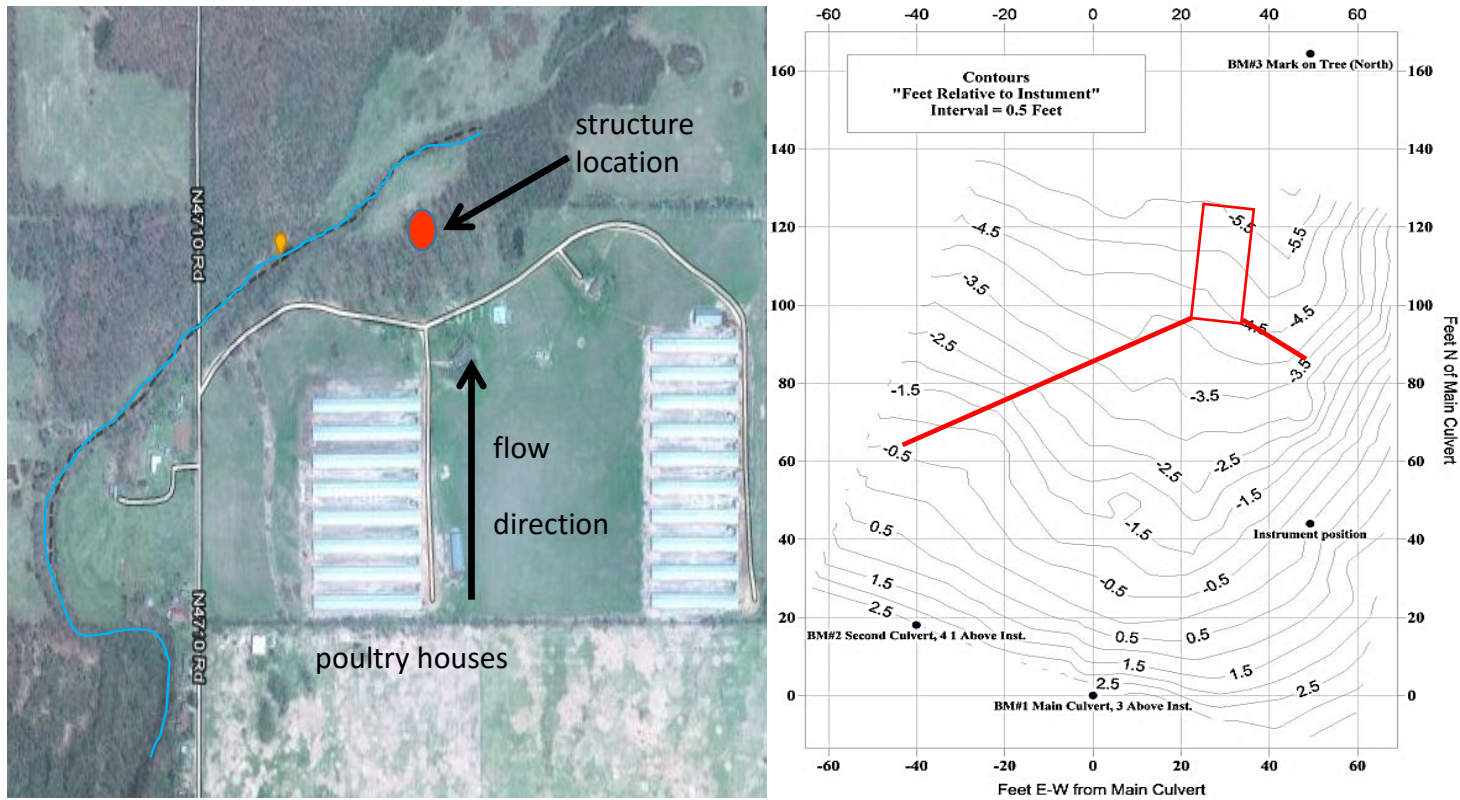


Figure 2.2. Aerial view of the site described in this paper in which the phosphorus (P) removal structure was constructed (left), and contour map showing (in red) the structure location and berms used to converge water into the structure (right).

runoff were taken and analyzed for dissolved P, which consistently showed dissolved P concentrations ranging from 1 to 2 mg L⁻¹ (2 ppm). Therefore, all three site requirements were met for this particular location regarding construction of a P removal structure.

Site Data Collection Required for Structure Design.

In addition to estimates of runoff dissolved P concentrations it was necessary to estimate the following:

- Peak flow rate
- Average annual flow volumes and dissolved P load
- Hydraulic head

The average annual flow volume and peak flow rate was calculated by using site information required for estimating the NRCS curve number (CN). This included soil type (used to determine hydrologic soil group), ground cover, greatest length of flow, and slope. Each parameter, except for soil type and flow length, was determined via site visit. The CN was 78 as the cover was mostly pasture. Curve number was used in conjunction with precipitation depth for the design storm in order to estimate peak runoff flow rate. In our case, we wanted to design the structure for a 2yr-24hr storm, which produces about 10 cm (4 in) of rainfall as estimated by standard USDA-NRCS rainfall tables.

The CN method resulted in an estimated runoff depth of 5 cm (2 in) for this watershed (2yr-24hr storm). Runoff depth was then used to calculate peak flow rate by the Soil-Cover-Complex method and “time of concentration” (USDA-SCS, 1986). The time of concentration was calculated using the CN at 24 minutes and the greatest length of flow was determined to be 331 m (1059 ft). Therefore the predicted peak discharge was calculated as 1.5 m³ min⁻¹ ha·cm⁻¹ (0.9 ft³ s⁻¹ acre·inch⁻¹). Based on the size of the watershed, this was equal to about 27 m³ min⁻¹ (16 ft³ s⁻¹).

Unfortunately, it would require 100 subsurface drainage pipes with 10.16 cm diameter to handle this flow rate, so we chose a more reasonable goal of $2.8 \text{ m}^3 \text{ min}^{-1}$ ($1.6 \text{ ft}^3 \text{ s}^{-1}$).

Annual flow volume is necessary in order to estimate annual dissolved P load. This was achieved by the runoff coefficient method, which was simply based on cover, watershed area, and average annual rainfall depth (USDA-SCS, 1986). For an average annual rainfall depth of 112 cm (44 in), the average annual runoff volume at the site was determined to be 30 cm yr^{-1} (12 in yr^{-1}) or $1.1 \text{ ha} \cdot \text{m}$ ($9 \text{ acre} \cdot \text{ft}$). Using the highest observed dissolved P concentrations for this site (2 mg L^{-1} ; 2 ppm) and average annual runoff volume, the resulting average annual P load was estimated at 22 kg P yr^{-1} (48.5 lbs yr^{-1}).

Hydraulic head is necessary to achieve flow through the P removal structure. Hydraulic head is the elevation difference between the entry point of flow into the structure and the elevation of the water body receiving the discharged water. While this may seem simple, hydraulic head often has to be manipulated in extremely flat landscapes such as those common to coastal plain regions. The site used for this case study had ample topographic relief necessary to generate the required hydraulic head. In order to estimate flow rates through the structure hydraulic head was estimated by the elevation survey (figure 2.2).

Sizing the P Removal Structure

Required Mass of PSM. The necessary mass of PSM was determined from:

- Annual P load
- Typical dissolved P concentration in runoff (or drainage) water to be treated
- P removal goal (i.e. the % of the annual P load that is desired to be removed)
- Characteristics of the locally available PSM

An annual P load of 22 kg (48.5) was calculated in the previous section based on the highest observed dissolved P concentration of 2 mg L^{-1} (2 ppm). The structure was designed to remove

~50% of the load in year one. This removal goal was chosen to limit the size of the structure and subsequent construction costs. Proper design requires development of a “design curve” for the PSM utilized in the structure. A design curve is simply a quantitative description of the relationship between dissolved P loading to the PSM and the % discrete P removal (figure 2.3). This must be determined in a flow-through setting. A batch P sorption experiment will not

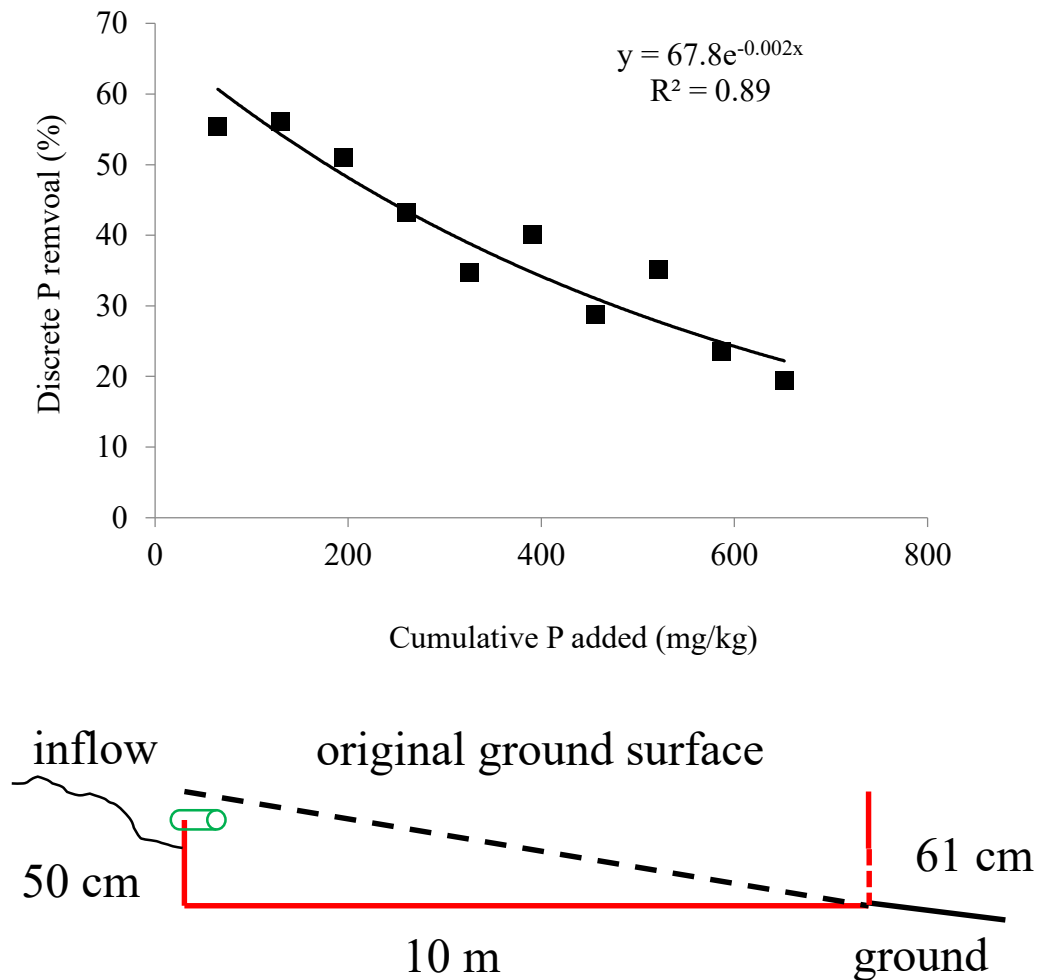


Figure 2.3. Example (upper) of a phosphorus (P) removal curve as determined by a flow-through P sorption experiment conducted on a P sorbing material, and (lower) side cutaway diagram of the P removal structure constructed on a poultry farm.

suffice. A batch sorption experiment in this context is only useful as an index to compare different PSMs, not to quantify how much P they would remove from a flowing solution. Penn

and McGrath (2011) and Stoner et al. (2012) provide examples and discussion of flow-through versus batch P sorption experiments and their utility in determining discrete P removal.

A design curve is specific with regard to the retention time (i.e. contact time) and the inflow P concentration that is moving through the PSM. The design curve in figure 2.3 is specific to an inflow P concentration of 2 mg P L^{-1} (2 ppm) and a retention time of 30 seconds. In other words, it takes 30 seconds for the solution to pass through the PSM. As you would expect, the P sorption is initially very high, but with further P loading the PSM is not able to sorb as much P as it did previously. The shape of the curve varies between PSMs, retention times, and inflow P concentrations. A detailed discussion of design curves is provided by Stoner et al. (2012).

The design curve equation can be solved different ways to provide the desired output. Including:

1. Estimate the lifetime of the structure if a given mass of a specific PSM is to be placed in the structure. In this case, “lifetime” is defined as the amount of time until the P removal structure is no longer able to sorb P that flows into it.
2. Upon integration of the design curve, estimate how much P will be removed by the structure during that lifetime.
3. Upon integration of the design curve, estimate how much of the PSM (i.e. mass) will be necessary to remove a desired amount of P under the condition of the design curve.

An example of how to use design curve equations for proper design is found in Penn et al. (2012) and Stoner et al. (2012). At this particular site we used the design curve to determine the appropriate amount of PSM to achieve the desired P removal (option 3 above). In designing the structure we considered several locally available PSMs. An annual P load of 22 kg (48.5 lbs), inflow P concentration of 2 mg L^{-1} (2 ppm), and the design curve for each potential material were used to estimate the mass required of each material (Table 2.1). Other PSMs may be available in different regions.

Because of the difficulty associated with conducting a flow-through P sorption experiment, a model was developed for predicting the equation of a design curve for a specific PSM under a given retention time, inflow P concentration, and selected PSM characteristics (chemical and physical). This model was developed for the following reasons:

- Conducting a flow-through experiment for every single individual PSM sample and every possible flow condition (i.e. inflow P concentration and retention time) is extremely time consuming and expensive.
- There is variation in P sorption behavior between different PSMs, and among the same type of PSMs that come from different sources and produced at different times.
- It is easier and less expensive to measure certain chemical and physical characteristics of PSMs and then predict a design curve than it is to conduct many flow-through P sorption experiments.

Data from over 1000 flow-through experiments conducted on different PSMs under various conditions was used to develop a model to predict the equation for a design curve unique to any unknown material under given flow conditions. It was determined that among practical retention times for treating runoff and subsurface drainage (from seconds up to 20 minutes), retention time usually has little impact on P removal (Stoner et al., 2012). This is true for materials that dominantly remove P via fast kinetics by Al and Fe sorption (ligand exchange) and for Ca-rich materials that have relatively high pH. For example, flue gas gypsum is an example of a Ca-rich material that is not highly buffered with regard to pH, and therefore the retention time does have a dramatic impact on P removal in a flow-through setting. Gypsum is one of the few materials that display this behavior.

While the details of this model for predicting the design curve will not be discussed here, the design curve is at the heart of the current program being developed, which essentially helps one

to design a site-specific P removal structure in the same manner in which this paper describes.

The design program can be found at www.phrog.okstate.edu.

Orientation of the PSMs. This part of the design is flexible and somewhat unique to the site. While PSMs can be oriented in different ways, the water must flow through the material in an amount of time (i.e. retention time) that is sufficiently short enough to treat most of the water. For example, one may design the water flow from the bottom of the sorption bed upward, laterally, or from the top downward. An advantage to flow design from the top downward is that it is free-draining and avoids saturation with water during non-flow events, avoiding dissolution of P sorbed onto Fe-rich PSMs. Regardless of the water flow direction through the material, flow rate is dependent on hydraulic head, thickness of the PSM layer, and hydraulic conductivity of the PSM. In any of those situations, the standard Darcy Equation can be used to design the structure after you have determined the required mass of PSM, peak design flow rate, and site limitations such as area and slope (i.e. hydraulic head).

Often, the most limiting factor in structure design is hydraulic conductivity of the PSM. The dichotomy is that PSMs which have the best P sorption ability tend to have poor hydraulic conductivity, and PSMs with large hydraulic conductivity have low P sorption ability. Using a material with a low hydraulic conductivity translates to designing a structure that has a larger area, since thickness of the sorption bed must be lower in order to achieve a reasonable flow rate.

Determining the layout of the structure for a particular PSM is a function of the following parameters:

- Required mass of PSM
- Hydraulic conductivity of PSM
- Porosity of PSM
- Bulk density of PSM

- Target peak flow rate for structure
- Maximum area for structure at site
- Maximum hydraulic head at site

Table 2.1 shows potential layouts for several PSMs local to the site. Each scenario can handle our minimum flow rate ($2.8 \text{ m}^3 \text{ min}^{-1}$; $1.6 \text{ ft}^3 \text{ s}^{-1}$).

Table 2.1 clearly shows that PSMs with lower conductivity (WTR, AMDR, and fly ash) tend to have a greater P sorption ability, lower conductivity, and therefore require relatively small amounts of PSM and large area. On the other hand, use of the sieved steel slag also requires a large amount of area, not because of limited hydraulic conductivity, but because of the physical constraint of housing a large mass of material. We utilized treated slag since it was a “happy medium” between the low hydraulic conductivity-high P sorption materials and the high hydraulic conductivity-low P sorption materials such as the sieved steel slag. The suitable layout for each PSM in table 2.1 was estimated using the software developed for designing P removal structures (www.phrog.okstate.edu).

Table 2.1. Required mass, area, and depth of several phosphorus sorbing materials (PSMs) for removing the indicated percent of the year 1 P load (22 kg) and treat the peak flow rate of 2.8 m³ min⁻¹ (1.6 ft³ s⁻¹) on a poultry farm located in Eastern Oklahoma. Calculations made based on respective design curves (figure 2.3) and material and site characteristics. Lifetime indicates the number of years in which the theoretical structure would be able to remove P at this site under current conditions.

| PSM | Mass (Mg) | Cumulative year 1 removal (%) | Lifetime (yrs) | Hydraulic conductivity (cm s ⁻¹) | Area (m ²) | PSM depth (cm) |
|--------------------------|-------------------|-------------------------------|----------------|--|------------------------|----------------|
| WTR* | 7 | 37 | 21 | 0.01 | 286 | 2.3 |
| AMDR† | 4 | 50 | 7 | 0.009 | 225 | 2.2 |
| Fly ash‡ | 3 (plus 95% sand) | 50 | 3.6 | 0.03 (mixed with 95% sand) | 406 | 13 |
| >6.35 cm slag§ | 171 | 21 | 1.4 | 1.0 | 190 | 50 |
| Treated > 6.35 cm slag** | 36 | 45 | 3.5 | 1.0 | 40 | 50 |

*WTR: Water treatment residuals from the AB-Jewel treatment plant located in Tulsa, OK

† AMDR: acid mine drainage residuals from southeast OK

‡ Fly ash from Muskogee, OK, mixed with 95% sand (60 Mg sand)

§ Electric arc furnace steel slag from Ft. Smith, AR (Tube City IMS).

** Steel slag treated for increased P sorption

Site Preparation for Construction of the Structure

Since there was no drainage ditch or subsurface drainage outlet at the site, it was necessary to manipulate flow to converge at a single point. Flow was only somewhat concentrated along the gravel road in front of the poultry houses and on the East-West gravel road. Runoff from the field flowed to the gravel road, which acted as a natural drainage swale. Earthen berms were constructed to direct flow to this swale and then the P removal structure (figure 2.2). Berms were seeded with tall fescue and covered with an erosion control mat.

The foundation for the structure (figure 2.2) was excavated and the material was used for berm construction. We elected to use treated slag screened to greater than 6.35 cm (0.25 in). Using the design curve equation we found that 36 Mg of slag was required. In order to meet desired flow rate of $2.8 \text{ m}^3 \text{ min}^{-1}$ ($1.6 \text{ ft}^3 \text{ s}^{-1}$) the material was arranged to 10 m (33 ft) long by 4 m (13 ft) wide by 0.52 m (20 in) deep. The foundation was made by cutting into the ground on the upslope side, producing a 10 m (33 ft) long flat surface that was 0.52 m (20 in) deep on the upslope side (figure 2.3).

Hydraulic head is critical to force water through the PSMs, which is a function of the slope of the site. As mentioned previously, some sites have very low topographic relief, such as ditch drained fields in coastal plain regions, and therefore hydraulic head must be manipulated. A proven solution to this problem is incorporating flow control structures into filter design to increase hydraulic head, thereby increasing flow rate through the PSM and maintaining a more buffered and constant flow rate.

Construction and Installation of Structure

For this site, a simple bed-style structure where water flows through the PSM from the top into subsurface drainage pipes was utilized. The frame was 6.35 mm (0.25 in) carbon steel and the structure was constructed in modular form for hand assembly in the field.

Figure 2.4a shows the structure from the perspective of the downhill (drainage) side looking up

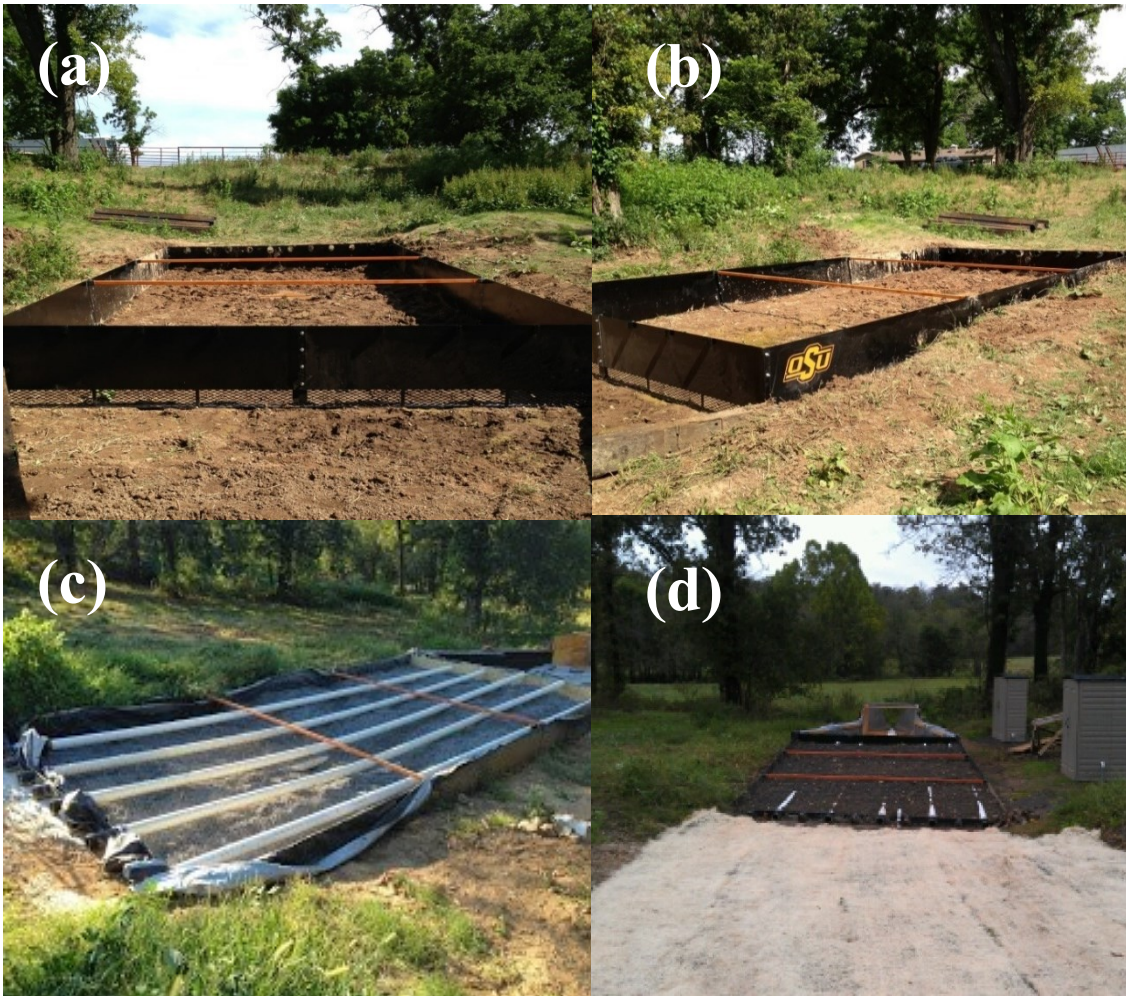


Figure 2.4. The frame of the phosphorus (P) removal structure from the perspective of looking from the downhill (drainage) side toward the uphill (inflow) side (top left), side view (top right), structure partly filled with slag showing the attached inflow perforated pipes (bottom left), and the complete structure from the perspective of looking from the inflow toward the drainage side (bottom right). Note the H flume for monitoring flow rates.

toward the uphill (inflow) side. Runoff enters the structure on the uphill side through four-inch diameter pipes connected to perforated pipes located just below the surface, for the purpose of distributing runoff throughout the entire bed of PSMs (figures 2.4b and c). Note the expanded metal on the drainage side. The deep perforated pipes will drain treated water to the expanded metal, where the water can then exit the structure. The discharge side of the structure was designed to be removed when the PSMs become saturated with P, providing access for a skid-steer to drive in and remove the material. The completed structure is shown in figure 2.4d.

The discharge side is fitted with an H flume for monitoring flow rate. Two automatic samplers were installed to monitor inflow and outflow P concentrations and flow rates. Testing P concentrations alone is not sufficient to completely assess performance of a P removal structure. By also recording flow rates in real time the cumulative volume of water passing through the structure can be calculated along with the total mass or load of P removed by the structure. Ultimately, load reductions are what are required to benefit water quality. An illustration of this principle is described in Sharpley et al. (2013). Briefly, the authors showed that the portion of the watershed that delivered 72% of the P load to the stream had the lowest runoff P concentration while the area that had the highest runoff P concentration delivered only about 1% of the load. This also illustrates why the EPA regulates P loss through “total maximum daily loads” (TMDLs).

The site described in this paper is currently being used, not only as a research site, but also to demonstrate this new tool for controlling dissolved P losses from terrestrial legacy P sources to stakeholders, including state and federal agencies, non-profit organizations, producers, and the general public. There are also similar research and demonstration sites located in ditch-drained fields and poultry farms on the Delmarva Peninsula (Maryland, USA). Demonstrations and field-days will be conducted at these sites for several years. Please contact the authors for more information on future extension activities at these sites.

Structure Monitoring and Data Analysis

Two 6712 ISCO (Teledyne Isco Inc., Lincoln, NE) automatic samplers were used to collect inflow and outflow samples, i.e. treated water, during runoff events. All of the effluent from the structure was channeled into the 0.9 m H flume which was used in conjunction with an ISCO 730 bubbler module to measure flow rate (1 minute intervals). The sampler was programmed to trigger both inflow and outflow sampling when flow through the structure was detected by the

bubbler module. During a flow event, 800 mL samples were taken every 15 minutes, each deposited in an individual bottle. Samples were tested for P using the Murphy-Riley molybdenum blue method on a Spectronic 21D at 880 μ m (Murphy and Riley, 1962). The P removal for each event was calculated as the percentage of the difference between the inflow and outflow P load, where P load is simply concentration times the flow volume. The P load was summed for each 1 minute interval over each flow event. The resulting discrete P removal percentage was plotted versus the cumulative P added to the structure and fitted to an exponential regression equation. Removal predictions were made using a chemical characterization of the treated steel slag input into the universal flow-through model (Stoner et al., 2012).

A randomly selected set of 18 inflow outflow pairs were tested for Na, Ca, Mg, K, S, P, Fe, Zn, Cu, Mn, Al, Ni, B, As, Cd, Cr, Ba, Pb, and Co using inductively coupled argon plasma analyzer (ICP-AES). The concentration change for each pair was calculated with negative changes labelled as sorption events and positive changes labelled as release events. The change in concentration during release events (the portion attributable to the PSM) was compared with EPA drinking water standards (USEPA, 2009).

Performance of the P Removal Structure

During the first 21 mo of monitoring, the P removal structure was subjected to a total of 36 runoff events that triggered sampling (Table 2.2). Precipitation for this period totaled

Table 2.2. Summary of the conditions and performance of the poultry farm phosphorus (P) removal structure during the first 21 mo of monitoring.

| | |
|---|-------|
| Number of runoff events | 36 |
| Maximum flow rate, m ³ min ⁻¹ | 2.60 |
| Maximum P concentration, mg L ⁻¹ | 14.73 |
| Flow weighted P concentration, mg L ⁻¹ | 4.27 |
| Total P input to structure, mg P kg ⁻¹ PSM | 93.5 |
| Total P removed by structure, mg P kg ⁻¹ PSM | 53.8 |

204.6 cm with the largest event, 7.5 cm, occurring on Oct. 10, 2014. The highest flow rate through the structure, $2.60 \text{ m}^3 \text{ min}^{-1}$, was associated with a precipitation event on June 25, 2014 that produced 2.9 cm over the course of 25 min. These findings are in agreement with a previous study and highlight the necessity for structures to be designed to treat the highest flow rates that are likely to occur at a site (Penn and McGrath, 2011). The maximum dissolved P concentration measured in influent was 14.73 mg L^{-1} which was well in excess of the average of 2 mg L^{-1} assumed in the structure design process. However, when the total P load was averaged across all of the flow through the structure (i.e. flow-weighted), it was 4.27 mg L^{-1} which was similar to the grab samples utilized in the design process. The structure removed a total of 53.8 of the $93.5 \text{ mg P kg}^{-1}$ PSM that has entered the structure, i.e. 58% cumulative removal thus far. The cumulative P removal has not decreased to the 45% goal, so the structure will continue to be monitored. Regardless, when normalized for cumulative dissolved P entering the structure, it removed P similar to what was predicted based on the universal flow-through model (figures 2.5 and 2.6).

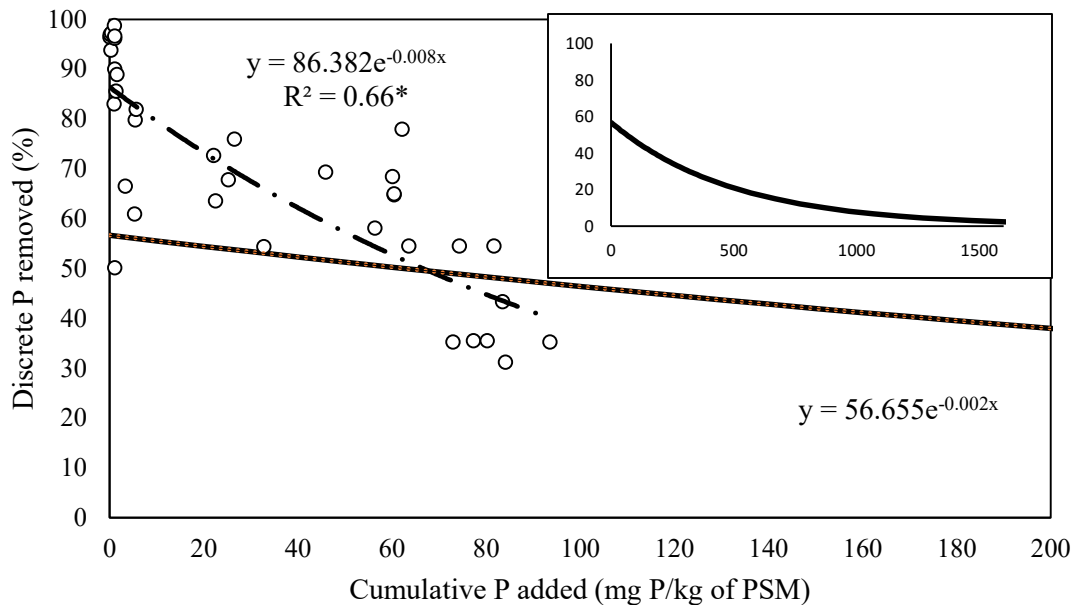


Figure 2.5. Predicted vs measured discrete dissolved phosphorus (P) removal for the poultry farm P removal structure described in this case study. Individual points are the measured discrete P removal from 36 runoff events. The equation and R^2 are shown for the exponential regression of the measured data points depicted as a dashed line. The solid line is the model predicted design curve shown with its equation (full curve shown in inset). *Significant at the 0.05 level.

The estimation of annual runoff volume used in sizing this structure was higher than the actual runoff produced at the site, so the annual P load that entered the structure was much lower than the value used in design of the structure. The smaller annual P load produced means that the structure will chronologically last longer than predicted. This highlights the need for some sort of

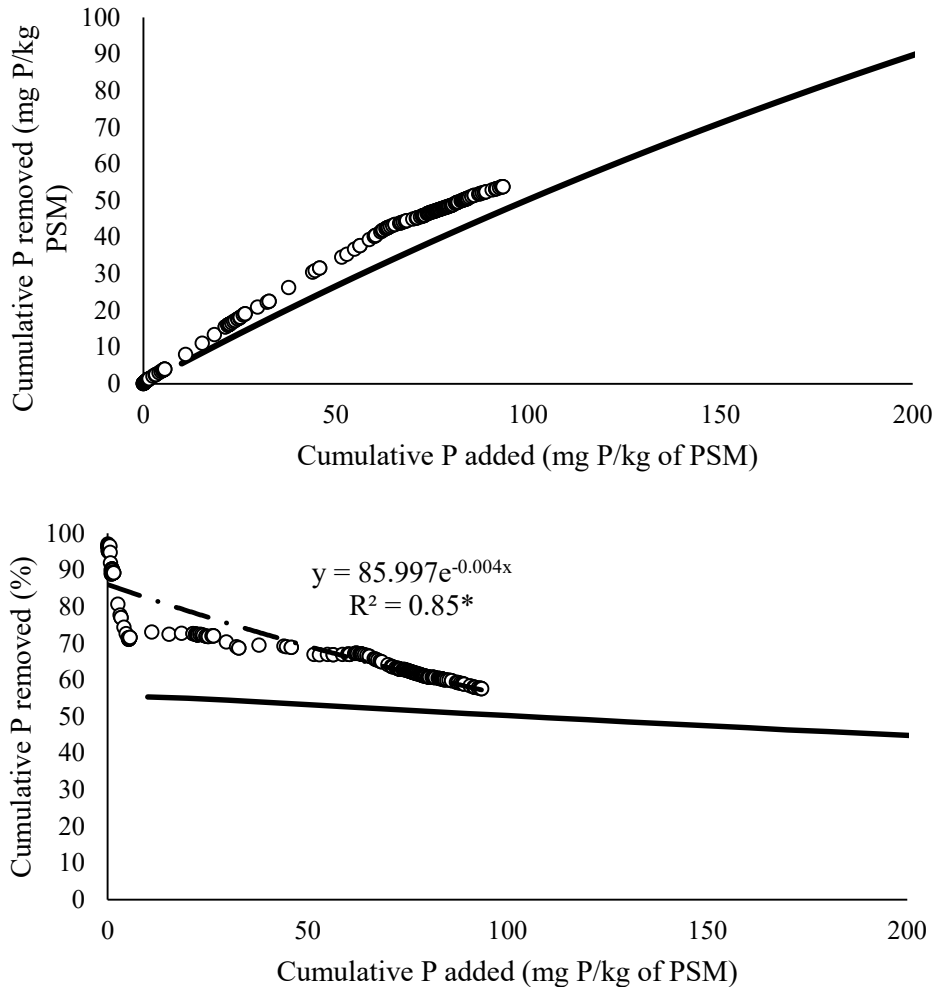


Figure 2.6. Predicted vs measured cumulative dissolved phosphorus (P) removal for the poultry farm P removal structure described in this case study. Individual points are the measured cumulative P removal plotted as mg P removed kg⁻¹ PSM (upper) and as a percentage (lower). The equation and R² are shown for the exponential regression of the measured data points depicted as a dashed line (lower). The solid line is the cumulative removal predicted using the universal flow-through model (upper and lower). *Significant at the 0.05 level.

annual monitoring for these structures to assess performance of the PSM. Constant monitoring is not necessary if the structure was properly built using the model, but an annual grab sample to assess removal coupled with precipitation data for the site could be used to gauge the current

performance of the structure. If the site is an area that is affected by drought then the runoff volume will decrease thereby reducing the load entering the structure. This reduction in load will increase the chronological lifetime of the PSM since it was designed for an average year, for this particular site.

The number of samples per event varied from 1 to 24 pairs, so the discrete P removal and P added to the structure were used to create a flow-weighted average for each event to determine the discrete removal curve (figure 2.5). The universal flow-through model predicted a design curve with a slope of -0.002 and a y-intercept of 56.655 compared with the measured discrete removal curve which had a slope of -0.008 and y-intercept of 86.382. Integration of the predicted and the actual discrete P removal curve results in the cumulative P removal (Stoner et al., 2012). After integrating the design curve produced by the model, the predicted cumulative P removal to date for this structure, was observed to be 49.0 mg P kg⁻¹ PSM, or 52.4%. These predicted values are very similar to the actual cumulative removal of 53.8 mg P kg⁻¹ PSM, or 57.5%. The actual cumulative P removal curves, both as mg P removed kg⁻¹ PSM and as a percentage, show agreement with the model predictions (figure 2.6). The actual cumulative removal, when plotted as cumulative removed (mg P kg⁻¹ PSM) versus cumulative P loading to the structure (mg P kg⁻¹ PSM), followed the same trend as the model prediction, but slightly under predicted P removal.

The structure will outlast the designed chronological lifetime due to an overestimation of the annual P load at the site. However, the model prediction overestimates the cumulative P removal. Assuming the current removal trend and annual P loading rate continue, the structure will reach 45% cumulative P removal at 3.3 yr compared with the model prediction of 4.3 yr. If the model prediction was used to schedule the cleanout of PSM, the actual cumulative removal would be 38% not 45%. This over estimation by the model is due to the shape of the predicted design curve. Instead of being a sharp, exponential decline like the actual removal data, it appears flat,

nearly linear at a cumulative P loading of 200 mg kg^{-1} . The exponential shape of the curve is more evident over a greater cumulative P loading (figure 2.5 inset).

The model under-predicted the y-intercept of the discrete P removal curve (figure 2.5), which is likely an artifact of the flow-through method used to develop the model for materials rich in Fe and Al. The affinity of P for such materials is generally much higher than Ca materials (Stoner et al., 2012). In order to capture the majority of the removal curve within 5 h, the mass of PSM used in each laboratory flow-through experiment was inversely related to its P affinity. The smaller mass of PSM led to a larger P loading ($\text{mg P kg}^{-1} \text{ PSM}$) before the first outflow solution was taken from the flow-through cell, so discrete % P removal was typically much less than 100% for the first sampling point. Having no data points near 100% removal influenced the regression resulting in the model's under estimation of the y-intercept. The universal flow-through model for Al/Fe rich materials could be improved by repeating the flow-through experiments used to develop the model, utilizing a larger mass and greater monitoring period in excess of 5 h, but this would be expensive and time consuming. Instead, the model can be improved by assuming a y-intercept of 95% for the discrete curve with a linear decrease until reaching the first point predicted by the current model. This would result in a closer fit to measured removal data and increased accuracy at lower loading rates. The additional area under the curve due to this change should not have much impact on the cumulative removal curve, since addition of the linear portion to the prediction would cover a small portion of the overall cumulative loading. Regardless of the model under-prediction of the discrete curve y-intercept, the cumulative P removal was well predicted by the model. Ultimately, it is the cumulative prediction of P removal that is the most important, as this is what is used to determine the size of the P removal structure, and also to guide cleanout schedules.

Some of the later runoff events contained samples with almost no P sorption occurring mid-way through the runoff event. The pipes used as a manifold to evenly distribute the influent were

uncovered at that time due to settling of the slag. This allowed a portion of the influent to bypass the media layer and exit the structure untreated. Caps were recently placed on the pipes to ensure this would not occur in the future. This highlights the importance of a design that ensures that the influent makes substantive contact with the media layer prior to exiting,

Effluent Safety

Safety of the effluent is always a concern when using an industrial by-product as a PSM. Of the 18 sample pairs (matched inflow and outflow) tested there were 5 elements that increased in concentration after treatment. Ca was released in all 18 sample pairs which is not surprising given the amount of Ca present in the slag. There were 15 release events involving S with 8 of them exceeding the secondary drinking water standard of $250 \text{ mg L}^{-1} \text{ SO}_4$ which involves taste and odor (USEPA, 2009). Mo was released in 10 events with a maximum difference of 0.06 mg L^{-1} . There were 9 release and 9 sorption events for Ba with the maximum difference of 0.02 mg L^{-1} well below the drinking water standard of 2 mg L^{-1} . Cr was found in 3 sets with 1 sorption event and 2 release events with a maximum release of 0.01 mg L^{-1} which is below the standard for total Cr of 0.1 mg L^{-1} . Ideally there would be no release from the structure, but these concentrations are of no concern.

The use of EPA drinking water standards was chosen as a gauge for safety due to the lack of regulations regarding discharge from these structures. While the effluent is not being directly used as a drinking water source, the structure drains into the Green Creek approximately 1,200 m from the Westville Reservoir. Safety of the PSM and resulting effluent should always be considered when building a P removal structure, but these results, which are similar to a previous study, show that steel slag can be used safely (Penn et al., 2012).

Summary

The P removal structure constructed on a poultry farm was designed using the universal flow-through model to remove 45% of the cumulative P load for 1 y. The annual volume of runoff was estimated using the runoff coefficient method, but the estimate was greater than the actual runoff produced which led to an overestimation of annual P load. Due to this overestimation of the load, the structure has continued to remove dissolved P for a greater time period than predicted.

However, based on the cumulative P load that entered the structure, normalized per unit mass of PSM, the structure is removing P as predicted. The structure was able to remove 57.5% of the P load that entered it over the course of 21 mo. The agreement between the model predictions and actual removal data for this structure even with the differences between expected and measured P concentrations and flow volume, help support the validity of the model and this design process.

Even though the predictions were reasonably close, the model needs to be updated in order to more accurately predict the y-intercept of the discrete P removal curve for Fe and Al materials. In order to predict the actual mass of P removed, the PSM characterization, as well as estimates of annual P load must be accurate.

Widespread Implementation and Future Research

Widespread adoption of P removal structures in the United States will depend on economic viability. For this technology to be economically viable the value of clean water, or conversely the cost of non-point P losses have to be internalized to the end user. To date, even with an increasingly aggressive regulatory approach, the reality is that the cost of non-point pollution is external to the market. For this technology to be sustained there has to be economic incentive for private enterprise to build and maintain the structures. However, it might initially require government investment (e.g. cost-share programs) to initiate widespread implementation of P removal structures. This type of early cost support is typically viewed as a mechanism to offset

risk for early adopters. There are entities such as golf courses, municipalities, or home owners association that are willing to voluntarily bare the cost of P removal structure construction because they place value on reducing P loading, either as a matter of public image or the intrinsic value of clean water. On the other hand, many agricultural producers are less likely to adsorb the cost of P removal structure construction, because of the complete absence of economic incentive and the profit margins in agriculture typically would not support investment in the technology purely for intrinsic value. In either case there is a need for competent and trained individuals to provide the service of design and construction of the structures; such a need would create a market for entrepreneurs.

Beyond initial support from a cost share program, nutrient trading coupled with regulatory limits could eventually provide the economic incentive for construction of structures. For example, the Chesapeake Bay watershed is under a total maximum daily load (TMDL) limit imposed by the USEPA and most Bay states have initiated trading programs. These programs allow nutrient point sources to purchase “credits” from non-point sources to allow for discharge beyond their cap. These programs are thought to allow for future growth. The non-point sources install BMP’s to remove the credited amount of nutrients, plus some efficiency factor to account for uncertainty associated with quantifying nutrient reduction through most non-point BMP’s. For example, a point source might pay for 10 fold more N credits than they will actually be able to discharge. Phosphorus filters provide clear advantages over other types of BMP’s in such cap and trade systems. First they provide more certain and verifiable nutrient load reductions than have been typically associated with BMPs in the past. Nutrient trading is often confounded by the simultaneous implementation of other BMPs that also contribute to nutrient loading reductions, making it difficult to determine whether nutrient loadings were reduced by nutrient trading or by other factors. The concept of additionality has emerged from the environmental economics literature, referring to the additional quantity of nutrient reduction which results from, and only

from, the active presence of nutrient trading. Additionality is an important concept and it is now commonly accepted that additionality should be established before projects are implemented. A desirable feature of P removal structures is that additionality is readily established due to both their operational features and their location. Measurements can be taken at the outlet of the P removal structures to quantify the change in P levels relative to upstream, unfiltered water that might be influenced by other upstream BMPs. It is also expected that the P filtration structure, by providing a transparent accounting of the nutrient reduction, will reduce the risk and uncertainty often associated with the verification of nutrient trading, enabling markets to operate more efficiently.

Future research should focus on examining the economic potential and cost of widespread implementation. While the structure highlighted in this paper utilized a frame made of steel, this is not always necessary and therefore costs could be greatly reduced by using earthen berms or other material. In addition, an assessment of P loading “hot spots” would permit one to target critical areas in order to maximize efficiency and minimize costs, i.e. “precision conservation” (Delgado et al., 2011). Last, there is also a need to further examine beneficial reuse of the spent PSMs.

REFERENCES

- Claveau-Mallet, D., S. Wallace, and Y. Comeau. 2011. Model of phosphorus precipitation and crystal formation in electric arc furnace steel slag filters. *Environmental Science and Technology* 46:1465-1470.
- Daroub S.H., T.A. Lang, O.A. Diaz, and S. Grunwald. 2009. Long-term water quality trends after implementing best management practices in South Florida. *Journal of Environmental Quality* 38:1683–1693
- Delgado, J.A., R. Khosla, and T. Mueller. 2011. Recent advances in precision (target) conservation. *Journal of Soil and Water Conservation*. 66:167-170.
- Deng, N., L. Huaien, and D. Shi. 2011. Preliminary experimental study on effectiveness of vegetative filter strip to pollutants in surface runoff. *Journal of Water Resources Protection*. 3:222-227.
- Klimeski, A., W.J. Chardon, E. Turtola, and R. Uusitalo. 2012. Potential and limitations of phosphate retention media in water protection: A process-based review of laboratory and field-scale tests. *Agricultural and Food Science* 21:206-223.

Lyngsie, G., O.K. Borggaard, and H.C.B. Hansen. 2013. A three-step test of phosphate sorption efficiency of potential agricultural drainage filter materials. *Water Research*. In print.

Online at <http://www.sciencedirect.com/science/article/pii/S0043135413008877>

Murphy J., Riley J.P. (1962) A modified single solution method for the determination of phosphate in natural waters. *Analytica Chimica Acta* 27:31-36. DOI: [http://dx.doi.org/10.1016/S0003-2670\(00\)88444-5](http://dx.doi.org/10.1016/S0003-2670(00)88444-5).

Penn, C.J. and J.M. McGrath. 2011. Predicting phosphorus sorption onto normal and modified slag using a flow-through approach. *Journal of Water Resources Protection*. 3:235-244.

Penn, C.J., J.M. McGrath, E. Rounds, G. Fox, and D. Heeren. 2012. Trapping phosphorus in runoff with a phosphorus removal structure. *Journal of Environmental Quality* 41:672-679.

Sharpley, A.N., H.P. Jarvie, A.Buda, L. May, B. Spears, and P. Kleinman. 2013. Phosphorus legacy: overcoming the effects of past management practices to mitigate future water quality impairment. *Journal of Environmental Quality*. 42(5):1308-1326.

Sharpley, A.N., P.J.A. Kleinman, P. Jordan, L. Bergström, and A.L. Allen. 2009. Evaluating the success of phosphorus management from field to watershed. *Journal of Environmental Quality* 38:1981–1988.

Stoner, D., C.J. Penn, J.M. McGrath, and J.G. Warren. 2012. Phosphorus removal with by-products in a flow-through setting. *Journal of Environmental Quality* 41:654-663.

USDA-SCS, 1986. Urban hydrology for small watersheds. Technical release No. 55, U.S.

Government Printing Office, Washington, D.C.

USEPA. (2009) National Primary Drinking Water Regulations & National Secondary Drinking Water Regulation, in: O. o. Water (Ed.), Environmental Protection Agency, Washington, DC.

Vadas, P.A., M.S. Srinivasan, P.J. Kleinman, J.P. Schmidt, and A.L. Allen. 2007. Hydrology and groundwater nutrient concentrations in a ditch-drained agroecosystem. *Journal of Soil and Water Conservation* 62:178–188.

Vohla, C., M. Koiv, H.J. Bavor, F. Chazarenc, and U. Mander. 2011. Filter materials for phosphorus removal from wastewater in treatment wetlands-a review. *Ecological Engineering*. 37:70-89.

CHAPTER III

VALIDATION OF THE UNIVERSAL FLOW-THROUGH PHOSPHORUS SORPTION MODEL

Abstract

Phosphorus (P) removal structures have been shown to decrease dissolved P loss from agricultural and urban areas which may reduce the threat of eutrophication. In order to design or quantify performance of these structures, the relationship between discrete and cumulative removal with cumulative P loading must be determined, either by individual flow-through experiments or model prediction. The objective of this study was to compare discrete and cumulative P removal curves predicted by the universal flow-through model with measured curves for 14 sets of observations at 3 different experimental scales. The experiments included nine laboratory flow-through experiments, two pilot-scale structure, and three full scale field experiments conducted at two different sites. Materials tested included eight acid mine drainage residuals (AMDRs), electric arc furnace (EAF) steel slag sieved to >0.5 mm and another sieved to >6.35 mm, and a treated EAF steel slag sieved to >6.35 mm. The intercept and slope of predicted P removal curves were compared with the measured curve using a paired t-test. The mean difference was not found to be significantly different from 0 with a p-value of 0.6845 and 0.8567 for the y-intercept and slope, respectively. The ability of the model to predict P removal for various materials, retention times, and P concentrations in both controlled settings and field structures validate its use in design and quantification of these structures. This ability to predict P

sorption without constant monitoring is vital to widespread adoption of P removal structures, especially for meeting discharge regulations and nutrient trading programs.

Introduction

Cultural eutrophication reduces the ability of surface water bodies to provide drinking water, serve as a means of recreation, and sustain a diverse group of organisms (Carpenter et al., 1998). While both nitrogen (N) and phosphorus (P) are required for algae growth, P cannot be fixed from the atmosphere, so P is the most limiting nutrient for eutrophication (Schindler et al., 2008). Phosphorus sources to surface waters include effluent from waste water treatment plants, runoff from agricultural land and urban areas, and domestic septic systems which release both dissolved and particulate P (Carpenter et al., 1998). Agriculture has been identified as a major contributor of P due to mismanagement of nutrients with over application of chemical fertilizer or manure, allowing soil P levels to accumulate beyond plant needs. Soils with high P levels will release small amounts of dissolved P in runoff for years or even decades providing a “legacy” of P that will continue even after adoption of BMPs and cessation of P additions (Sharpley et al., 2013). The dissolved P released from such soils is of relatively low concentration, but it is 100% bioavailable upon reaching an aquatic ecosystem which could result in algae growth.

Conventional BMPs focus on reduction in particulate P through erosion prevention, but do little to reduce transport of dissolved P and can even increase losses of dissolved P (Darch et al., 2015; Sharpley and Smith, 1994). Materials with a high affinity for P have been used to reduce solubility of soil P in efforts to reduce dissolved P transport in runoff, tile drainage, and other effluents (Claveau-Mallet et al., 2013; Gallimore et al., 1999; McDowell et al., 2008; Penn et al., 2011). These P sorbing materials (PSMs) are able to reduce dissolved P concentrations in runoff, but they have a finite ability to sorb P, requiring additional material for continued reductions. In order to facilitate this process, PSMs have been used as a replaceable filter media in large landscape filters, or P removal structures, that were strategically placed in areas receiving runoff with high concentrations of dissolved P (Penn et al., 2014; Penn et al., 2007; Penn et al., 2012). Most PSMs are able to remove P from solution by two main mechanisms: ligand exchange

onto Fe and Al materials and precipitation of Ca phosphates (Karczmarczyk and Bus, 2014; Klimeski et al., 2012; Lyngsie et al., 2015; Stoner et al., 2012). These mechanisms are a function of different chemical characteristics of the PSM and are favored in different solution conditions, which also provide a means of modelling P sorption.

Using a series of flow-through experiments, an individual model was developed for predicting P sorption onto steel slag under various flow conditions, but it was only able to accurately predict sorption for that specific slag sample due to the high spatial and temporal variability in slag produced from steel mills (Penn and McGrath, 2011; Penn et al., 2012; Wang, 2012). The individual model only required the retention time (RT) of the water and the inflow dissolved P concentration, so it was unable to take into account variation in chemical characteristics between slag samples which would affect the ability of the PSM to sorb P. These experiments exposed the need for a universal flow-through model that could be used to predict P sorption for any PSM at a variety of RTs and P concentrations, as a function of PSM properties.

In order to develop this model, fourteen PSMs that included Fe, Al, and Ca materials were characterized both chemically and physically and then subjected to flow-through experiments at 5 different RTs and 5 different P concentrations (Stoner et al., 2012). For each flow-through experiment the discrete P removal, as a percentage, was plotted versus the cumulative loading of P in units of mg of P added per kg of PSM and then fitted with an exponential regression. The resulting curve, referred to hereafter as the “design curve”, quantifies the ability of a PSM to sorb P under those specific conditions and can be used to design a P removal structure to meet specified performance goals (Penn et al., 2014). The design curve is then integrated with respect to P loading in order to calculate cumulative P removal instead of discrete P removal. Chemical characteristics of the twelve PSMs were used, in conjunction with the RT and P concentration, to predict the Y intercept and slope of the design curve. This resulted in two separate models, one for Ca materials and one for Fe and Al materials, that were capable

of estimating the design curves using RT, P concentration, and a variety of chemical characteristics of the PSM (Stoner et al., 2012).

The design curve is integral to one of the most important aspects of designing a P removal structure: determination of the mass of PSM required to meet the user's performance goals, namely the percentage of the annual P load to remove and how long the material lifetime. In order to calculate the mass required three things must be known: the annual load of P that will enter the P removal structure, the P loading of the PSM that occurs at the point in which desired P removal (percentage) is achieved, and the desired number of years before the PSM will be spent (i.e. the intended lifetime; (Penn et al., 2014). Several equations were developed for this process by Stoner et al. (2012) and Penn et al. (2012), and is demonstrated in practice by Penn et al. (2014). This process allows for the structure to be designed to meet certain performance goals unlike previous P removal structures that were designed simply to meet a specific flow rate or to fit in a certain area.

While the design process that was developed allowed a P removal structure to be designed to remove a certain percentage of P over a desired lifetime, fit within a certain area, and be able to handle a specific flow rate, this was a cumbersome process. In order to disseminate this research and facilitate implementation of this BMP, we developed software that utilized the model and incorporated flow calculations to streamline the design process. The Phosphorus Removal Online Guidance (PhROG) software allows the user to design bed and ditch P removal structures or to quantify the performance of existing P removal structures. The user inputs size and flow constraints, removal goals, and characteristics of the PSM into the software which designs a structure that meets those constraints and goals, if possible. The flow characteristics through the PSM and subsurface drainage are calculated using certain assumptions which allow for Darcy flow and Manning's equation to be used. The ability of the PSM to remove P from the water is estimated using the universal flow-through model, so the accuracy of the design or

quantification rests on the accuracy of that model. The model has been used estimate P sorption in a variety of settings at different scales, including laboratory flow-through experiments, pilot-scale structures, and field scale structures. The objective of this study was to compare discrete and cumulative P removal vs. P loading, as predicted by the model, to measured values from a variety of experiments.

Materials and Methods

Chemical Characterization of PSMs

PSMs were analyzed for Na, Ca, Mg, K, S, P, Fe, Zn, Cu, Mn, Al, Ni, B, As, Cd, Cr, Ba, Pb, and Co following acid digestion using a modified EPA Method 3050 with the mass of sample reduced to 0.5g and the resulting solution tested by inductively coupled argon plasma analyzer (ICP-AES) (USEPA, 1996). Samples with particle size greater than 2mm were crushed prior to digestion to ensure a complete digestion, but particles were left whole for the remaining tests to ensure that the exposed portion would be the only portion able to react during testing to more accurately simulate how the material would react in a filter. The amorphous Fe and Al of the materials was extracted using a 0.2 M ammonium oxalate/oxalic acid solution buffered at pH 3. A solid to solution ratio of 1:40 was used with the samples shaken for 2 hours in the dark, centrifuged at 2,000 rpm, and then filtered using Whatman 42 filter papers prior to analysis for Fe, Al, and P using ICP-AES (McKeague and Day, 1966). For each material the pH was measured using a 1:5 solid to deionized water ratio using a meter. The equivalents of acid required to reduce the pH below 6, i.e. the buffer index, was measured using 2 g of sample equilibrated with 10 ml of deionized water for 30 min that was stirred at 0 and 15 min. After 30 min the sample was titrated to an endpoint of 6 using dilute HCl.

Physical Characterization of PSMs

Particle size distribution curves were determined for each PSM using the ASTM D 422 standard method for particle size analysis of soils which utilizes a combination of sieves and a hydrometer method when the particle size was small enough to warrant the hydrometer (Standard, 2007). Samples were submersed in a 5% sodium metaphosphate solution, placed on a shaker table on high for 16 h, poured into 1 L graduated cylinders, and brought to volume with deionized water. Hydrometer readings were taken at 2, 5, 15, 30, 60, 250, and 1440 min using a 152H hydrometer. After the 1440 min reading, the solution was poured onto a #200 sieve, washed using tap water, dried at 105°C, and then passed through a series of sieves ranging from a #10 to a #200 U.S. Standard sieve. The results from both the hydrometer and sieve testing were plotted with the diameter in mm versus the percent finer by mass and then subjected to a second order polynomial regression resulting in the particle distribution curve.

Solution analysis of effluent

All water samples were tested for dissolved P using the Murphy-Riley method and a Spectronic 21D at 880 μm (Murphy and Riley, 1962). When possible, samples were tested the same day as collected, and kept refrigerated at 4° C if testing was delayed.

Regarding effluent safety, eighteen sets of inflow-outflow samples from the poultry farm P removal structure (described below) were randomly chosen for further testing. The subset of the paired inflow and outflow samples were analyzed for Na, Ca, Mg, K, S, P, Fe, Zn, Cu, Mn, Al, Ni, B, As, Cd, Cr, Ba, Pb, and Co using ICP-AES.

Validation Scenarios

Controlled Setting

Laboratory flow-through testing of PSMs

Eight samples of acid mine drainage residuals (AMDR1-8) were obtained from treatment systems located in eastern Oklahoma. One steel slag (Slag1) sample collected from the Tube City IMS steel mill located in Ft. Smith, Arkansas was sieved to >6.35 mm and treated using a patent pending process. Each material was tested for dissolved P removal under flow-through conditions in the laboratory, and then compared to predicted P removal using the PhROG software. The flow-through experiments were completed using a setup previously described by (DeSutter et al., 2006; Lyngsie et al., 2015; Penn and McGrath, 2011; Stoner et al., 2012). A solution made from sodium phosphate and deionized water was made and placed into a 2.5 liter Mariotte bottle that was used to keep a constant head in a 47 mm diameter plastic cell containing the PSM sitting atop a 0.45 μm filter. The mass of PSM varied with the P affinity of that material, so all samples were brought up to 5 g total using acid-washed, lab-grade sand (pure Si sand, 14808-60-7; Arcos Organics, Morris Plains, NJ) to normalize the pore volume. The addition of the sand allowed for different RTs to be achieved by varying the flow rate given that the pore volume of all samples would be the same as 5 g of the sand, 1.26 cm^3 given a 40% porosity. The solution was pulled through the cell at a constant rate using a single channel variable-rate peristaltic pump (VWR variable rate “low flow” and “ultra low flow,” 61161-354 and 54856-070). For each flow-through cell, samples were taken at 0, 30, 60, 90, 120, 150, 180, 210, 240, 270, and 300 min after start of the experiment. The P concentration for each sample was tested and compared with the P concentration of the bottle used to supply the flow-through cell to calculate discrete removal at each sampling event. P loading was calculated using the individual bottle concentration and the flow rate of each peristaltic pump. For these series of experiments conducted on the AMDRs, a

retention time (RT; total pore volume divided by flow rate) of 0.7 minutes was utilized along with an inflow P concentration of 1 mg L⁻¹.

Pond Filter Structure

In order to test PSMs on a larger scale than a laboratory flow-through experiment, a filter was constructed next to a 405m² pond located at the Oklahoma State University Botanical Gardens. Both materials tested in this structure were collected from the Tube City IMS steel mill located in Ft. Smith, Arkansas on two separate occasions. The steel slag sample from one trip (Slag2) was sieved to 6.35 mm (retained) and the other steel slag sample (Slag1) was sieved to 6.35 mm (retained) and then treated. The pond receives runoff and subsurface drainage from adjacent turfgrass research plots which contribute to elevated levels of P within the pond, approximately 0.5 mg L⁻¹. This is the same structure Penn and McGrath (2011) described, but the tank used in their study was replaced with a 1136 L plastic stock tank. The stock tank was filled with PSM, and served as the flow-through cell with a 1/2 horsepower electric pump supplying water from the pond. Inflow pond water was evenly distributed over the PSMs by a manifold made of 1.27 cm diameter PVC pipe. The water was gravity-drained through the PSM layer which exited the stock tank outlet and released back into the pond via hose. The resulting RT for the materials tested under these conditions was approximately 10 min. Controlled by a timer, the pump was turned on for 20 h day⁻¹ with the off time during midday to allow the pump to cool. Inflow and outflow samples were taken 3 times daily coupled with a flow measurement at the outflow.

Field Structures

Golf Course Structure

A field P removal structure was constructed in Stillwater, Oklahoma at an outlet that drains a 63-ha watershed with land uses that consist of undeveloped areas, residential, and a golf

course (Penn et al., 2012). The structure is located in a ditch that drains into Stillwater Creek which is supplied by a culvert which delivers surface runoff, as well as overflow from a nearby pond. As described by Penn et al. (2012), the structure is a 2.4 m wide by 3 m long by 0.2 m deep box made of 6.35 mm thick carbon steel welded and painted in place (2010). A series of perforated PVC pipes were connected to structure inlets to promote even distribution of influent throughout the structure to help reduce uneven consumption of the PSM's sorption ability. Water exits the structure through one 10 cm diameter steel pipe located at the center of the downstream side that is connected a 15.2 cm diameter PVC drainage pipe. Samples were collected using a set of ISCO 6712 (Teledyne Isco Inc., Lincoln, NE) automatic samplers with the inflow samples collected near the culvert prior to entering the structure and outflow samples collected in the drainage pipe (Penn et al., 2012). Flow was monitored using an insert V-notch weir in the drainage pipe and a bubble line connected to an ISCO 730 flow module which took flow measurements every minute. When flow exceeded the programmed threshold it would trigger a sampling event at the outflow and the inflow. The range in dissolved P concentrations in inflow was from 0.25 to 1.5 mg L⁻¹, and the weighted RT was approximately 10 min. The original PSM placed in this structure was 2721 kg of a steel slag (Slag3) with a particle size > 6.35 mm, collected from the Tube City IMS steel mill located in Ft. Smith, Arkansas. After this PSM was no longer effective at removing P, it was replaced with steel slag (Slag4) from the same facility, except that the size fraction used was > 0.5 mm.

Poultry Farm Structure

A P removal structure was constructed at an outlet that drains 3.6 ha of a poultry farm in eastern Oklahoma (Penn et al., 2014). The site is located within the Illinois River Watershed which is designated as a scenic river, as such it is held to a higher standard concerning water quality. A site assessment began with a series of grab samples collected from runoff which were analyzed for dissolved P resulting in P concentrations of 1-2 mg L⁻¹. The annual runoff volume

and the peak flow rate for a 2-year, 24-hour storm was estimated using the Natural Resources Conservation Service curve number (CN), time of concentration, and the Soil-Cover-Complex method (USDA, 1986). The annual volume of runoff was estimated to be $1.11 \times 10^7 \text{ L y}^{-1}$ which makes the annual load of dissolved P leaving the site 22 kg, assuming an average P concentration of 2 mg L^{-1} . The structure was designed using the universal flow-through model with a goal of removing 45% of the annual P load for 1 year and able to handle a maximum flow rate of $2.8 \text{ m}^3 \text{ min}^{-1}$ ($1.6 \text{ ft}^3 \text{ s}^{-1}$) or $1/10^{\text{th}}$ of the estimated peak flow rate from a 2-year, 24-hour storm. The P removal structure was constructed using 6.35 mm painted carbon steel that was modular in design to facilitate transport and assembly on site. In order to house the appropriate mass of PSM needed to meet the performance goals, 36 Mg of a treated steel slag (Slag5) (sieved to achieve $>6.35 \text{ mm}$), the structure needed to be 10 m long by 4 m wide by 0.61 m deep (Penn et al., 2014). Ten 10.16 cm diameter perforated PVC pipes were used as a manifold buried just below the surface of the PSM layer to ensure even distribution of influent with another set of 10 pipes near the bottom of the PSM layer for drainage. Water flows into the upstream side of the structure, down through the PSM layer, into the subsurface drainage pipes, and then exits through an expanded metal grate at the bottom of the downstream side. The effluent then travels through an approach attached to a 0.9144 m H flume that is used, in conjunction with an ISCO 730 bubbler module, to measure flow rate. Two ISCO automatic samplers, housed near the structure in plastic buildings, were used to collect samples from the inflow and outflow, as well as monitor the flow (Penn et al., 2014).

Data analysis and modelling

Discrete P removal (%) was expressed as an exponential curve with discrete removal plotted as a function of the cumulative P added ($\text{mg P kg}^{-1} \text{ PSM}$), x in equation 3.1:

$$\text{Eq. 3.1 } \textit{crete P Removal} (\%) = be^{mx} .$$

Curves depicting actual removal data and curves based on model predictions are referred to as discrete P removal curves and design curves, respectively. The model was produced using data from flow-through experiments conducted on 14 materials at RTs of 0.5, 3, 6, 8, and 10 min and inflow P concentrations of 0.5, 1, 5, 10, and 15 mg L⁻¹ (Stoner et al., 2012). Multiple linear regression (MLR) was performed on the PSM's chemical and physical characteristics to predict the slope and intercept of the discrete removal curves. The PSMs were separated into two groups based on the dominant sorption mechanism, either ligand exchange onto Fe and Al materials or precipitation of Ca-phosphates in Ca materials. While there are two sets of models, one set per mechanism, the basic equation used is the same for both. The slope (m), and the y-intercept (b), of the design curve are predicted using equations 3.2a and 3.2b (Stoner et al., 2012).

$$\text{Eq. 3.2a } \log(-m) = (\alpha RT) + (\beta P) + \chi$$

$$\text{Eq. 3.2b } \log(b) = (\delta RT) + (\epsilon P) + \mu$$

The coefficients, α , β , and χ are predicted based on material chemical characteristics in order to predict the log of the negative slope of the design curve, along with the specified retention time (RT) and inflow P concentration (P). The intercept equation predicts the log of the design curve's y-intercept in the same manner using the prediction coefficients δ , ϵ , and μ . The prediction coefficients differ for the two groups of materials (Fe/Al and Ca) due to the chemical characteristics relevant to their sorption mechanism. The two broad sorption mechanism groups are separated using some of the same characteristics used to predict the coefficients shown in equations 3.2a and 3.2b. In order to be categorized as a Ca material, the PSM must meet 2 of the 3 criteria: the total Ca must be greater than the total Fe + Al, pH >8, and buffer index >0.2. Materials not meeting 2 of the 3 are considered Fe and Al materials with two exceptions, materials that have a pH >8.5 or materials that contain 50 times more Ca than Fe + Al, belong to

the Ca group. The cutoff pH of 8.5 was chosen since ligand exchange is not favored at high pH values due to hydroxyl competition for available sites (Antelo et al., 2005; Essington, 2004).

Within the Ca-P precipitation group, materials are further divided into RT sensitive and non-sensitive materials based on pH and buffer index. For example, certain Ca materials, such as some gypsum samples, have pH values near neutral and low buffer indexes (less than 0.1 eq kg⁻¹) which would not meet 2 of the 3 requirements for a Ca material. However, these poorly buffered Ca materials lack the chemical potential necessary to quickly precipitate Ca-phosphates, so they are considered RT sensitive materials. Unlike Fe and Al materials, P removal of RT sensitive materials are significantly affected by RT with increased time increasing P sorption (Stoner et al., 2012).

The actual coefficient values cannot be listed due to it being proprietary information (patented), but the general effect of chemical characteristics on them can be discussed. The chemical characteristics used to produce the prediction coefficients include: pH, buffer index, amorphous Fe and Al, mean particle size, and total Al, Ca, and Fe. The total amount of an element present is used to determine the availability of that element for sorption. As the element increases, so does the likelihood it will be in contact with the water and sorb P. Amorphous Fe and Al minerals have a large density of terminal hydroxides, the site of ligand exchange, compared to crystalline minerals, so increased amorphous Fe and Al result in increased P affinity. Precipitation of Ca-phosphates is favored in alkaline conditions, so an increased pH and the ability to maintain it, a high buffer index, increase the P sorption potential of Ca materials. The mean particle size of both groups will increase the effectiveness since as particle size decreases surface area to volume ratio increases. A large surface area to volume ratio indicates an increasing contact between the material and solution. All of these characteristics influence the solution conditions and therefore the mechanisms of P sorption, which can alter the shape of the design curve.

After the discrete removal curve or design curve is determined, can be integrated to produce a cumulative P removal curve prior to use in designing or quantifying a P removal structure. Calculation of cumulative P removal (%) at any cumulative P loading (x), is shown in equation 3.3:

$$\text{Eq. 3.3 } \textit{Cumulative P removed (\%)} = \frac{\int_0^x (be^{mx})dx}{x}.$$

Dividing the integrated discrete removal curve or design curve by 100 instead of the cumulative P loading results in the cumulative P removal in mg P kg⁻¹ PSM, as shown in equation 3.4:

$$\text{Eq. 3.4 } \textit{Cumulative P removed (mg kg}^{-1}\text{)} = \frac{\int_0^x (be^{mx})dx}{100}.$$

The loading at which the PSM's cumulative P removal (%) reaches 1%, i.e. when the PSM is spent, can be determined by using the slope and intercept from the discrete removal curve or design curve:

$$\text{Eq. 3.5 } \textit{Maximum P Added (mg kg}^{-1}\text{)} = \frac{\ln(b)}{-m}.$$

Input of the maximum P added into either equation 3.3 or 3.4 will result in the maximum cumulative P removed in percent or mg kg⁻¹, respectively.

For each set of observations in this paper, an exponential regression was performed using on measured removal data, resulting in the discrete removal curve. The discrete curve was used to estimate the maximum P added and produce the cumulative removal curve (both as a percentage and mg kg⁻¹). A chemical and physical characterization of each PSM was input into the previously described universal flow-through model to predict the slope and intercept of the design curve. This design curve was used to estimate the maximum P added and produce the cumulative removal curve (both as a percentage and mg kg⁻¹). Comparisons were made between the slope and intercept of the measured and predicted discrete removal curve, the cumulative removal (both

as a percentage and mg kg^{-1}), and the maximum P loading. For a more detailed discussion of the model development and calculations refer to Stoner et al. (2012).

Statistical analysis

Comparison of the slope and intercepts for the measured discrete P removal_flow-through model was performed using the SAS statistical software package (Institute, 2011). The intercept and slope of the model predicted design curve were compared to the measured discrete P removal curve for each set of observations using a paired t test. The maximum P loading and cumulative P removal estimated using equations 3.3, 3.4, and 3.5 for both the model predicted design curve and the measured discrete removal curve were compared using a paired t test.

Results and Discussion

Overall Design Curve Estimation

Actual P removal data from 14 sets of observations, including laboratory flow-through experiments, the pilot-scale structure, and two field structures, were compared to model predictions of the discrete P removal curve, maximum P loading, and cumulative P removal with the paired t test results shown in Table 3.1. There was no significant difference found between the

Table 3.1. Results from paired t-tests used to compare the predicted and measured values for the y-intercept and slope of the discrete P removal curves, the maximum phosphorus (P) loading when the material is spent, and the maximum cumulative P removal (mg kg^{-1} and %). The actual data was collected from laboratory flow-through experiments, a pilot-scale filter, and two field structures that were not used in creation of the model. $n=14$, $\alpha=0.05$.

| Validation Scenario | P(Difference = 0) | | | |
|---------------------|-------------------|-------------|-----------------------------------|---------------------------------------|
| | Slope | Y-intercept | Max P loading mg kg^{-1} | Max P Removal mg kg^{-1} (%) |
| Overall | 0.8567 | 0.7091 | 0.0484* | 0.1199 (0.7065) |

model predicted slope and y-intercept and the measured values, with a p value of 0.8567 and 0.7091, respectively. The predicted and measured maximum P loading of the PSM was

significantly different at the 0.05 level. This disagreement between the model predicted and actual maximum loading is due to deviation in slope and intercept values for the design curve, particularly for Fe and Al materials. Fortunately, the impact of over prediction of maximum P loading is somewhat minimal since this only effects the predicted lifetime of a P removal structure, at the point at which the PSM is spent. The over predictions in maximum P load can occur due to an under estimation of the slope or overestimation of the y-intercept; an underestimation of the slope has greater impact on deviation of P loading as overestimation of the y-intercept increases. Overestimation of the maximum P loading is evident for AMDR3, 4, 5, 8, and the poultry farm structure in table 3.2 (i.e. only for Al/Fe PSMs), which mostly appears to be due to an underestimation of slope. However, the poultry farm structure is the only case in which the PSM has not been spent, and therefore the values are based on current trends; it is likely that the large difference between measured and predicted maximum P loading will decrease when the data set is completed.

Table 3.2. Model-predicted and measured slope and intercept of the exponential phosphorus (P) removal curve (equation 3.1) for each validation scenario, along with the resulting maximum P loading (mg P kg⁻¹; equation 3.5) at which the material will no longer sorb P. The maximum cumulative P removal is shown as both mg P kg⁻¹ of material and a percentage (equations 3.3 and 3.4).

| Validation Scenario | Material | Predicted | | | | Measured | | | |
|-------------------------|----------|-----------|-------------|-------------------------------|-----------------------------------|----------|-------------|-------------------------------|-----------------------------------|
| | | Slope | Y-intercept | P loading mg kg ⁻¹ | P Removal mg kg ⁻¹ (%) | Slope | Y-intercept | P loading mg kg ⁻¹ | P Removal mg kg ⁻¹ (%) |
| Laboratory flow-through | AMDR1 | -2.0E-04 | 38 | 18189 | 1850 (10.2) | -2.0E-04 | 18 | 14383 | 838 (5.8) |
| Laboratory flow-through | AMDR2 | -1.0E-04 | 36 | 35892 | 3520 (9.8) | -2.0E-04 | 78 | 21807 | 3868 (17.7) |
| Laboratory flow-through | AMDR3 | -4.0E-05 | 23 | 77875 | 5383 (6.9) | -1.0E-04 | 22 | 31132 | 2149 (6.9) |
| Laboratory flow-through | AMDR4 | -5.0E-05 | 49 | 77750 | 9558 (12.3) | -1.0E-04 | 66 | 41833 | 6458 (15.4) |
| Laboratory flow-through | AMDR5 | -5.0E-05 | 28 | 66653 | 5402 (8.1) | -9.0E-05 | 21 | 33968 | 2252 (6.6) |
| Laboratory flow-through | AMDR6 | -2.0E-04 | 40 | 18504 | 1974 (10.7) | -1.0E-04 | 43 | 37608 | 4198 (11.2) |
| Laboratory flow-through | AMDR7 | -9.0E-05 | 37 | 39982 | 3949 (9.9) | -1.0E-04 | 33 | 34851 | 3163 (9.1) |
| Laboratory flow-through | AMDR8 | -3.0E-05 | 20 | 100421 | 6447 (6.4) | -1.0E-04 | 59 | 40837 | 5836 (14.3) |
| Laboratory flow-through | Slag1 | -2.0E-03 | 57 | 2018 | 278 (13.8) | -2.0E-03 | 65 | 2089 | 321 (15.4) |
| Pond filter structure | Slag2 | -2.2E-02 | 93 | 206 | 42 (20.3) | -1.1E-02 | 45 | 347 | 40 (11.6) |
| Pond filter structure | Slag1 | -2.0E-03 | 56 | 2012 | 275 (13.7) | -2.0E-03 | 42 | 1869 | 205 (11.0) |
| Golf course structure | Slag3 | -2.7E-02 | 91 | 167 | 33 (19.9) | -1.4E-02 | 95 | 326 | 67 (20.7) |
| Golf course structure | Slag4 | -1.5E-02 | 80 | 292 | 53 (18.0) | -3.4E-02 | 64 | 122 | 19 (15.2) |
| Poultry farm structure | Slag5 | -2.0E-03 | 57 | 2018 | 278 (13.8) | -1.2E-02 | 89 | 374 | 73 (19.6) |

AMDR: Acid mine drainage residuals (AMDRs)

Slag1 Treated electric arc furnace (EAF) steel slag sieved to >6.35mm

Slag2 EAF steel slag >6.35mm

Slag3 EAF steel slag >6.35mm

Slag4 EAF steel slag >0.5mm

Slag5 Treated EAF steel slag sieved to >6.35mm

The measured and predicted cumulative P removal was not significantly different when considered as a percentage with a p value of 0.7065, but this value decreases 0.1199 for removal in mg kg^{-1} . Since the cumulative removal is calculated using the area under the curve, any deviation from the prediction of the design curve's shape will be more pronounced given that this integration covers the entirety of the curve. At P loading rates less than the maximum, i.e. the x-intercept, the shape of the design curve can be flatter and have a smaller y-intercept than the actual removal curve, yet accurately predict removal. Regardless of the cases where there was deviation in the slope and y-intercept, the area under the curves, and therefore predicted P removal, was not different between measured and predicted values. The use of the model could be restricted to P loadings much less than the x-intercept, so the impact of curve shape would be less pronounced.

The universal flow-through model did a reasonable job of predicting the design curve when compared with actual removal data in a variety of settings with both Fe and Al-based materials and Ca-based materials. The ability to predict the design curve reduces the effort required to design a P removal structure or quantify an existing one by eliminating the need for a flow-through experiment. Each flow-through experiment had a specific RT and P concentration, so to investigate other RTs and P concentrations, the experiment would need to be repeated for each combination. However, by using the model, various scenarios can be easily investigated requiring nothing more than the initial characterization of the PSM and information from the site or conditions in question, since the model takes into account RT and inflow P concentration as input by the user. Accurate prediction of the discrete P removal curve parameters is critical since they are used to calculate P loading at the desired removal goal, or for quantifying current performance of an existing P removal structure.

When designing a structure, the mass of PSM required to meet the desired removal goal is calculated by dividing the annual P loading ($\text{mg P L}^{-1} \text{y}^{-1}$) by the P loading at the desired

cumulative removal goal (mg P kg^{-1} PSM), as estimated from the cumulative P removal curve, and multiplying the result by the desired lifetime (years). The cumulative P removal curve is determined by integration of the predicted discrete P removal curve (i.e. design curve) as described in equations 3.3 and 3.4. For quantification of P removal for an existing structure, the current cumulative P load is input into the design curve equation (equation 3.1) resulting in the current discrete P removal, which is then integrated to determine cumulative P removal. The accuracy for either design or prediction is dependent on the model's ability to predict the equation for the design curve and the quality of the inputs, including the characteristics of PSM, annual flow volume, RT, and average P concentration. Considering variability of climate and P concentration in the three field experiments, the model still provided a good estimate of the design curve.

Example Validation Scenarios

Laboratory Flow-Through

One example of a laboratory flow-through validation scenario is shown in Fig. 3.1. This particular example is for an acid mine drainage residual (AMDR) from northeastern Oklahoma, tested using a P concentration of 1 mg L^{-1} and a RT of 0.71 min. Each point shown on the discrete P removal curve in Fig. 1a represents the percentage of P removed at that sampling time, as a function of the cumulative load of P that has flowed through the PSM. The dashed black line is the exponential regression curve, or experimental discrete P removal curve, which has an intercept of 32.626, slope of -1×10^{-4} , and an R^2 of 0.3797. The solid black line is the design curve estimated using the universal flow-through model which has an intercept of 36.54 and a slope of -9×10^{-5} . The model prediction was close to the actual curve produced by the flow-through experiment, but the R^2 of the experimental discrete removal curve was 0.3797 which was significant at 0.1 level. The sample taken at 240 min after the start of the experiment was

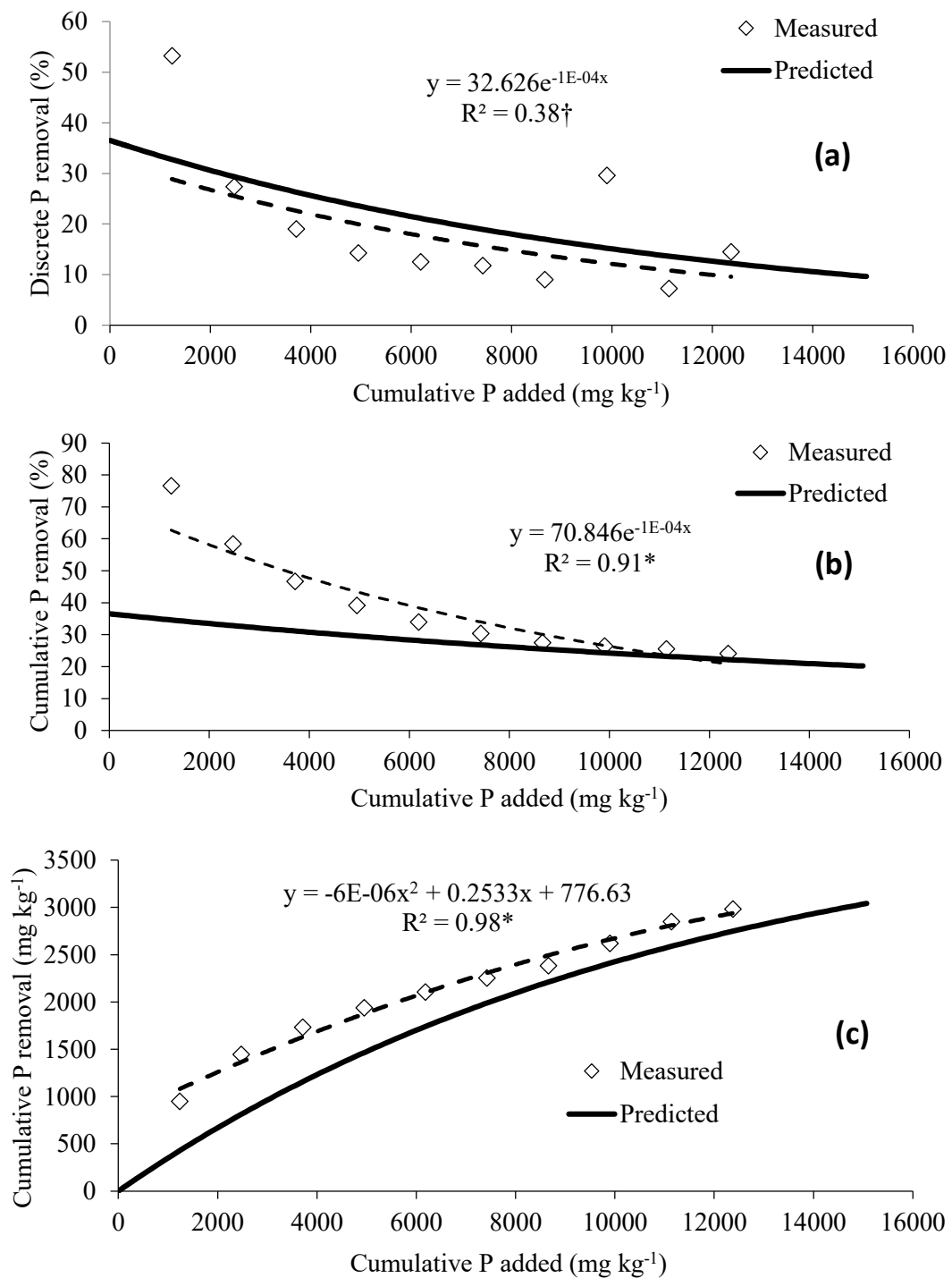


Figure 3.1. Predicted and measured values for phosphorus (P) removal by an acid mine drainage residual (AMDR), as a function of P loading, under laboratory flow-through conditions using a P concentration of 1 mg L⁻¹ and a retention time (RT) of 0.71 min. (a) discrete P removal, (b) cumulative P removal expressed as a %, and (c) cumulative P removal expressed as mg kg⁻¹ PSM. †Significant at the 0.1 level

measured at nearly 30% removal which exceeded the previous and following data point, which is odd. Given its deviation from the overall trend, if this one point was removed then the R^2 would increase to 0.6276 resulting in a much better fit that is significant at the 0.05 level.

While the discrete P removal curve (i.e. design curve) is essential for the design process of a P removal structure, it is not the only means of gauging the ability of a PSM to remove P. Shown in Figure 3.1b and c, the cumulative P removal curve is the cumulative P removed in % and mg P kg^{-1} of PSM, respectively, plotted versus the cumulative P added in mg P kg^{-1} of PSM. The cumulative curve, determined by integration of the discrete P removal curve (equations 3.3 and 3.4), removes some of the noise present in the discrete curve due to the way it is calculated and presented resulting in a clearer picture of the PSM's ability to sorb P. The points pictured in Figure 3.1b and c are data points from the flow-through shown with a second order polynomial regression curve. The figure also shows the predicted cumulative curve produced from the design curve in Fig. 3.1a; the model slightly under predicted the cumulative P removed by the AMDR. In order to obtain an accurate estimation of the performance of a PSM, it is important to consider the entire curve instead of attempting to predict at any given discrete point in time (i.e. loading). Overall the agreement of both curves was adequate for design purposes.

If this curve was to be used in sizing a P removal structure, for a cumulative removal goal of 25% for example, then a value of 25% would need to be entered into the cumulative P removal curve equation (Fig. 3.1b and equation 3.3), which when solved for cumulative P loading (x) will result in the P cumulative loading of the PSM that corresponds with the 25% removal goal. In this case, the P loading at the 25% goal would be $2662 \text{ mg P kg}^{-1} \text{ PSM}$. If this PSM was used to treat runoff from the poultry farm site described earlier, one would simply divide the annual load of 22 kg P by the loading at goal of $2662 \text{ mg P kg}^{-1} \text{ PSM}$, resulting in a required PSM mass of 8,264 kg. This PSM mass of 8,264 kg would achieve a cumulative 25% P removal over 1 y, so if a longer lifetime was desired then then one could multiply this PSM mass by the desired lifetime,

in years. For quantifying an existing structure, the process is simply reversed. The mass of PSM in the structure and the P load that entered the structure is known or estimated, thus simple division of the P load by the PSM mass will determine the current P loading of the PSM. This current loading of the PSM can be entered into the design curve (i.e. discrete P removal) equation (Fig. 3.1a) to determine the current discrete P removal of the structure, and also input into the cumulative P removal curve equation (Fig. 3.1b and c) to estimate the cumulative P removal of the structure, up to that point. The amount of time associated with a specified cumulative or discrete P removal can also be estimated by inserting the discrete or cumulative P removal percentage value of interest into the appropriate curve equation (Figs. 3.1a and b), solving for corresponding P load (x value), and then dividing the product of the PSM mass and P loading by the annual inflow P load. Similarly, the absolute lifetime of the structure (i.e. the point in which no P removal occurs) can be estimated by using equation 3.5, and using the resulting value in the same process. The determination or estimation of the design curve is the most difficult part of the design and quantification process since all sizing and performance calculations that rely on it are relatively straightforward.

Pond Filter Structure

The second example of a validation scenario was an experiment performed at the pond filter structure using a treated EAF steel slag that was sieved to > 6.35 mm (Slag1). The discrete P removal curve is pictured in Fig. 3.2a with individual samples represented by points and a fitted exponential regression curve. The measured discrete P removal curve had a y-intercept of 41.986 and a slope of -0.002, compared to the predicted curve with a y-intercept of 55.95 and a slope of -0.002. The model predicted the exact experimental slope, but the experimental y-intercept was over-predicted by the model. The result of over estimating the y- intercept is apparent in the cumulative removal curves shown in Figs. 3.2b and c. The estimated cumulative removal curve is higher than the measured P removal at around 250 mg P added kg⁻¹ PSM, and remains high. Even

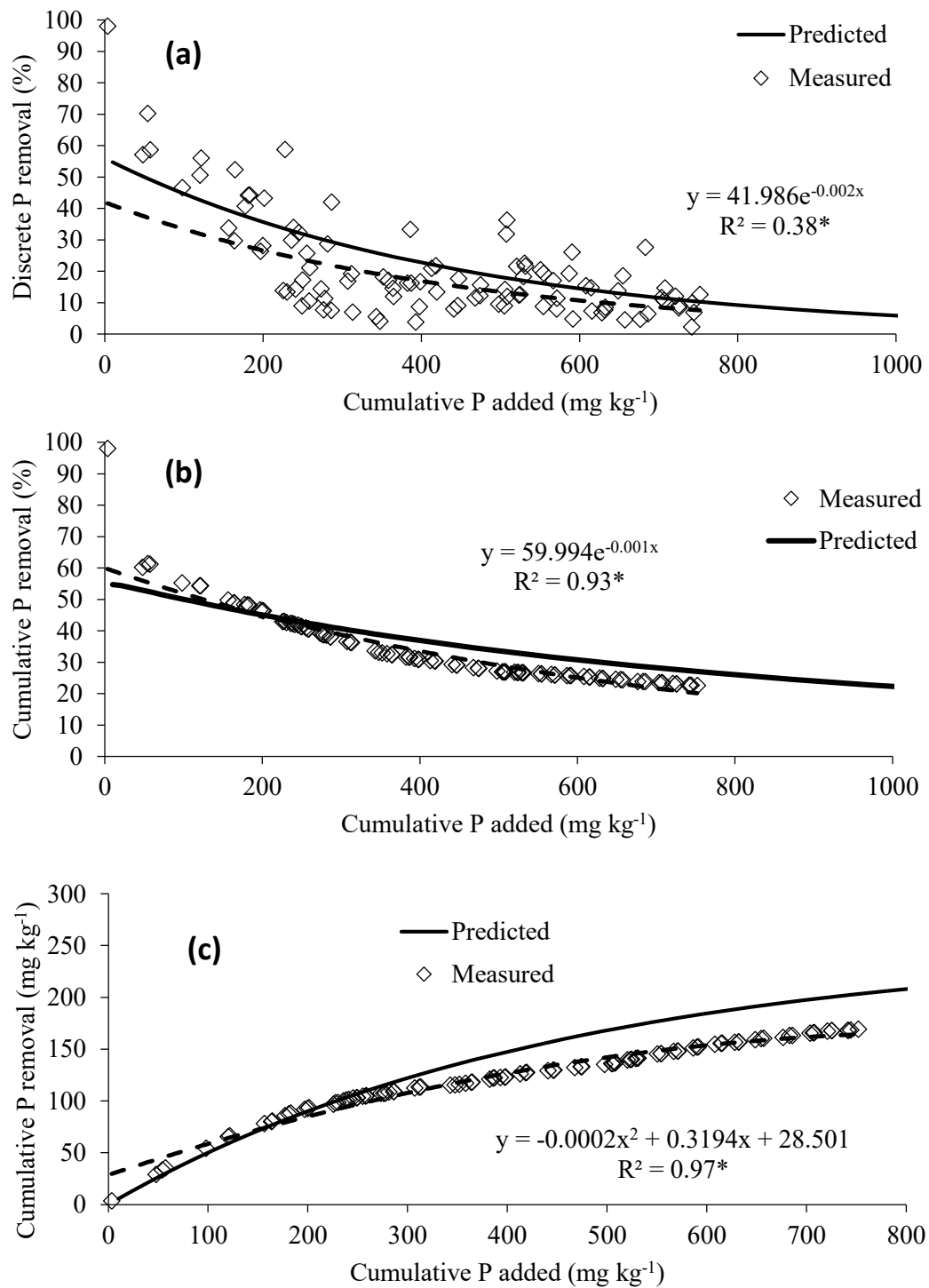


Figure 3.2. Predicted and measured values for phosphorus (P) removal by treated steel slag, as a function of P loading, in a pilot scale flow-through pond filter with a P concentration of 0.5 mg L⁻¹ and a retention time (RT) of 10 min. (a) discrete P removal, (b) cumulative P removal expressed as a %, and (c) cumulative P removal expressed as mg kg⁻¹ PSM.

though the structure removed less P than predicted, the model prediction was close enough to be usable for design purposes since it could provide a relatively accurate estimate of the mass required to meet certain goals. For quantification of an existing structure, model estimation is much less expensive and easier than the continuous monitoring of the structure required to obtain similar data.

Golf Course Structure

The third example validation scenario examines a field structure constructed and monitored at a golf course using an EAF steel slag (Slag3) that was sieved to 6.35 mm and greater, but did not receive the chemical treatment used in the previous example. Inflow and outflow (i.e. treated water) sample pairs were used to calculate the discrete P removal and, in conjunction with flow data, allowed for calculation of P loading (Penn et al., 2012). The discrete removal of the structure was monitored until the PSM was spent; results are shown in Figure 3.3. Unlike the previous two examples which utilized pumps, the flow rate and P concentration input to this structure was variable due to the precipitation and irrigation events which produced the runoff entering the structure. The variability in flow rates led to different RTs throughout the lifetime of the PSM making it more difficult to estimate P removal since RT, an input to the P universal P flow-through model, can have a profound impact on P removal for certain PSMs. The RT input into the model for this structure was 10 min, as determined by calculations based on a flow-weighted average, and also measurements with Rhodamine tracer (Penn et al., 2012). Flow-weighted dissolved P concentration input into the model was 0.69 mg L^{-1} .

The discrete P removal by the structure shows discrepancies from the expected exponential decay seen in more controlled settings, which is likely explained by the differing RTs that occurred for various flow events. The steel slag used in this structure was a Ca based material, therefore removes P by precipitation of Ca-phosphates; this particular material was

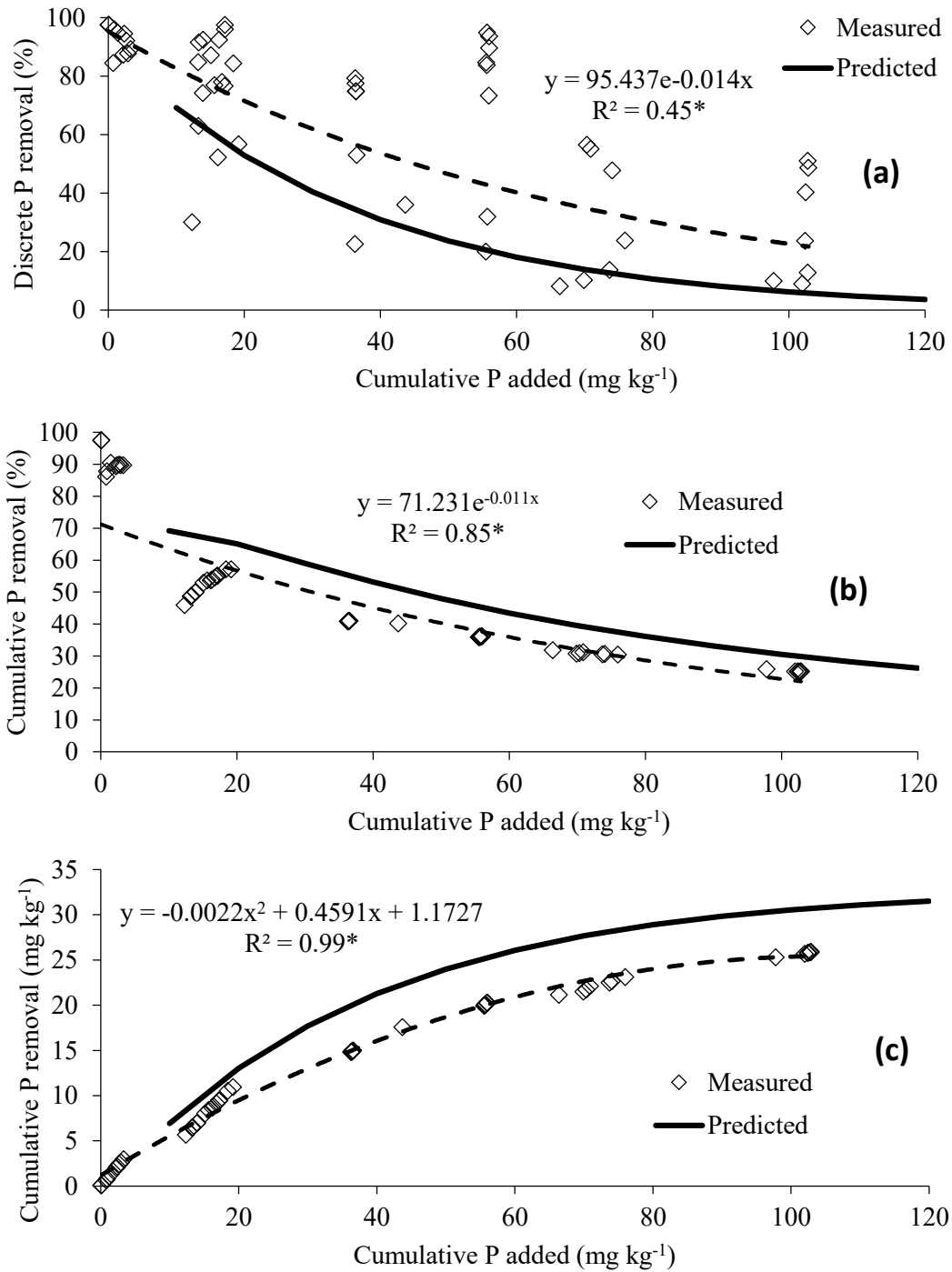


Figure 3.3. Predicted and measured values for phosphorus (P) removal by steel slag (>6.35 mm), as a function of P loading, for a field scale P removal structure located on a golf course. Flow-weighted inflow dissolved P concentration was 0.69 mg L⁻¹ and a weighted retention time (RT) of 10 min. (a) discrete P removal, (b) cumulative P removal expressed as a %, and (c) cumulative P removal expressed as mg kg⁻¹ PSM.

categorized as being sensitive to RT base on chemical characterization. For flow events with low flow rates, the RT of the structure will increase leading to increased sorption for RT-sensitive materials, which explains the sampling events with almost 100% removal halfway through the life of the PSM (Stoner et al., 2012). The measured discrete curve had a slope of -0.014 and y-intercept of 95.437 compared to the model prediction of -0.027 and 90.521 which was close, but lead to an under estimation of the discrete curve. The cumulative removal curve in Fig. 3.3b and c shows an over estimation of cumulative removal. The removal shown in the discrete graph was for each individual event with no distinction given to the flow rate for the event. The events with near 100% removal later in the life of the filter occurred during events with very low flow rates (i.e. long RT), so the portion of the total load removed was small. The cumulative removal curve shows removal as a function of P loading, so the high discrete removal does not impact the curve shape when the flow rate is lower i.e. the cumulative curve somewhat normalizes P removal. The cumulative P removal of the structure was slightly overestimated by the model. The agreement between the model prediction and the experimental data shows the ability of the model to accurately estimate P removal even with the variations in flow and RT, which affected removal. While the universal flow-through model did not exactly predict P removal, it was much improved compared to a previous model developed for and individual steel slag material previously tested (Penn et al., 2012; Wang, 2012).

Effluent Safety

Since industrial by-products are the most common PSMs, effluent safety must be considered. For the Poultry farm structure, a subset of 18 pairs (inflow-outflow) of samples were tested for a variety of elements. The concentration of the outflow was compared to the inflow for each pair with any decrease in the outflow compared to the inflow considered a sorption event and any increase considered a release event. The results shown in Table 3.3 are the five elements that had one or more release events. The number of sorption and release events are shown for

Table 3.3. Influent and effluent water analysis from a subset of 18 random outflow and inflow sample pairs from the poultry farm P removal structure, conducted for safety assessment. All the samples were tested for Na, Ca, Mg, K, S, P, Fe, Zn, Cu, Mn, Al, Ni, B, As, Cd, Cr, Ba, Pb, and Co using inductively coupled plasma atomic emission spectroscopy (ICP-AES). Each pair was compared with the difference between the effluent concentration and influent concentration being reported below as release with the minimum and maximum release shown. Negative values for release indicate a reduction in concentration and are listed as sorption events. Positive values indicate an increase in concentration after passing through the filter and are listed as release events. EPA drinking water standards, both primary and secondary, is shown for comparison.

| | Release Events | Sorption Events | Minimum Release (mg L ⁻¹) | Maximum Release (mg L ⁻¹) | EPA Standard (mg L ⁻¹) |
|----|----------------|-----------------|---|---|--|
| Ca | 18 | 0 | 6.20 | 226 | None |
| S | 15 | 3 | -56.7 | 606 | 250 (SO ₄) |
| Mo | 10 | 2 | -0.03 | 0.06 | None |
| Ba | 9 | 9 | -0.01 | 0.02 | 2.0 |
| Cr | 2 | 1 | -0.01 | 0.01 | 0.1 |

each element, with the majority of the release events from Ca and S, which was not surprising given the high Ca and S of the PSM in question. While there is no standard for Ca in drinking water, the EPA has a secondary standard for sulfate of 250 mg SO₄ L⁻¹, roughly 83.44 mg S L⁻¹, due to taste and odor (USEPA, 2009). The S tested in the water samples was total and no speciation was completed, but given that SO₄ is the most common form of inorganic S found in oxidized soils, it is a safe assumption that most of the S present was SO₄ (Dick et al., 2008). Solution Mo was released in 10 of the 18 pairs, but the maximum difference between the inflow and outflow was relatively low at 0.06 mg L⁻¹ and there is no current EPA standard. There was an even split of sorption and release events for Ba for the 18 sample pairs, but the maximum release event only increased the Ba concentration by 0.02 mg L⁻¹. The EPA drinking water standard for Ba is 2 mg L⁻¹, so the increase due to the filter is not a major safety issue especially since this was still acceptable to use as drinking water. The last element, Cr in excess of 0.1 mg L⁻¹ can cause allergic dermatitis (USEPA, 2009), a painful skin condition, but the highest amount released was 0.01 mg L⁻¹. There were 3 sample pairs with measurable Cr, with 2 of them releasing 0.01 mg L⁻¹ and one of them removing 0.01 mg L⁻¹ that was present in the influent. While the release of any Cr is not ideal, the concentration released by the structure is not high enough to warrant concern.

The elements released were all compared to drinking water standards in order to gauge potential risk, although the effluent was an appreciable distance from a drinking water source. The outflow of the structure is released approximately 100 m from Green Creek and 1,200 m from the Westville Reservoir. While safety must be addressed before an industrial by-product can be used in a P removal structure, this data set along with a previous study which tested effluent for heavy metals over the course of 5 mo, showed that steel slag can potentially be used safely (Penn et al., 2012).

Conclusion

P removal structures have been proven as an effective means of reducing dissolved P loss from sites, but in order to design or quantify their P removal, the PSM's ability to sorb P must be known (Bryant et al., 2012; McDowell et al., 2008; Penn et al., 2007; Penn et al., 2012). The design curve, which is the relationship between the discrete P removal and cumulative P loading to a PSM, is used for designing these structures to meet performance goals or to quantify existing structures. Without accurate design curve predictions, design of a P removal structures to meet performance goals or predict performance of existing structures is not possible without individual flow-through experiments and constant monitoring, respectively. The universal flow-through model predicts the design curve using chemical characteristics of the PSM in question, the P concentration, and the RT of the structure. In order to streamline the design process the model was incorporated into the PhROG software which allows the user to design a structure or predict P removal for an existing structure, by reporting P removal and flow performance. Since prediction of P removal is essential to the proper design or prediction of a P removal structure, the use of the universal flow-through model is critical to the PhROG software. The design curves predicted by the universal flow-through model were not significantly different from the experimentally determined design curves from the 14 sets of observations used in this validation. The model was able to predict curves for a variety of RTs, P concentrations, and PSMs in controlled settings, as well as field structures subjected to variable influent conditions. This validation of the model allows for more confidence in its use as the basis for the PhROG software, but additional work is required. The model needs to be refined to improve design curve predictions, particularly for Fe and Al materials. The ability to predict P removal without constant monitoring makes the P removal structure a viable means of meeting P discharge regulations and could be used in nutrient trading programs.

If P removal structures are going to become widely adopted, the safety of the effluent and disposal of spent material must be considered since many common PSMs are industrial by-products (Klimeski et al., 2012; Stoner et al., 2012). Of the samples tested from the effluent of the poultry farm structure, which utilized a treated steel slag, there were no samples that exceeded the EPA drinking water standards. Disposing of spent PSMs that are industrial by-products is less of a concern since there is a waste stream already in place that should be unaffected. For other spent materials, the part 503 biosolids rule are a good guideline to assess the suitability of land application, but as this BMP becomes more widespread regulations concerning safety should be implemented.

REFERENCES

- Antelo J., Avena M., Fiol S., López R., Arce F. (2005) Effects of pH and ionic strength on the adsorption of phosphate and arsenate at the goethite–water interface. *Journal of Colloid and Interface Science* 285:476-486.
- Bryant R.B., Buda A.R., Kleinman P.J.A., Church C.D., Saporito L.S., Folmar G.J., Bose S., Allen A.L. (2012) Using Flue Gas Desulfurization Gypsum to Remove Dissolved Phosphorus from Agricultural Drainage Waters. *Journal of Environmental Quality* 41:664-671. DOI: 10.2134/jeq2011.0294.
- Carpenter S.R., Caraco N.F., Correll D.L., Howarth R.W., Sharpley A.N., Smith V.H. (1998) Nonpoint Pollution of Surface Waters with Phosphorus and Nitrogen. *Ecological Applications* 8:559-568. DOI: 10.2307/2641247.
- Claveau-Mallet D., Wallace S., Comeau Y. (2011) Model of Phosphorus Precipitation and Crystal Formation in Electric Arc Furnace Steel Slag Filters. *Environmental Science & Technology* 46:1465-1470. DOI: 10.1021/es2024884.
- Claveau-Mallet D., Wallace S., Comeau Y. (2013) Removal of phosphorus, fluoride and metals from a gypsum mining leachate using steel slag filters. *Water Research* 47:1512-1520. DOI: <http://dx.doi.org/10.1016/j.watres.2012.11.048>.
- Darch T., Carswell A., Blackwell M.S.A., Hawkins J.M.B., Haygarth P.M., Chadwick D. (2015) Dissolved Phosphorus Retention in Buffer Strips: Influence of Slope and Soil Type. *Journal of Environmental Quality*. DOI: 10.2134/jeq2014.10.0440.

- DeSutter T.M., Pierzynski G.M., Baker L.R. (2006) Flow-Through and Batch Methods for Determining Calcium-Magnesium and Magnesium-Calcium Selectivity. *Soil Science Society of America Journal* 70:550-554.
- Dick W.A., Kost D., Chen L. (2008) Availability of Sulfur to Crops from Soil and Other Sources, in: J. Jez (Ed.), *Sulfur: A Missing Link between Soils, Crops, and Nutrition*, American Society of Agronomy, Crop Science Society of America, Soil Science Society of America, Madison, WI. pp. 59-82.
- Essington M.E. (2004) *Soil and Water Chemistry: An Integrative Approach*. 1st ed. CRC Press, Boca Raton, Florida.
- Gallimore L.E., Basta N.T., Storm D.E., Payton M.E., Huhnke R.H., Smolen M.D. (1999) Water Treatment Residual to Reduce Nutrients in Surface Runoff from Agricultural Land. *J. Environ. Qual.* 28:1474-1478. DOI: 10.2134/jeq1999.00472425002800050012x.
- Institute S. (2011) *SAS/IML 9.3 User's Guide* SAS Institute.
- Karczmarczyk A., Bus A. (2014) Testing of reactive materials for phosphorus removal from water and wastewater—comparative study. *Annals of Warsaw University of Life Sciences-SGGW. Land Reclamation* 46:57-67.
- Klimeski A., Chardon W.J., Turtola E., Uusitalo R. (2012) Potential and limitations of phosphate retention media in water protection: A process-based review of laboratory and field-scale tests. *Agricultural and Food Science* 21:206-223.
- Lyngsie G., Penn C.J., Pedersen H.L., Borggaard O.K., Hansen H.C. (2015) Modelling of phosphate retention by Ca- and Fe-rich filter materials under flow-through conditions. *Ecological Engineering* 75:93-102.
- McDowell R., Sharpley A., Bourke W. (2008) Treatment of drainage water with industrial by-products to prevent phosphorus loss from tile-drained land. *Journal of environmental quality* 37:1575-1582.

- McKeague J., Day J.H. (1966) Dithionite-and oxalate-extractable Fe and Al as aids in differentiating various classes of soils. *Canadian Journal of Soil Science* 46:13-22.
- Murphy J., Riley J.P. (1962) A modified single solution method for the determination of phosphate in natural waters. *Analytica Chimica Acta* 27:31-36. DOI: [http://dx.doi.org/10.1016/S0003-2670\(00\)88444-5](http://dx.doi.org/10.1016/S0003-2670(00)88444-5).
- Penn C., McGrath J., Bowen J., Wilson S. (2014) Phosphorus removal structures: A management option for legacy phosphorus. *Journal of Soil and Water Conservation* 69:51A-56A.
- Penn C.J., Bryant R.B., Callahan M.P., McGrath J.M. (2011) Use of Industrial By-products to Sorb and Retain Phosphorus. *Communications in Soil Science and Plant Analysis* 42:633-644. DOI: 10.1080/00103624.2011.550374.
- Penn C.J., Bryant R.B., Kleinman P.J.A., Allen A.L. (2007) Removing dissolved phosphorus from drainage ditch water with phosphorus sorbing materials. *Journal of Soil and Water Conservation* 62:269-276.
- Penn C.J., McGrath J.M. (2011) Predicting Phosphorus Sorption onto Steel Slag Using a Flow-through approach with Application to a Pilot Scale System. *Journal of Water Resource and Protection* 03:235-244.
- Penn C.J., McGrath J.M., Rounds E., Fox G., Heeren D. (2012) Trapping Phosphorus in Runoff with a Phosphorus Removal Structure. *J. Environ. Qual.* 41:672-679. DOI: 10.2134/jeq2011.0045.
- Schindler D.W., Hecky R.E., Findlay D.L., Stainton M.P., Parker B.R., Paterson M.J., Beaty K.G., Lyng M., Kasian S.E. (2008) Eutrophication of lakes cannot be controlled by reducing nitrogen input: Results of a 37-year whole-ecosystem experiment. *Proceedings of the National Academy of Sciences of the United States of America* 105:11254-11258. DOI: 10.1073/pnas.0805108105.

- Sharpley A., Jarvie H.P., Buda A., May L., Spears B., Kleinman P. (2013) Phosphorus Legacy: Overcoming the Effects of Past Management Practices to Mitigate Future Water Quality Impairment. *J. Environ. Qual.* 42:1308-1326. DOI: 10.2134/jeq2013.03.0098.
- Sharpley A.N., Smith S. (1994) Wheat tillage and water quality in the Southern Plains. *Soil and Tillage Research* 30:33-48.
- Standard A. (2007) D422–63 (2007) Standard test method for particle-size analysis of soils. ASTM International, West Conshohocken. doi 10:1520.
- Stoner D., Penn C., McGrath J., Warren J. (2012) Phosphorus Removal with By-Products in a Flow-Through Setting. *J. Environ. Qual.* 41:654-663. DOI: 10.2134/jeq2011.0049.
- USDA S. (1986) Urban hydrology for small watersheds. Technical release 55:2-6.
- USEPA. (1996) Method 3050B Acid Digestion of Sediments, Sludges, and Soils, Environmental Protection Agency.
- USEPA. (2009) National Primary Drinking Water Regulations & National Secondary Drinking Water Regulation, in: O. o. Water (Ed.), Environmental Protection Agency, Washington, DC.
- Wang Z. (2012) Phosphorus Reduction in Runoff Using a Steel Slag Trench Filter System, Oklahoma State University.

CHAPTER IV

HANDBOOK FOR THE PHOSPHORUS REMOVAL ONLINE GUIDANCE (PHROG)

DESIGN SOFTWARE

Abstract

Excess phosphorus (P) in waterways leads to eutrophication reducing water quality. Conventional best management practices (BMPs) reduce particulate P loss, but do little for dissolved P loss. The transport of dissolved P in runoff and tile drain effluent can be reduced by construction of landscape filters that use P sorption materials (PSMs). In order for P removal structures to handle the incoming water at the site, meet desired removal goals (P removal and lifetime), and continue functioning for a reasonable amount of time, they must be specifically designed for each individual location and PSM. The design process requires characterization of the site regarding flow and P loading, the discrete P removal curve (% P removal as a function of cumulative P loading) to be measured or estimated (via universal flow-through model) for the PSM of interest, and the ability to calculate flow through the structure. In order to streamline the design process, the universal flow-through model, along with certain flow calculations, were incorporated into design software. Phosphorus Removal Online Guidance (PhROG) was developed using Mathematica programming software, resulting in a user-friendly interface. PhROG allows the user to easily design P removal structures, both for a bed or ditch, or to quantify the performance of an existing structure using characteristics of the site and the PSM of their choice. Required software inputs, explanation of site and PSM characterization, description of how the software

operates, and illustration of several structure design scenarios are highlighted. Years of experience building structures and conducting research have been condensed into PhROG, resulting in a straightforward tool that makes designing and quantifying P removal structures a simple process.

Introduction

Water quantity and quality is an issue that will become increasingly important with rising population and climate change (Schewe et al., 2014). Of the 42,458 waterways that are sufficiently impaired to be listed on the United States Environmental Protection Agency's (USEPA) 303(d) list, nutrients are the cause of 7,705 water bodies (USEPA, 2011). Excess nutrients introduced into a water body leads to an increase in primary producer growth, typically algae, which interferes with water treatment facilities, overall decreased biodiversity, illness in humans and animals, and decreased dissolved oxygen leading to fish kills (Carpenter et al., 1998; Codd, 2000; Dodds, 2002). The two primary nutrients associated with eutrophication are nitrogen and phosphorus (P), but with no atmospheric source of P it is the most limiting nutrient in freshwater. Nitrogen is mobile within soil and can be lost through volatilization unlike P which is relatively immobile, so P loss can be harder to control using conventional best management practices (BMPs). (Tisdale et al., 1993). Phosphorus loss from a site is either dissolved P which is bioavailable or particulate P which may desorb from the sediment carrying it or may even sorb more P depending on conditions. There is an inherent lag time between adoption of BMPs concerning P and reductions in P lost from a site, especially in soils that are built up with P which creates a "legacy" source of P that can be a problem for years to come. These high P soils will release dissolved P for years or even to decades to come (Sharpley et al., 2013). Conventional BMPs focus on proper fertilizer additions and techniques that prevent a site from becoming built up with excess P and from losses. This is primarily achieved through prevention of runoff losses after P application and also prevention of erosion of soil particles which, most likely, have P attached to them (Sharpley et al., 2000). One BMP for sites that already have excessive soil P include phytoremediation which uses plants to uptake the nutrient followed by biomass removal, thereby reducing the soil P at that location. "Mining" the phosphorous with plants can achieve lower P values in the soil, but it will take many years (Kratovich et al., 2006). Another BMP for

reducing P losses from high P soils is the addition of soil amendments to bind P and reduce solubility, which reduces the loss of dissolved P (Delorme et al., 2000; Fenton et al., 2012; Gallimore et al., 1999; Gotcher et al., 2014). Addition of soil amendments that tie up P will reduce the amount of dissolved P leaving a site, but material will need to continue to be added to maintain low dissolved P concentrations in runoff (Penn and Bryant, 2006). Even if P sorbing materials (PSMs) are added to a soil for reducing the solubility of P, such P is still present within the watershed, and may still be transported in particulate form or solubility may increase as chemical conditions change.

As an alternative, a P removal structure can be placed in a ditch, tile drain outlet, or some other type of hydraulically active area to capture overland flow from an agricultural field or urban area. A P removal structure is essentially a landscape-scale filter that contains a PSM, which sorbs P from passing water thereby immobilizing it within the structure. The structure is constructed in such a manner that the PSM can be removed and replaced after it is no longer able to remove P from passing water (Penn et al., 2007). The replacement of the spent PSM allows P to be truly removed from the site, rather than temporarily reducing the solubility. All P removal structures share three components: the filter utilizes a solid material that has an affinity for P (a PSM), the PSM is contained within the structure, and the PSM can be removed and replaced when it is saturated with P, but their form can vary greatly (Penn et al., 2014). The P Removal Online Guidance (PhROG) software was developed to help the user design a P removal structure with specific goals for P removal and lifetime of the structure, or to quantify how much P a current structure will remove and how long it will last. This document was written to help guide the user through the required inputs for the software, how to obtain the required inputs for site and PSM characterization, illustrate the interactions between input and output variables, and communicate common pitfalls to avoid when designing a structure.

Design Curve

The first step to designing a P removal structure is to estimate how much P a material (i.e. PSM) will be able to remove from the water. While P batch isotherms are easier and less expensive to complete than conducting a flow-through sorption experiment, it does not accurately simulate the real world conditions of a filter which will be subject to continuous additions of P rich water during runoff events, the removal of reaction products, and limited contact time. The differences in P sorption between a batch test and a flow-through can be significant due to the inherent differences in the time of contact between the material and the solution and the continuous addition of a constant P concentration, which is low compared to traditional methods for batch isotherms (Penn and McGrath, 2011). In order to accurately estimate the amount of P a filter can sorb, the test conditions need to be as close to those in the field; a design curve must be determined either directly through a flow-through experiment or estimated through a model. A design curve is simply a mathematical relationship that quantifies the change in P sorption onto a PSM with cumulative P loading of the material, under specific conditions of contact time (retention time) and inflow dissolved P concentration (Fig. 4.1). Simply put, the design curve is an essential tool for properly designing a P removal structure for a particular location.

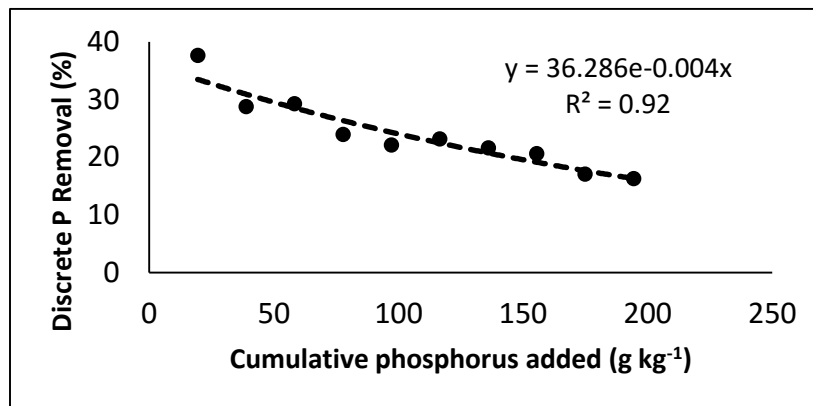


Figure 4.1 Data from a flow through of a treated EAF steel slag at a retention time of 0.71 min and a P concentration of 1 mg L⁻¹ are shown with the discrete P removal percentage plotted versus the mg of cumulative P added per kg of material. The equation and r-squared are shown for an exponential regression.

Sizing a filter using the design curve

One of the main variables controlling the size of a P removal structure is the mass of PSM required to meet performance goals, which can be calculated using the design curve. Several factors must be known in order to calculate PSM mass and the structure in general, including the equation for design curve specific to the PSM, inflow dissolved P concentration, retention time, cumulative P removal goal, desired lifetime of the filter, and the annual P load. The design curve, or a discrete removal curve like the one shown in Fig. 4.1, have to be integrated prior to being used to estimate the mass of PSM required for a P removal structure. Once integrated the cumulative P removal curve, as shown in Fig. 4.2, is the cumulative percent of P removed plotted versus the cumulative P added to the PSM. Once one has a removal goal chosen, such as 50%, input that into the cumulative curve and solve for x. The result, 435, is the cumulative P load at which the removal goal is met. The inflow dissolved P concentration and the desired retention time indirectly impact the design (or performance) of a P removal structure because these two variables directly dictate the shape of the design curve. All of these factors must be input into PhROG in order to make a proper design or to predict the performance of an existing structure.

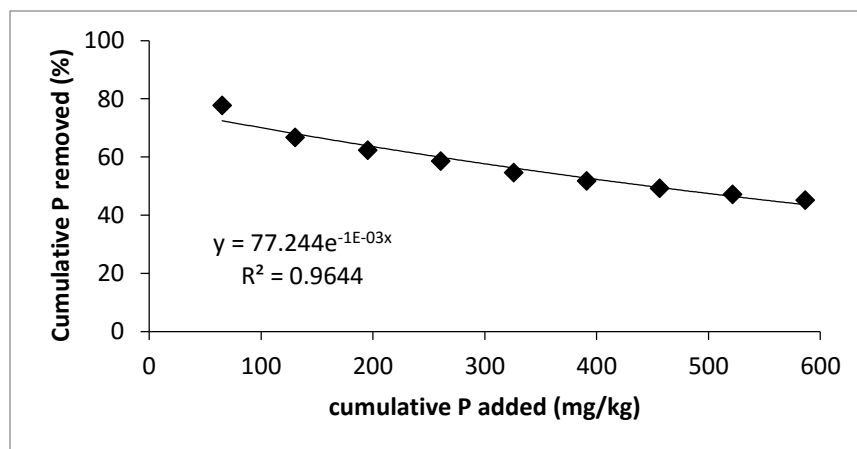


Figure 4.2 The discrete P removal curve of a treated EAF steel slag at a retention time of 0.28 min and a P concentration of 1 mg L^{-1} was integrated resulting in the cumulative P removal curve shown here. The cumulative P removal as a percentage is plotted versus the cumulative P additions in mg kg^{-1} of slag. The equation and r-squared are shown for an exponential regression.

The annual P load is calculated by multiplying the average dissolved P concentration by the annual flow volume, which can be estimated using Rational Runoff method, produced at that site resulting in a mass of dissolved P that will pass through that outlet each year (Eq. 4.1). The

$$\text{Eq.4.1 Annual P Load} = \text{Annual Flow Volume}(L) * \text{Average Dissolved P}(mg L^{-1})$$

annual P load can be calculated if the P loading in mass of P per unit area and the contributing area are known (Eq. 4.2). If the average dissolved P concentration is known, then the result from

$$\text{Eq. 4.2 Annual P Load} = P \text{ Loading}(\text{mass P area}^{-1}) * \text{Contributing Area}$$

Equation 4.2 can be used to estimate the annual flow volume (Eq. 4.3). Once the annual P load is

$$\text{Eq. 4.3 Annual Flow Volume}(L) = \text{Annual P Load}(mg) / \text{Average Dissolved P}(mg L^{-1})$$

estimated, the desired percentage of that load to be removed by the filter and the lifetime of the filter need to be decided upon. The removal goal, lifetime, and size of the filter are connected since removing more P or increasing the time between cleanouts (the lifetime of the material) will increase the mass required and subsequent size of the filter. If the size of the filter is a concern due to limited space, then the lifetime or removal goal could be reduced. The cumulative P loading to the PSM that will occur at the time of reaching the desired cumulative P removal (i.e. desired lifetime) can be calculated using equation 4.4 shown below:

$$\text{Eq. 4.4 Cumulative P load} = (-b - \text{goal} * \text{ProductLog}[(-b) / (e^{\frac{b}{\text{goal}}} * \text{goal})]) / (m * \text{goal}).$$

Where Cumulative P load is in units of mg P kg⁻¹ PSM, “goal” is the desired cumulative P removal (%), over the desired lifetime, “b” and “m” are the slope and intercept of the design curve, respectively (Fig. 4.1). The cumulative P load to the PSM calculated from equation 4.1 can then be used in equation 4.5 in order to estimate the required mass of PSM:

$$\text{Eq. 4.5 Mass of PSM} = \frac{(\text{desired lifetime} * \text{annual P load})}{\text{cumulative P load}}.$$

Where “mass of PSM” is in kg, “desired lifetime” is the desired lifetime of the structure in yrs, “annual P load” (mg) is determined from equation 4.4. Since the mass of PSM required is a function of the PSM’s affinity for dissolved P, site hydrology, and desired performance goals, these calculations have to be re-calculated if any of those three variables change. The PhROG software performs most of these calculations for the user, allowing them to simulate a variety of scenarios, such as using different PSMs or altering performance goals.

Estimating the equation for a design curve

Measuring a design curve directly requires conducting a flow-through experiment which is relatively straight forward, but does require a peristaltic pump, flow-through cell, and P source. The P solution is stored in a Mariotte bottle that utilizes atmospheric pressure to maintain a constant head in the cell holding the material sample while a peristaltic pump pulls the solution through the cell at a constant flow rate as shown in Fig. 4.3 (DeSutter et al., 2006; Lyngsie et al., 2015; Stoner et al., 2012). Outflow solution samples (i.e. treated water) are taken at known time increments and analyzed for dissolved P, which is then used to calculate discrete P removal by knowing the inflow P concentration, flow rate, and timing of sampling. This information is used with the mass of PSM utilized in the experiment in order to calculate cumulative P loading.

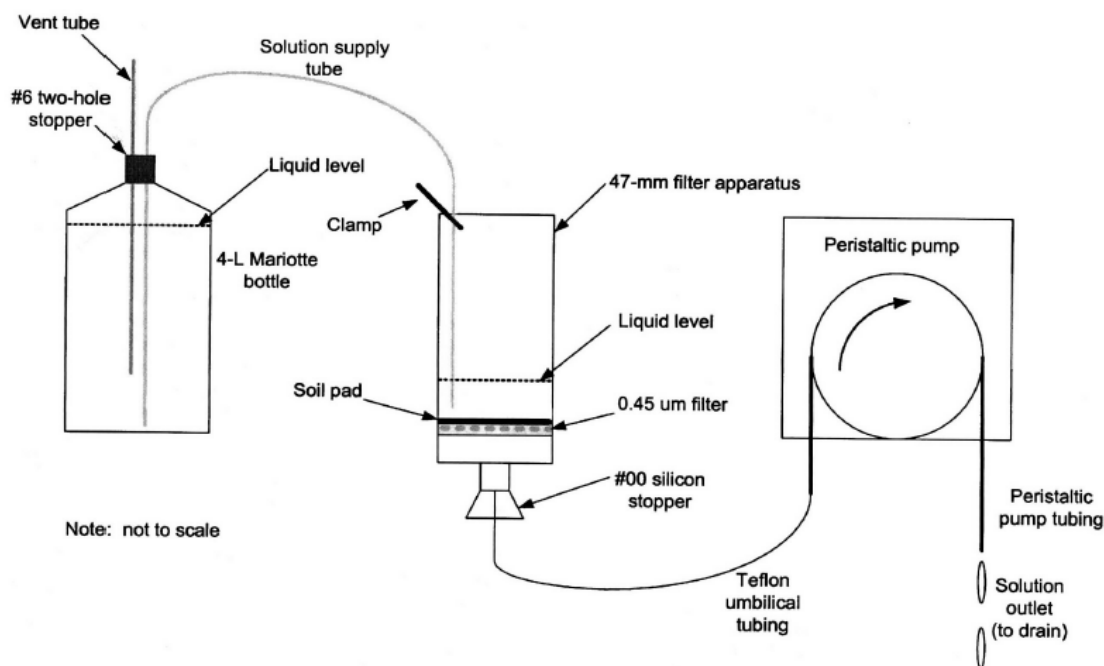


Figure 2.3. The flow-through set up is shown with the Mariotte bottle holding the P solution which supplies the cell containing the P sorbing material of known mass. The flow rate is maintained by a peristaltic pump which draws the solution through the cell. Diagram source: DeSutter et al. 2006.

The flow rate of the solution will change the retention time which can have an impact on the sorption capability of the PSM, depending on the chemical characteristics of the PSM (Stoner et al., 2012). Retention time is estimated by:

$$\text{Eq. 4.6 Retention time} = \frac{\text{pore volume}}{\text{flow rate}}$$

Essentially, the retention time is the time required for the inflow solution to pass through the PSM. If a material is sensitive to retention time, then an increase in retention time will increase P removal.

The concentration of P in the solution can also impact the sorption capability of the material with a certain baseline concentration required to drive the reaction, known as the equilibrium P concentration (Froelich, 1988). In general, a higher dissolved P concentration will promote more efficient P sorption compared to lower concentrations. Given the variability of

sorption, it is important that the P concentration and retention time used in the flow-through experiments are similar to actual field conditions in order to correctly design the size of the filter to meet the user's goals.

To estimate the design curve without the need to execute a flow-through experiment, a model was developed that correlated certain chemical characteristics of PSMs with their ability to sorb P in a flow-through setting, as a function of retention time and inflow P concentration. These chemical characteristics can be inputted into the model, along with inflow dissolved P concentrations and desired retention time (Lyngsie et al., 2015; Stoner et al., 2012). This model is the foundation of the PhROG software providing design curves used in both the design and quantification of P removal structures. The necessary chemical characterization required to predict a design curve with the PhROG software will be discussed in later sections.

Impact of Material Physical Characteristics on P Removal Structure Design and Performance

Flow through the filter will be dictated by certain physical characteristics of the PSM used in the structure. It is necessary to know the saturated hydraulic conductivity of the material, bulk density, and porosity. The bulk density is a measurement of the mass per unit volume; PhROG uses units of grams per cubic centimeter. Porosity is the proportion of empty volume in a material to the solids volume (Hillel, 2004). When the software calculates the proper orientation of the material, the bulk density is required since it relates the mass of material to the volume required to accommodate it. If the bulk density is inaccurate then the dimensions of the structure will not be able to hold the mass required to meet the user's removal goals, so accurate measurements are important. Porosity is an important aspect when calculating the retention time of the structure which can perform a significant role in the sorption capability of the material if it is sensitive to retention time (Lyngsie et al., 2015; Stoner et al., 2012). The saturated hydraulic conductivity is the most important physical characteristic since it determines how much water can

pass through the material in a given time, and will directly affect how the material is orientated at the site, primarily, how deep the material can be and still achieve the minimum flow rates the user requires.

The flow through the structure is calculated in two distinct parts, downward flow down through the material feeding the subsurface drainage layer, and flow of the water exiting the structure through the subsurface drainage layer. Darcy's Law is used to estimate the flow through the material with the assumption that the water is flowing down through the surface of the PSM layer (a in Fig. 4.4) into the subsurface drainage layer (b in Fig. 4.4).

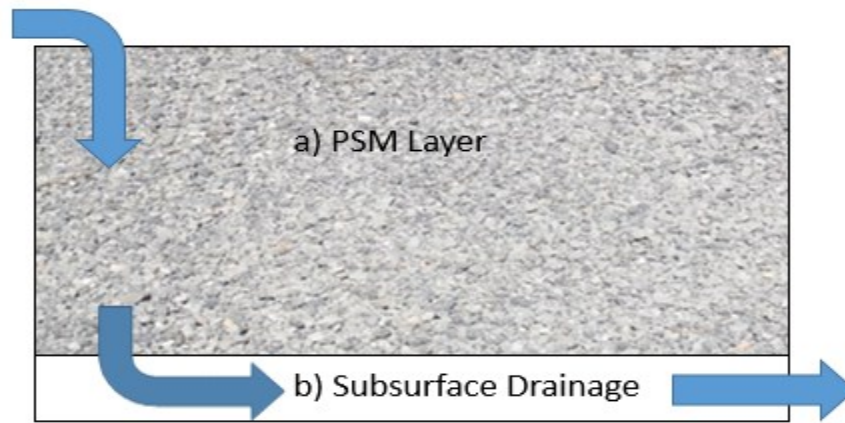


Figure 4.4. A cutaway side view of a P removal structure that shows the water flow through the P sorbing material (PSM) layer (a), downward into the subsurface drainage layer (b).

Calculating flow rate using Darcy's Law is straight forward requiring only a few inputs, specifically the saturated hydraulic conductivity of the material, the cross sectional area of the filter, hydraulic head, and the length (i.e. distance) water has to flow as shown in equation 4.7.

$$\text{Eq. 4.7 } Q = \text{Saturated Hydraulic Conductivity} \times \text{Cross Sectional Area} \times \frac{\text{head}}{\text{length}}$$

The saturated hydraulic conductivity is a constant value for a given material, and can be defined as the ratio of the discharge of water through a saturated material, to the driving force of water. Saturated hydraulic conductivity has units of a length per unit time, such as centimeters per second (Hillel, 2004). The cross sectional area of the filter is important since the larger the

area the more water can pass through it. In our case, the cross sectional area will be the area of the structure since we are calculating water flowing down through the material into the drainage layer. The hydraulic gradient, which is the hydraulic head divided by length, is a measure of the driving force of the water (Hillel, 2004). Given our filter's orientation, the hydraulic head is simply the difference in elevation between the inlet and outlet of the filter, and the length is simply the depth of PSM. By looking at the equation, it becomes apparent how the flow through the PSM can be increased. Since the hydraulic conductivity of a material can only be changed by altering the particle size distribution, possibly by sieving to reduce the smaller particles (in steel slag, for example) or additions of a larger sized particle such as sand (to fly ash, for example), the flow can be altered only by changing the area and gradient. Increasing the area of the filter will directly increase the rate (and therefore volume) that water that can flow through it. The gradient is a ratio of the head to the length it has to travel through the material. Since the elevation change for water flowing into a structure is mostly determined by the topography of the site only being altered by earthwork, the depth of material is the easiest way to change the gradient. Decreasing the depth of PSM and therefore the length that water has to travel before reaching the drainage layer increases flow rate, but consider that the depth of PSM also cannot be less than the diameter of the pipes used to drain the structure. The depth of material should also be deep enough that it is possible to achieve a relatively uniform depth across the area of the filter. The software will constrain the depth to be deeper than the pipe diameter, less than or equal to the hydraulic head, and to be at least 2cm which is a manageable depth for spreading material.

Characterization of PSMs

Methods of Physical Characterization

The PSM's physical characteristics are required for using the PhROG software since it necessary for both design and quantification of existing structures. The bulk density can be

measured simply with some rudimentary tools. By placing the material in a container of known volume (such as a graduated cylinder) and then weighing that material, bulk density is simply the mass divided by volume. It is important that the material not be compacted when measuring the bulk density, so limit the amount of settling by not excessively tapping the cylinder when smoothing the top of the material. Given that 1ml is equal to 1cm³, the bulk density is the mass on the scale in grams divided by the volume reading of the cylinder resulting in a value with units of g per cm³ as shown in equation 4.8.

$$\text{Eq. 4.8 } \textit{Bulk Density} = \textit{Mass of Material}(g) / \textit{Volume of Container}(cm^3)$$

The particle density is determined since it can be used in conjunction with the bulk density to estimate the porosity (Hillel, 2004). To find the particle density, add 25ml of water, preferably deionized, to a 50ml graduated cylinder and pour in 20g of material. Ensure that there are no air bubbles and then take a reading of the cylinder's volume. The particle density is the mass of material used (20g) divided by the increase in volume (Final Volume – 25ml) resulting in a value with units of g per cm³ as shown in equation 4.9.

$$\text{Eq. 4.9 } \textit{Particle Density} = \textit{Mass of Material}(g) / (\textit{Final Volume} - \textit{Initial Volume})(cm^3)$$

The porosity can be estimated using the bulk density and the particle density by subtracting the quotient of the bulk density and the particle density from 1 as shown in equation 4.10.

$$\text{Eq. 4.10 } \textit{Porosity} = 1 - (\textit{bulk density} / \textit{particle density})$$

Although these measurements are straight forward, but given the amount of variability that can be present within a material it is important that these measurements are replicated several times to ensure that they are accurately representing the actual value for the material as a whole. Unfortunately, the hydraulic conductivity of a material is more difficult to measure directly unless one can gain access to a permeameter. Many private civil engineering testing laboratories offer

testing for hydraulic conductivity. However, if the user has a data on the particle distribution curve for the material (which can also be measured by a private testing laboratory) then the hydraulic conductivity can be estimated using one of two models depending on whether it is predominated by smaller particle sizes like a soil or larger sizes like a gravel (Canga et al., 2013; Salarashayeri and Siosemarde, 2012). The particle distribution curve can be determined using ASTM method D422-63 which incorporates sieving with hydrometer measurements of a slurry made with the PSM (Standard, 2007). The curve can be used to find d_x values which represent the particle size in mm that X% of all particles are smaller than; these values can be used to estimate hydraulic conductivity. Once the curve is plotted, a polynomial regression can be fitted to it allowing the user to input the X from d_x , for example 10 to find d_{10} , into the regression equation. A sample particle distribution curve and regression equation are shown in Fig. 4.5.

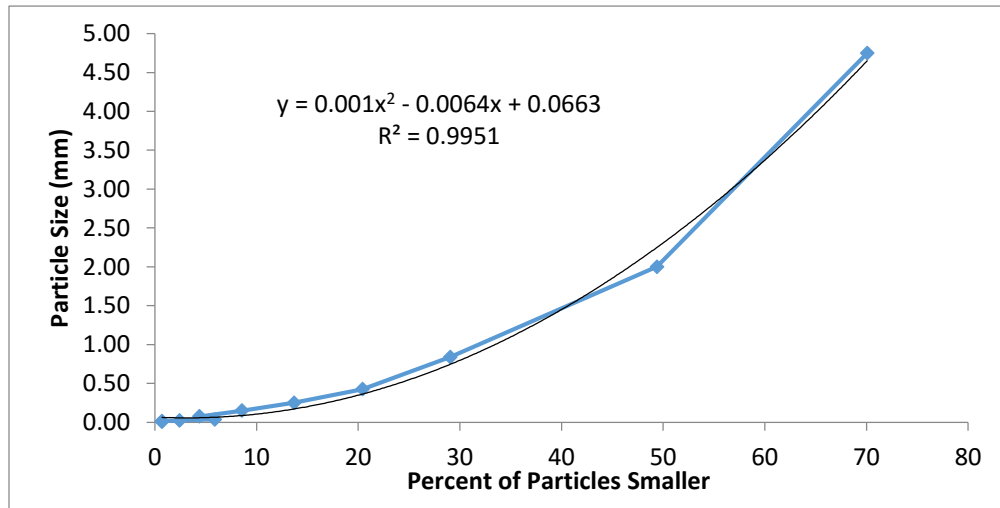


Figure 4.5. A sample particle size distribution curve for a material is shown with the particle size in mm shown versus the percent of particles finer than that diameter.

Equation 4.11 was developed on soils, so it is better used for materials that contain smaller particles, such as acid mine drainage residuals and other soil-like materials (Salarashayeri and Siosemarde, 2012).

$$\text{Eq. 4.11 Saturated Hydraulic Conductivity } \left(\frac{m}{day} \right) = 10.06 + 118.54(d_{10}) - 12.50(d_{50}) - 7.32(d_{60})$$

Equation 4.12 was developed using larger sized porous materials that may be found in a variety of filters, so it is better suited for coarser materials, such as steel slag (Canga et al., 2013).

$$\text{Eq. 4.12 } \log(\text{Saturated Hydraulic Conductivity } \left(\frac{\text{cm}}{\text{day}}\right)) = 4.66 + 0.63 \times \log(d_{20}) + 0.94 \times \log(d_{50})$$

If direct measurement of the hydraulic conductivity or estimation using the two previous equations is not possible, then average values for a material can be used, but it is not advisable due to high variability within materials. Since most of the popular PSMs are by-products, there is not the same quality control to ensure uniformity that one would observe compared to manufactured PSMs, thus it is vital to ensure the sample is representative.

Methods of Chemical Characterization

The chemical characteristics of the PSM can be used to estimate the design curve as well as to ensure that the material is safe to dispose of after use (Lyngsie et al., 2015; Stoner et al., 2012). Two separate models were developed by characterizing PSMs and performing flow-through P sorption experiments under various conditions of P concentrations and retention times, with many different PSMs (Stoner et al., 2012). Materials are separated into two models by the dominate mechanism of P sorption, either iron (Fe) and aluminum (Al), or calcium (Ca). The Fe and Al dominated materials will mostly sorb P through ligand exchange which is relatively fast and irreversible (Essington, 2004; Hsu, 1964; Sigg and Stumm, 1981; Stoner et al., 2012). Materials that are dominated by Ca will sorb P through precipitation of Ca phosphate minerals which are relatively stable with little P released once formed (Claveau-Mallet et al., 2011; Grubb et al., 2011; Johansson and Gustafsson, 2000). The P removal efficiency of these two mechanisms vary with different solution environments, to which the PSM may have some influence. This influence on solution chemical conditions can often enhance the P sorption mechanism. This increased ability to sorb P allows for a smaller mass requirement of PSM to reach performance

goals, ultimately allowing for smaller structures that need to be cleaned out less often than those containing a lower quality PSM.

The two main groups of P sorption mechanisms are separated using pH of the material, ability to buffer the pH at 6 or above (buffer index), and the total amount of Ca, Fe, and Al present. Also any material that has a pH greater than 8.5 is automatically considered a Ca material since ligand exchange, the dominant mechanism in Fe and Al rich materials, will be poor in those materials at high pH due to competition with hydroxides and surface repulsion (Antelo et al., 2005; Essington, 2004). Since the two groups rely on different mechanisms there will be different chemical characteristics that will aid P sorption, which will be discussed separately.

Ca Materials

Ca materials rely on precipitation of Ca phosphates, so the first characteristic of interest is the Ca content of the PSM. The total amount of Ca present in the PSM has to be determined, so the sample needs to be digested by subjecting it to hot acid and hydrogen peroxide to break down minerals and organics present (USEPA, 1996). The solution remaining after digestion can then be tested using by inductively coupled argon plasma analyzer (ICP-AES) or atomic absorption (AA) for Ca, Fe, Al, and any trace metals which might limit disposal options after use in a structure. As the Ca present in the sample increases there is a greater possibility of soluble Ca being available for precipitation with P. While Ca has to be present for precipitation to occur, there also needs to be adequate chemical pressure to drive the reaction in a timely fashion. The pH of the material and its ability to buffer it within the desired range is vital to the formation of Ca phosphates. The higher the pH is the more chemical pressure that is applied to the system allowing for faster precipitation, although the reaction will still occur with less chemical pressure. If the pH is less than 7 and the PSM is poorly buffered (buffer index less than 0.1 eq of acid kg⁻¹ of PSM) it will take longer for the reaction to occur, so the retention time of the structure must be increased so

that the P-rich water is in contact with the PSM for a longer time. For these materials that are sensitive to retention time, the structure must have a retention time of 10 min or the ability to sorb P decreases dramatically thereby increasing the required mass of PSM required to meet the desired P removal goals. Testing pH can be accomplished by equilibrating 3g of the PSM with 15ml of deionized water and then using a calibrated pH meter or pH color-indicator strips. The buffer index requires titration of the PSM (1:5 solid:water ratio) with an acidic solution (usually hydrochloric acid) to endpoint pH of 6. Calculating the buffer index requires multiplying the normality of the acid by the volume of titrant added during the titration and dividing by the sample mass; the PhROG software requires that buffer index be in units of equivalents per kg of PSM.

Fe and Al Materials

Both Fe and Al materials rely on ligand exchange for sorbing P. Just like Ca materials, the first characteristic to examine at is the total amount of Fe and Al present in the PSM by digesting a sample and then testing for elements present. The results are expressed in units of mg kg⁻¹ for each element after the digestate concentration is multiplied by the sample volume and then divided by the initial sample mass. Just like the Ca materials, increasing concentrations of total Fe and Al in a PSM increase the likelihood that those elements will be able to react with P, but for Fe and Al the form present also makes a difference. Minerals are present in either a pure crystalline form that has very structured repeating patterns, an amorphous form that has no discernable pattern, or something in between (Essington, 2004). Amorphous minerals have two advantages over crystalline ones; they have a larger surface area per unit mass and have more terminal hydroxides exposed. The large surface area per unit mass means that more of the mineral is exposed to the solution and can therefore react with it. Since terminal hydroxides are sites where ligand exchange occur, the PSM's affinity for P will increase with greater surface area and density of terminal hydroxides. Amorphous Fe and Al are extracted with an ammonium oxalate

solution buffered at pH 3 that is shaken for 2 hr in the dark with the resulting solution tested for Fe and Al using ICP-AES or AA (McKeague and Day, 1966). For this extraction, the solids to solution ratio traditionally used is 1:40.

Site Requirements for a Phosphorus Removal Structure

P removal structures are only viable under certain conditions and will have to be custom designed for each location. There are several site requirements for a P removal structure:

- Flow convergence to a single point where the water can be directed into a P removal structure, or the ability to manipulate the landscape to achieve this. A ditch is an example of a landscape feature that serves as a point where water converges, and therefore a good potential interaction point for placement of a P removal structure. Another example of a point of concentrated flow that may already exist, is a subsurface drainage pipe such as a tile drain.
- Appreciable dissolved P concentrations in flow. This typically occurs in areas where soil test P is high.
- Hydraulic head, which is required to “push” water through a PSM. In practical terms, the hydraulic head is a function of the slope of the site (i.e. change in elevation) or the depth of a ditch if a structure is to be built in a drainage ditch, or ultimately drain into a ditch.
- Sufficient space to accommodate the PSM.
- Hydrologic connectivity to surface waters. In other words, P from runoff or drainage water cannot cause problems in aquatic systems if it is unlikely to reach surface waters.

The topography of the site plays a vital role in transport of water to the structure and the rate of flow through it, so properly positioning the structure and if necessary, use of berms, will help channel runoff into the structure. The maximum hydraulic head is simply the amount of elevation

change across a certain known distance (in units of inches for PhROG input). Flow of water through the material is determined in part by the hydraulic head.

Structures will only be successful in areas with a large concentration of dissolved P present in runoff, thus, it is essential to obtain some estimate of both the typical dissolved P concentration and average annual load at the site of interest.

Site Characterization

In order to properly design a site-specific P removal structure to achieve defined removal goals, several site characteristics must be obtained:

- Peak flow rate for various size storm events
- Average annual flow volume and dissolved P load
- Typical dissolved P concentrations
- Hydraulic head

Peak Flow Rate and Annual Flow Volume

Input of peak flow rate into the PhROG software is critical since this will allow PhROG to design a structure that will be able handle a flow rate equal to or greater than the peak flow rate. Simply put, water must be able to flow through the P removal structure in order for the structure to remove P; therefore, it is important that the structure be designed to be able to handle flow rates produced from appreciable sized storms since large storm events tend to deliver the greatest P loads to surface waters.

Estimation of the peak flow rate for different size storms (i.e. storm return period) can be completed using techniques such as the Curve Number Method developed by the National Resource Conservation Service (NRCS), or a computer model which utilizes these methods such

as the Soil and Water Assessment Tool (SWAT) (Arnold et al., 1998; NRCS, 2004). Certain information about the site is required to use the Curve Number Method (Jarrett, 1997), including:

- Hydrologic group of the soils present
- Contributing area
- Percent area of the different land uses/ground cover in that area
- Hydraulic length, which is the distance from the furthest point in the contributing area to the outlet
- Average slope of the watershed
- Depth of precipitation for storm events of interest

The depths of precipitation for various sized storm events can be obtained by USDA rainfall tables that ultimately come from the National Oceanic and Atmospheric Administration (USDA, 1986). This is specific to region and is typically obtained by viewing maps for storms of a specified return period. Choosing an appropriate storm size is important because storm size is proportional to runoff flow rates and volumes, therefore the required structure size will be larger for storms with a less frequent return period (i.e. larger storms).

For example, a user may be interested in designing a structure that can treat flow from a 2 year-24 hr storm, which means that this size storm is likely to only occur once every 2 years. Ultimately, the result is a depth of rainfall. This depth of rainfall is used with the other listed required information for estimating the peak runoff flow rate at the site. Much of that information can be obtained using aerial maps, soil survey, and computer programs such as the Water Erosion Prediction Project (WEPP) available at <http://milford.nserl.purdue.edu> (Elliot et al., 2000). However, this process does require that some variables are obtained directly from visiting the site. The NRCS provides this service of determining curve number as one component of the process for designing various best management practices. Also, many environmental

consulting agencies are equipped to estimate curve number or estimate peak flow rates by other methods.

Accurately estimating the annual flow volume is important since it, along with average P concentration, will dictate the load of P that enters that structure. The load of P, or mass, will play a large role in the design of a structure since more PSM and therefore a larger structure will be needed as the P load increases. Similar to estimating peak runoff flow rates, the average annual runoff volume can be obtained by techniques such as the Rational Runoff Coefficient method, which is simply based on cover, contributing area, and average annual rainfall depth (Jarrett, 1997). Some common values for the runoff coefficient used in Eq. 4.13 are shown in table 4.1.

Eq. 4.13 $Annual\ Runoff = Runoff\ Coefficient * Annual\ Rainfall * Area$

Table 4.1. The Runoff Coefficient for a variety of soil types, vegetation, and topographies are shown (Jarrett, 1997).

| Vegetation | Topography | Runoff Coefficient | | |
|------------|------------|------------------------------|---------------------------------|-------------------------|
| | | Open Sandy Loam ¹ | Clay and Silt Loam ² | Tight Clay ³ |
| Pasture | Flat | 0.1 | 0.3 | 0.4 |
| | Rolling | 0.16 | 0.36 | 0.55 |
| | Hilly | 0.22 | 0.42 | 0.6 |
| Cultivated | Flat | 0.3 | 0.5 | 0.6 |
| | Rolling | 0.4 | 0.6 | 0.7 |
| | Hilly | 0.52 | 0.72 | 0.8 |

¹Soil types assumed to be equivalent to Hydrologic Group A.

²Soil types assumed to be equivalent to Hydrologic Group B and C.

³Soil types assumed to be equivalent to Hydrologic Group D.

Estimation of Dissolved P Concentrations

For estimating typical dissolved P concentrations in flow, simple “grab” samples can be taken during several flow events, followed by analysis for dissolved P. It is vital that the samples used to determine the average P concentration are taken during different sized events and times of

year since runoff and drainage P concentration will vary at a site (Sharpley et al., 2008a). One can also estimate dissolved P concentrations in runoff and subsurface drainage based on the soil test P values and soil type; for this approach, there are several sources in the literature that describe the relationships between soil test P concentrations and dissolved P concentrations in runoff (Vadas et al., 2005). Dissolved P loss can be correlated with routine nutrient testing, such as Mehlich-3 and Bray-1, or a water extraction as shown in Eq. 4.14 and 4.15 (Vadas et al., 2005). Estimates of

$$\text{Eq. 4.14 } \textit{Dissolved P}(\mu\text{g L}^{-1}) = 2.0 * \textit{Soil Test Value}(\text{mg kg}^{-1}) + 43.5$$

$$\text{Eq. 4.15 } \textit{Dissolved P}(\mu\text{g L}^{-1}) = 11.2 * \textit{Water - Extractable P}(\text{mg kg}^{-1}) + 66.9$$

typical dissolved P concentrations is directly used by the software to help estimate the appropriate design curve, and it is also used to calculate the dissolved P loading at the site. Loading is estimated by multiplying the dissolved P concentration by the annual volume of water leaving a site, which results in the mass of P that is transported from the site in one year.

Hydraulic Head and Area for Structure

The maximum area the user is willing to set aside for a filter must be determined. In practice, this involves visiting the site and marking the corners with flags or stakes to help with subsequent measurements. Once the maximum length is determined, the elevation difference between each end needs to be measured (Fig. 4.6). This value, known as the hydraulic head, is an

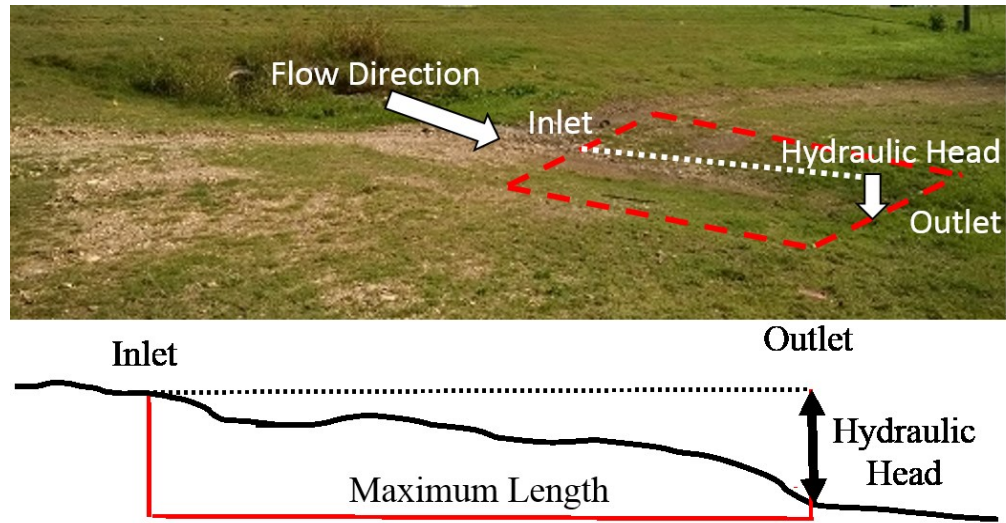


Figure 4.6. A proposed site for P removal structure is shown (upper) with the maximum allowable area for the structure enclosed by a dashed line. The hydraulic head, the elevation difference from inlet to outlet, is shown at the site (upper) and in a cutaway diagram (lower).

important factor controlling the amount of water that can flow through a structure. Having a free draining structure is especially important if an iron-rich material is used as a PSM, long term saturated conditions will lead to a reduced state of the iron which decreases the material's sorption capacity and releases a foul smell due to bacterial reduction of sulfur (Pratt et al., 2007).

In the case of a ditch P removal structure, the user is required to provide input on the dimensions of the drainage ditch: top and bottom width and depth (Fig. 4.7). The depth of the ditch ultimately controls the hydraulic head for a ditch P removal structure. In some cases where a P removal structure is desired to treat tile drains, the P removal structure will consist of a buried PSM bed. In that case, the hydraulic head available for draining the structure is ultimately the elevation difference between the tile drain and the bottom of the ditch at the tile drain outlet.



Figure 4.7. A drainage ditch fed by a tile drained agricultural field in Ohio is shown with top width, bottom width, and depth marked.

Proper Drainage of P removal Structures

After the water flows down through the material in the P removal structure, it has been treated. However, the treated water must exit the structure to allow untreated water to enter into it. Thus, a subsurface drainage layer, such as the one shown in Fig. 4.8, is required for most structures. Without the drainage layer, the flow through a P removal structure would be severely limited since it would rely solely on lateral Darcy flow through the PSM layer. Due to its use in research and demonstration filters, as well as its availability at local hardware stores, perforated PVC pipe is recommended for use in the subsurface drainage layer. The factors affecting flow



Figure 4.8. The subsurface drainage layer of a P removal structure was exposed prior to the addition of steel slag. The drainage layer used 10.16 cm diameter perforated PVC pipes.

rate of water in the pipe are the slope of the pipe, which affects the velocity of the water and the friction water is subjected to by the roughness, and diameter of the pipe (Jarrett, 1997). As shown in Eq. 4.16, the relationship between flow rate and pipe diameter is not linear, so a doubling of pipe diameter results in much more than doubling of flow. The dramatic effect of pipe diameter

$$\text{Eq. 4.16 } \textit{Flow rate}(cfs) = 0.463 * \left(\frac{\textit{Pipe diameter}(inch)}{12} \right)^{\frac{8}{3}} * \frac{\textit{Pipe Slope}^{0.5}}{0.015}$$

on flow becomes important in designing a structure since the cost and ease of installation can vary with different sizes of pipe. The equation shown is for PVC only since pipes made from different materials will slow water flow to a different degree thus requiring a different roughness coefficient. The PhROG software requires that the user specify the diameter and slope of the pipe to be used to drain the structure. Based on the flow rate for each pipe, PhROG will determine how many of the specified drainage pipes will be required to meet or exceed the target flow rate for the structure, and also satisfy the specified retention time (for retention time sensitive materials).

Required Site Inputs and Specifications into the Software

The design and prediction of P removal structures is based on the site inputs which are mostly average values, so the lifetime and removal are only as accurate as the inputs. All design recommendations are based on an average annual P load. If rainfall is significantly less than normal, the total amount of P removed will be less than expected over that time period, and the lifetime will increase, since less runoff is produced and thus less P loading to the structure than expected over that time period. The upside of this is that the material will last longer than expected.

Design Structure vs. Predicting Performance of an Existing Structure

The PhROG software provides two different tabs that allow a user to either design a P removal structure (“Design Structure”) based on constraints and desired P removal goals, or predict the performance of an already existing P removal structure (Fig. 4.9).

Design a new structure

Design Structure Existing Structure

Desired Retention Time (min) 0

Average Dissolved P Concentration (mg/L) 0

Annual Flow Volume (gallons) 0

Desired Removal Goal (%) 0

Desired Lifetime (years) 0

Drainage Pipe Diameter (inches) 0

Drainage Pipe Slope (decimal) 0

Quantify an existing one

Design Structure Existing Structure

Average Phosphorus Concentration (mg/L) 0

Annual Flow Volume (gallons) 0

Subsurface Drainage (Backward Required)

Drainage Pipe Diameter (inches) 0

Drainage Pipe Slope (decimal) 0

Number of Subsurface Drainage Pipes 0

Figure 4.9. The “Design Structure” tab and “Existing Structure” tab from the PhROG software are shown. Only one of these two will be visible at a time, but both are shown to highlight the different inputs.

Two Broad Styles for P Removal Structures: Bed vs. Ditch Structure

Regardless of whether the user is designing a structure or predicting the performance of an existing structure, the PhROG software allow the user to specify between a bed of PSMs located on the surface or surface, and a P removal structure constructed within a ditch. This is found by clicking on the tabs labeled with the terms, “Bed” or “Ditch”. However, the “Design

Structure” tab must be selected with the “Design Bed Size” or “Design Ditch Size” tabs, in order to design those structures. Likewise, the “Existing Structure” tab must be selected with either the “Existing Bed Size” or “Existing Ditch Size” tabs, when the intention is to quantify the performance of a ditch or bed P removal structure that already exists (Fig. 4.10).

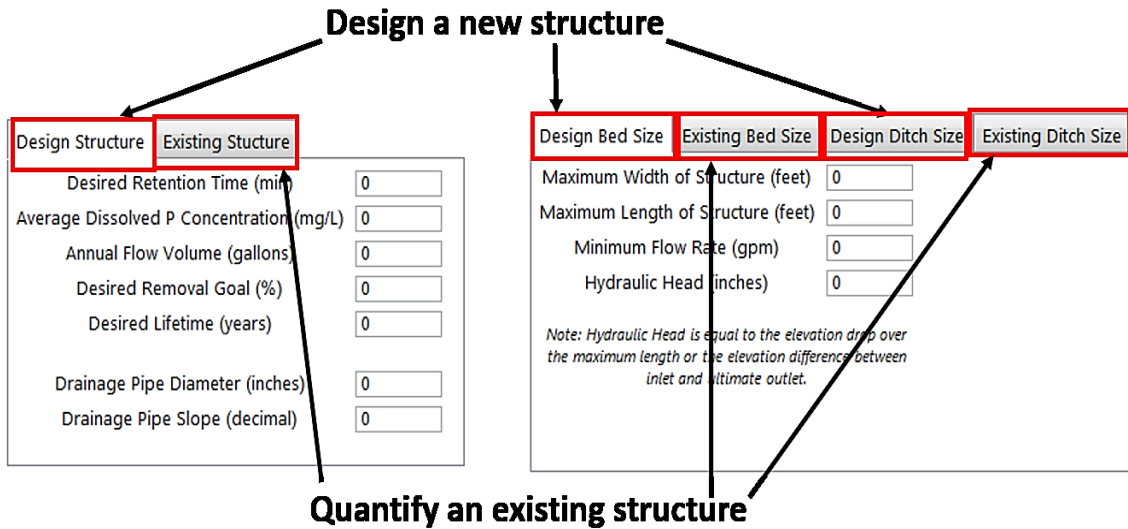


Figure 4.10. A screenshot of the PhROG software is shown with the corresponding tabs for designing or quantifying a bed or ditch structure.

As previously discussed, drainage ditches present a simple and readily accessible point for construction of a P removal structure. The inputs for bed and ditch structures are mostly the same, although there are some major differences that are highlighted below.

Specific Inputs for Structure Design

Chemical and Physical Characteristics of PSM to be Used

The required chemical and physical characterization of the PSMs to be used in the P removal structure was previously discussed. It is critical that the user input the actual values for the material of interest that will potentially be utilized in the structure instead of relying on previously measured values for the same type of material collected at a different time or location. Tremendous variability may occur between the same types of PSMs, even if they are collected

from the same location. Input for chemical and physical characteristics of the PSM is show in Fig. 4.11.

Chemical characteristics

Estimate Design Curve | Manually Input Design Curve ($y=be^{mx}$)

Total P Removal (optional)

Mean Particle Size of Filter Media (mm)

Average Total Phosphorus Concentration (mg/L)

Average Sediment Concentration (mg/L)

Deposition Rate (grams of sediment/minute of flow)

Ammonium Oxalate Aluminum (mg/kg)

Ammonium Oxalate Iron (mg/kg)

Buffer Index (equivalents of acid per kg of material to reduce pH to 6)

Mean Particle Size (mm)

pH

Total Aluminum (mg/kg)

Total Calcium (mg/kg)

Total Iron (mg/kg)

Material Physical Characteristics

Bulk Density (g/cm^3)

Hydraulic Conductivity (cm/sec)

Porosity (decimal)

Physical characteristics

Figure 4.11. The “Estimate Design Curve” and “Material Physical Characteristics” tabs of the PhROG software are shown highlighted. These tabs are used to input the chemical and physical characteristics of the PSM.

As previously discussed, the software determines if a PSM is Ca-based or Al/Fe-based. If the PSM is Ca-based, then it determines if it is sensitive to retention time or not. Precipitation of Ca phosphates can be a slower process than other forms of sorption, so in order for it to occur quick enough to treat runoff, an appreciable amount of chemical pressure is required. The pH of the PSM and its ability to buffer pH above 6 are what dictates how fast precipitation can occur.

The hydraulic conductivity of the PSM will have a large impact on the design of the structure since it dictates flow through a material. For materials with a very low hydraulic conductivity, the depth of material will need to be somewhat shallow, forcing the structure to be larger in area to achieve higher flow rates. Materials with large hydraulic conductivity can be stacked deeper and still achieve high flow rates. The bulk density of the PSM will partly dictate the mass and volume of PSMs required, and the porosity will additionally have an impact on the retention time of the structure.

Site Characteristics and Constraints

Desired retention time: minutes - The user must input the retention time they desire for the structure, but depending on the material used, the retention time they choose may not be a constraint. This is due to the fact that for some materials, retention time has little impact on the P sorption (Lyngsie et al., 2015; Stoner et al., 2012). The PhROG software is able to determine if a material is sensitive to retention time based on the material characterization. If a material is retention time sensitive, the retention time will automatically change from whatever the user inputs, to 10 min. This default of 10 min was chosen after experimentation using various retention times; this high retention time for materials sensitive to retention time will maximize P removal per unit mass, thereby decreasing the required mass of the PSM to achieve the desired performance goals (Stoner et al., 2012). For sensitive materials, the software will meet the 10 min retention time even if it has to sacrifice the minimum flow rate through the filter. The retention time is calculated by dividing how much water the filter can hold, its pore volume, by the maximum flow rate through the filter. The pore volume is the empty space present in the filter, so it is calculated by multiplying the porosity of the PSM by the volume of the PSM contained in the structure. For a given retention time, the pore volume and flow rate are proportional, so to achieve a larger flow rate and keep retention time the same, the pore volume must be increased. The software makes use of this relationship in a feature demonstrated later in a case study example.

Dissolved P concentration: mg/L – Ideally, flow-weighted dissolved P concentrations should be input by the user. Otherwise, the user should input typical dissolved P concentrations either determined by grab samples or by estimates based on soil test P values as previously discussed. This value directly impacts the P load entering the structure, and therefore is a major factor controlling the mass of the PSM required to meet the desired removal goal.

Annual flow volume: gallons – The annual flow volume is also necessary for the software to estimate the dissolved P load entering the structure. The larger the annual flow volume, the larger the dissolved P load, and thus a greater requirement for PSM mass. Methods for estimating annual flow volume were previously discussed.

Desired removal goal: % – This value is the cumulative percentage of dissolved P removal over a chosen time period, i.e. the desired lifetime. The greater the desired removal goal, the greater the required mass of PSM and size of structure. Realistic values must be chosen since some materials are not capable of removing extremely large percentages of dissolved P with appreciable P loading. If the user chooses a desired removal goal that is beyond the capacity of that particular PSM, then PhROG automatically reduces the desired removal goal to the maximum for that PSM. While some materials that are rich in Fe and Al oxides/hydroxides are able to remove high percentages of dissolved P with appreciable P loading, other materials such as gypsum are unable to do so.

Desired lifetime: years – The desired lifetime is used in conjunction with the desired removal goal, and therefore partly dictates how much PSM is required and how large the structure will need to be. This value is the number of years that is desired for the structure to last, until the desired removal goal (specified by user) is met.

Drainage pipe diameter: inches – In order for the software and the P removal structure to function, there must be subsurface drainage pipes used in the structure. The program allows the user to input a specific pipe diameter. The output of the software will include the number of pipes that the structure will require, for that specific pipe diameter, so it is easy to compare multiple pipe sizes. The pipe diameter the user chooses will depend on cost, availability, and ease of installation since using a larger size pipe will decrease the number needed possibly reducing transportation and construction costs. When PhROG calculates the required size of the P removal

structure, it takes into account the volume of the drainage pipes since this volume will not be filled with PSMs.

Drainage pipe slope: fraction (decimal) – The slope of the drainage pipe has a direct impact on the flow rate of water through the pipes. Flow rate from the pipes increases with increasing slope of the pipes. Therefore, this has similar implications and flexibility as choosing drainage pipe diameter.

Minimum flow rate through filter: gallons/min – The minimum flow rate through the filter is essentially the peak flow rate that the user desires for the structure to be able to handle. Simply put, the structure must be able to handle the high flow rates produced at that site in order to be able to remove appreciable dissolved P in water; the structures cannot remove P if water does not flow through them. Methods for estimating this value on a site-specific basis was previously discussed. This value has a tremendous impact on the orientation of the structure, specifically the depth of the PSM and the area or length of the structure.

Maximum decrease in ditch flow (ditches only): % - First, the hydraulic head for a ditch P removal structure is ultimately a function of the depth of the ditch, and PhROG takes this into account with the required inputs for a ditch P removal structure. While deep ditches are able to provide ample hydraulic head for pushing water through a thick layer of PSMs at a sufficient rate, there is a trade-off in the fact that the depth of PSM placed in a ditch is directly proportional to the loss of ditch flow capacity. Specifically, the ultimate purpose of a ditch is to quickly convey water off of the landscape; filling a ditch with a PSM will therefore decrease the ability of the ditch to convey water. For this reason, the PhROG software allows the user to specify the maximum amount of ditch flow capacity that they are willing to sacrifice in construction of the P removal structure. Thus, PhROG will limit the depth of the PSM, partly based on meeting the constraint of not exceeding this specified maximum decrease in ditch flow capacity.

Maximum length and width: feet – For a bed-style structure, this is the area constraint for a site, or it could ultimately be a cost restraint. Compared to a surface bed structure, a ditch P removal structure is already partly fixed in area, since the ditch itself provides the area for the PSM to be placed. In this case, the maximum length is the length of the ditch that ultimately dictates and limits the size of the ditch P removal structure. Thus, for design of a ditch P removal structure, the user must specify the maximum length of the ditch that may be utilized for the structure.

Hydraulic head: inches – As previously discussed, the hydraulic head is essentially the maximum change in elevation from the inlet of the structure to its potential drainage point. For a buried surface bed that treats a subsurface tile drain, this is the elevation difference between the point where the tile drain enters the P removal structure, and the bottom of the ditch where the tile ultimately drains into. Usually, the elevation of the point where the tile drain enters the P removal structure is very close to the elevation of the tile drain outlet in the ditch to which it drains to.

Ditch dimensions (ditch structures only): feet – The top and bottom width of the ditch, and the depth, are all required. The depth of a drainage ditch is essentially equal to the maximum amount of hydraulic head for a ditch P removal structure.

Ditch slope (ditch structures only): fraction (decimal) – The slope of the ditch affects the flow rate of water through that ditch. This is important when PhROG calculates the maximum decrease in ditch flow capacity due to placing a PSM in the ditch.

Manning's roughness coefficient (ditch structures only): unit less – This value partly describes the friction of water flowing through a ditch, as a function of the surface condition of the ditch. For example, grass, stone, or soil each result in different amounts of friction with flowing water, and therefore have a unique impact on the flow rate of water through the ditch. A few surfaces and corresponding Manning's roughness coefficients are shown in Table 4.2 (Jarrett, 1997).

Table 4.2. Selected channel types are shown with their Manning's roughness coefficient (Jarrett, 1997).

| Type of channel | Lining | Manning's Roughness Coefficient |
|-----------------|----------------------------|---------------------------------|
| Vegetation | Long (30.5 to 61.0 cm) | 0.08 |
| | Short (5.1 to 15.2 cm) | 0.04 |
| Earth Channels | Firm soil, sand or silt | 0.02 |
| | Stiff clay, alluvial silts | 0.025 |
| | Shales and hardpan | 0.025 |
| | Dredged earth channels | 0.028 |
| | Large ditch, no vegetation | 0.035 |
| | Small ditch, no vegetation | 0.04 |

Additional Factors for Predicting Existing Structures

Most of the same variables that were described for designing a P removal structure are also used for predicting the performance of an already existing P removal structure. However, there are some additional inputs for this process.

Number of drainage pipes – Simply input the actual number of drainage pipes that were used in the P removal structure. This is important for estimating the maximum flow rate through the structure.

Length and width of structure: feet – Input the actual dimensions of a bed structure, whether it was a surface or subsurface structure. For a ditch P removal structure, only the length of the structure is required since ditch dimensions will also be input.

Depth of PSM: inches – Input the depth of the PSM. This is important to estimating the maximum flow rate through the structure and retention time, along with the number and size of drainage pipes and material physical characteristics

Mass: tons – This value is the actual mass of the PSM used to construct the P removal structure.

Optional inputs: Total and Particulate P removal

If total or particulate P loss from a site is a major concern, then other BMPs are better suited to reduce erosion, thereby reducing total and particulate P transport from the site.

However, the PhROG software has the ability to estimate the total P removed by the P removal structure if the user provides a few additional inputs, although it will not alter the design. Fig. 4.29 shows the inputs required to estimate total P removal.

Mean particle size of PSM: mm – The mean diameter of the PSM particles. This variable is already required for other purposes in the PhROG software, which was previously discussed in detail.

Total P concentration: mg/L – Similar to dissolved P concentrations, the best input for this variable is a flow-weighted mean. But again, if that is not possible, a user may obtain some typical values for total P concentrations by capturing grab samples for the site during a variety of different sized storms. Also, values may be predicted from relationships developed between soil properties and losses in runoff/drainage. Programs such as SWAT are also able to predict total P concentrations in runoff. *Sediment concentration: mg/L* – Values for sediment concentration can be obtained as similar to dissolved P and total P concentrations.

Deposition rate: g/minute - Of the four inputs, particle size of the PSM, total P concentration, and sediment concentration are relatively straightforward to measure, but deposition rate is more difficult to estimate. Deposition rate is the grams of sediment that is delivered to the structure per

minute of flow. Since the flow rate and sediment concentration entering the structure will vary, measuring the deposition rate without constant monitoring will be difficult, but it can be estimated using certain assumptions. For our demonstration of the total P removal option shown below, we assumed that all of the annual flow volume would be delivered at the highest flow rate, so the minutes of flow could be calculated by dividing the annual flow volume by the peak flow rate; this resulting value (time) can then be divided into an estimate for annual sediment load (mass).

General Output from Software

Mass of PSM required: tons – Simply put, this is the required mass of the PSM that possesses the chemical characteristics that the user input into the software.

Depth of material: inches – The depth in which the PSM should be placed in the structure in order to treat the water at the desired flow rate retention time (if retention time sensitive material).

Depth of structure (bed structures only): inches – The total depth of the PSMs plus hydraulic head. Occasionally the software will estimate a depth of structure that is greater than the depth of the material in order to allow some depth of water to be “stacked up” on the PSM. This usually occurs for PSMs with very low hydraulic conductivity, in order to increase the hydraulic gradient and therefore meet the required flow rate.

Length (ditch structures only): feet - The required length of ditch to be filled with the PSM at the depth previously specified in the output.

Length and Width (bed structures only): feet - the required length and width of the bed of PSM at the depth previously specified in the output.

Number of pipes needed in structure: PhROG will choose the proper number of drainage pipes, of the specified diameter, in order to achieve proper flow through the structure, either to limit it in

order to meet a certain retention time or to meet or exceed the minimum flow requirement. Note that PhROG has a minimum PSM depth that is equal to the specified pipe diameter. This is done in order to ensure that the pipes are completely buried in the PSM. PhROG also considers the total volume of pipe in the structure when making length and width calculations.

Actual retention time: minutes – The estimated retention time (minimum) for the structure if it is built to the specifications described in the output. If the PSM is not sensitive to retention time, then the output will additionally state, “material not sensitive to RT changes”. If the PSM is sensitive to the retention time, then the software will produce a design that has a retention time equal to or greater than the desired retention time.

Actual maximum flow rate through PSM: gallons per minute – The software attempts to produce a design that meets or exceeds the desired flow rate. If the desired flow rate is not met, PhROG produces the message, “Flow rate not met”. If this occurs, then PhROG will additionally provide a suggestion for increasing the lifetime of the structure in order to meet the flow rate requirement (see below).

Actual decrease in flow of ditch (ditch structures only): % - This is the calculated value for the decrease in ditch flow capacity if the structure is built to the specifications described in the output.

Estimated lifetime to meet both minFR and RT: years – If the minimum flow rate is not met, then PhROG will calculate a suggestion for increasing the lifetime of the structure in order to meet both the flow rate and retention time (if retention time sensitive material). Increasing the lifetime will increase the mass of the PSM which will increase the area, and therefore the flow rate (Darcy flow) through the structure.

Annual P removal table – Year by year output of cumulative P removal presented as a percentage of the total mass of P that flowed into the structure up to that time. Cumulative P removal is also presented as a load (lbs). If the user chose to utilize the additional option of estimating total P and particulate P removal, then the table will additionally provide cumulative removal for those constituents as well. The final time listed in the annual P removal table is essentially the point at which the P removal structure will no longer be able to remove any dissolved P. i.e. the inflow dissolved P concentration will equal the treated water dissolved P concentration.

Case Studies

In order to highlight some of the various applications of P removal structures, several structures will be designed or quantified in the following sections using the PhROG software in an effort to illustrate how different factors affect design, and the flexibility of the software. These scenarios were chosen to help reinforce how performance goals, site hydrology, and the PSM characteristics interact to produce a viable structure and how to manipulate them to meet goals. Characteristics used for the sites and PSMs are real values whenever possible, so that these examples are as close to reality as possible. All screenshots shown in the following sections are taken from the current version of PhROG which can be obtained through Oklahoma State University.

Maryland Ditch Design

The eastern shore of Maryland is drained by a series of large ditches that help prevent water from ponding on the relatively flat farmland (Fig. 4.12). The agricultural land produces runoff that can be elevated in dissolved P which has caused problems with eutrophication in the Chesapeake Bay. In order to combat P loss, P removal structures have been built in these ditches intercept and treat runoff water before it reaches the Chesapeake Bay. The ditches are an ideal

interception point to treat runoff since the runoff naturally converges to them, in addition to the hydraulic head for pushing water through the PSMs, which is a function of the depth of the ditch.

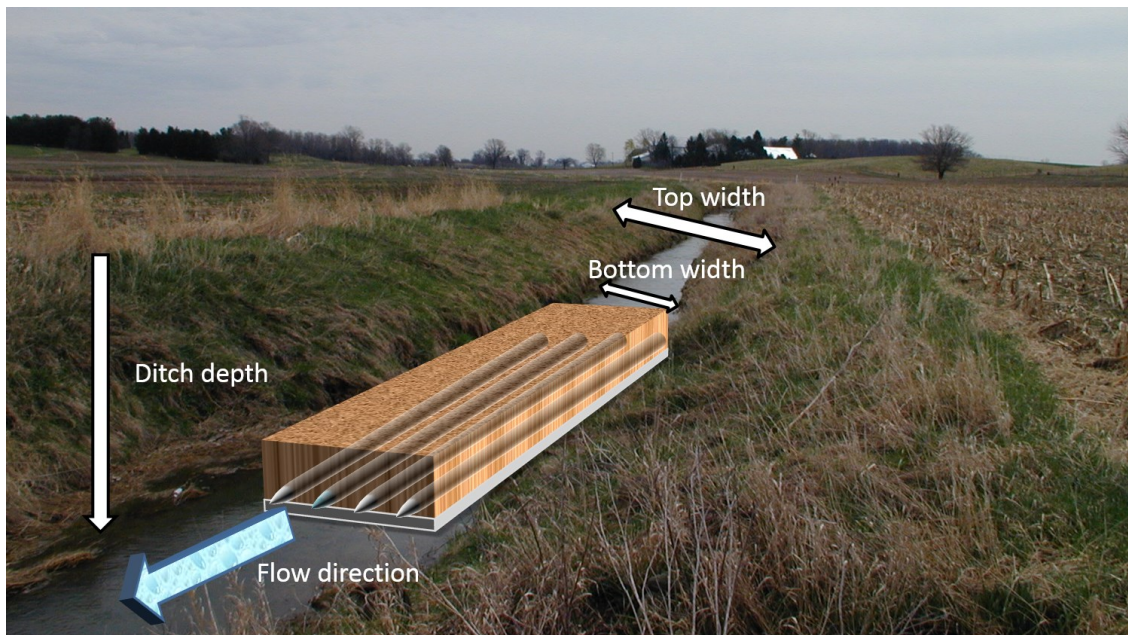


Figure 4.12. A diagram of a P removal structure is shown located in a ditch that drains agricultural fields. The ditch dimensions, top width, bottom, width, and depth, are marked with arrows.

This particular site is approximately 25 acres with an annual flow volume of 1 million gallons and an average dissolved P concentration of 1 mg L^{-1} ; this was input into the “Design Structure” tab shown in Fig. 4.13. The ditch is 12 ft wide at the top, 8 ft wide at the bottom, and 5 ft deep with a trapezoidal shape, which is common for drainage ditches in this region. We input the ditch dimensions, ditch slope, and the Manning’s Roughness Coefficient in the Design Ditch Size tab shown below (Fig. 4.13). The Manning’s Roughness Coefficient relates the condition of the ditch surface, concrete or long grass for example, to its ability to restrict flow (Jarrett, 1997).

Site Characteristics

| Design Structure | Existing Structure |
|--|--------------------|
| Desired Retention Time (min) | 10 |
| Average Dissolved P Concentration (mg/L) | 1 |
| Annual Flow Volume (gallons) | 1 000 000 |
| Desired Removal Goal (%) | 35 |
| Desired Lifetime (years) | 11 |
| Drainage Pipe Diameter (inches) | 4 |
| Drainage Pipe Slope (decimal) | 0.01 |

Ditch Characteristics

| Design Bed Size | Existing Bed Size | Design Ditch Size | Existing Ditch Size |
|--|-------------------|-------------------|---------------------|
| Minimum Flow Rate Through Filter (gpm) | | 400 | |
| Maximum Decrease in Ditch Flow (%) | | 35 | |
| Maximum Allowable Length (feet) | | 500 | |
| Ditch Top Width (feet) | | 12 | |
| Ditch Bottom Width (feet) | | 8 | |
| Ditch Depth (feet) | | 5 | |
| Ditch Slope (decimal) | | 0.001 | |
| Manning's Roughness Coefficient | | 0.07 | |

Figure 4.13. Two of the input tabs of the PhROG software are shown with values that correspond to the Maryland Swift ditch example. The site and ditch characteristics, namely loading and dimensions, are highlighted in red.

The minimum flow through the filter and the maximum decrease in ditch flow must be chosen by the user; these will vary from site to site. The minimum flow rate should be chosen with care since most of the P will be lost with larger events, so it is vital that the structure can handle high flow rates that are likely to occur at a site (Penn et al., 2012; Pionke et al., 1999; Sharpley et al., 2008b). The software also requires the maximum allowable decrease in flow capacity for the ditch after installation of the filter. Given that the purpose of ditches is to convey flow from runoff or tile drainage, it is important that the ditch can still meet the purpose it was designed for after installation of the filter. For this example we chose a minimum flow rate of 400 gpm and a maximum decrease in flow of 35% of the original; this was input into the Design Ditch Structure tab shown in Fig. 4.14. Also shown in this example, the user can input the maximum length of ditch that is able to be sacrificed for use as a P removal structure; in this case the maximum length is 500 ft.

The desired removal goal and the desired lifetime must be chosen by the user; these two values will greatly impact the size of the P removal structure. Specifically, the desired lifetime, desired P removal goal, and the affinity of the PSM for P (as quantified by the design curve) will be the biggest factors affecting the mass of PSM required, which directly impacts the size needed

for the structure. For this first example, we chose to remove 35% of the annual load for 1 year, so at the end of 1 year we would need to remove and replace the PSM in order to maintain the 35% removal.

Removal Goals

Constraints

| Design Structure | Existing Structure |
|--|--------------------------------------|
| Desired Retention Time (min) | <input type="text" value="10"/> |
| Average Dissolved P Concentration (mg/L) | <input type="text" value="1"/> |
| Annual Flow Volume (gallons) | <input type="text" value="1000000"/> |
| Desired Removal Goal (%) | <input type="text" value="35"/> |
| Desired Lifetime (years) | <input type="text" value="1"/> |
| Drainage Pipe Diameter (inches) | <input type="text" value="4"/> |
| Drainage Pipe Slope (decimal) | <input type="text" value="0.01"/> |

| Design Bed Size | Existing Bed Size | Design Ditch Size | Existing Ditch Size |
|--|------------------------------------|-------------------------------|-------------------------------|
| Minimum Flow Rate Through Filter (gpm) | <input type="text" value="400"/> | <input type="text" value=""/> | <input type="text" value=""/> |
| Maximum Decrease in Ditch Flow (%) | <input type="text" value="35"/> | <input type="text" value=""/> | <input type="text" value=""/> |
| Maximum Allowable Length (feet) | <input type="text" value="500"/> | <input type="text" value=""/> | <input type="text" value=""/> |
| Ditch Top Width (feet) | <input type="text" value="12"/> | <input type="text" value=""/> | <input type="text" value=""/> |
| Ditch Bottom Width (feet) | <input type="text" value="8"/> | <input type="text" value=""/> | <input type="text" value=""/> |
| Ditch Depth (feet) | <input type="text" value="5"/> | <input type="text" value=""/> | <input type="text" value=""/> |
| Ditch Slope (decimal) | <input type="text" value="0.001"/> | <input type="text" value=""/> | <input type="text" value=""/> |
| Manning's Roughness Coefficient | <input type="text" value="0.07"/> | <input type="text" value=""/> | <input type="text" value=""/> |

Figure 4.14. Two of the input tabs of the PhROG software are shown with values that correspond to the Maryland Swift ditch example. The removal goals and flow constraints are highlighted in red.

For this example we chose to use a 4 in diameter pipe with a slope of 0.01 (i.e. 1%) as shown below in Fig. 4.15.

Subsurface Drainage

| Design Structure | Existing Structure |
|--|--------------------------------------|
| Desired Retention Time (min) | <input type="text" value="10"/> |
| Average Dissolved P Concentration (mg/L) | <input type="text" value="1"/> |
| Annual Flow Volume (gallons) | <input type="text" value="1000000"/> |
| Desired Removal Goal (%) | <input type="text" value="35"/> |
| Desired Lifetime (years) | <input type="text" value="1"/> |
| Drainage Pipe Diameter (inches) | <input type="text" value="4"/> |
| Drainage Pipe Slope (decimal) | <input type="text" value="0.01"/> |

| Design Bed Size | Existing Bed Size | Design Ditch Size | Existing Ditch Size |
|--|------------------------------------|-------------------------------|-------------------------------|
| Minimum Flow Rate Through Filter (gpm) | <input type="text" value="400"/> | <input type="text" value=""/> | <input type="text" value=""/> |
| Maximum Decrease in Ditch Flow (%) | <input type="text" value="35"/> | <input type="text" value=""/> | <input type="text" value=""/> |
| Maximum Allowable Length (feet) | <input type="text" value="500"/> | <input type="text" value=""/> | <input type="text" value=""/> |
| Ditch Top Width (feet) | <input type="text" value="12"/> | <input type="text" value=""/> | <input type="text" value=""/> |
| Ditch Bottom Width (feet) | <input type="text" value="8"/> | <input type="text" value=""/> | <input type="text" value=""/> |
| Ditch Depth (feet) | <input type="text" value="5"/> | <input type="text" value=""/> | <input type="text" value=""/> |
| Ditch Slope (decimal) | <input type="text" value="0.001"/> | <input type="text" value=""/> | <input type="text" value=""/> |
| Manning's Roughness Coefficient | <input type="text" value="0.07"/> | <input type="text" value=""/> | <input type="text" value=""/> |

Figure 4.15. Two of the input tabs of the PhROG software are shown with values that correspond to the Maryland Swift ditch example. The section with subsurface drainage inputs is highlighted in red.

The next step is to choose a PSM to be used in this structure and then input the characteristics specific to that PSM. For this example we will use a flue-gas desulfurization gypsum which is an industrial by-product that is rich in Ca, but is poorly buffered at high pH values. In order for the

software to determine the proper group to place the PSM in, the user must input a variety of chemical characteristics shown in Fig. 4.16. All of these chemical characteristics are explained earlier in this paper, but these examples should highlight the impact they have on structure design. Values for this material were taken from a characterization completed on an actual material. Observation of the values in Fig. 16 shows that the amount of Ca present greatly

Chemical Characteristics

Estimate Design Curve
Manually Input Design Curve ($y=be^{mx}$)

Total P Removal (optional)

Mean Particle Size of Filter Media (mm)

Average Total Phosphorus Concentration (mg/L)

Average Sediment Concentration (mg/L)

Deposition Rate (grams of sediment/minute of flow)

Material Physical Characteristics

Bulk Density (g/cm³)

Hydraulic Conductivity (cm/sec)

Porosity (decimal)

| | |
|---|---------|
| Ammonium Oxalate Aluminum (mg/kg) | 56.32 |
| Ammonium Oxalate Iron (mg/kg) | 609.64 |
| Buffer Index (equivalents of acid per kg of material to reduce pH to 6) | 0.0318 |
| Mean Particle Size (mm) | 0.0412 |
| pH | 8.12 |
| Total Aluminum (mg/kg) | 781.85 |
| Total Calcium (mg/kg) | 209000. |
| Total Iron (mg/kg) | 1791.28 |

Figure 4.16. A screenshot of the PhROG software is shown with the chemical characteristics inputs highlighted in red.

outweighs the Fe and Al and the pH is close to the cutoff of 8.5 where ligand exchange is not favored, so this is a Ca-based material. Next, since the material is Ca-based, the retention time becomes an important factor since some Ca-based materials are sensitive to retention time with regard to P removal. Thus, based on the pH and buffer index, the Ca-based material in this example is retention time sensitive. In that case, PhROG automatically will set the desired retention time for 10 min in the case where a structure is being designed; that is not true when the software is predicting the performance of an existing structure. Fig. 4.17 shows the retention time set for 10 min.

Retention Time

| Design Structure | Existing Structure |
|--|--------------------|
| Desired Retention Time (min) | 10 |
| Average Dissolved P Concentration (mg/L) | 1 |
| Annual Flow Volume (gallons) | 1000000 |
| Desired Removal Goal (%) | 35 |
| Desired Lifetime (years) | 1 |
| Drainage Pipe Diameter (inches) | 4 |
| Drainage Pipe Slope (decimal) | 0.01 |

| Design Bed Size | Existing Bed Size | Design Ditch Size | Existing Ditch Size |
|--|-------------------|-------------------|---------------------|
| Minimum Flow Rate Through Filter (gpm) | | 400 | |
| Maximum Decrease in Ditch Flow (%) | | 35 | |
| Maximum Allowable Length (feet) | | 500 | |
| Ditch Top Width (feet) | | 12 | |
| Ditch Bottom Width (feet) | | 8 | |
| Ditch Depth (feet) | | 5 | |
| Ditch Slope (decimal) | | 0.001 | |
| Manning's Roughness Coefficient | | 0.07 | |

Figure 4.17. A screenshot of the PhROG software showing the desired structure retention time highlighted in red.

The only remaining inputs required are the physical characteristics of the PSM which are used in determining flow rate, depth of material, and the volume required to house the mass of material. For this material we used a value of 1.4 g cm^{-3} for the bulk density, 0.45 for the porosity, and 0.01 cm sec^{-1} for the hydraulic conductivity which were all input into the Material Physical Characteristics tab shown in Fig. 4.18. The bulk density is used to calculate the volume required for the structure, so the structure size given in the output will be incorrect if the bulk density is not reported accurately. The actual retention time is calculated using the porosity, so an accurate value for it is vital, especially for retention time sensitive materials.

Material Physical Characteristics

| | |
|----------------------------------|------|
| Bulk Density (g/cm^3) | 1.4 |
| Hydraulic Conductivity (cm/sec) | 0.01 |
| Porosity (decimal) | 0.45 |

Physical characteristics

Figure 4.18. A screenshot of the PhROG software showing the material physical characteristics highlighted in red.

The gypsum used in this example has a low hydraulic conductivity moving only 0.01 cm per sec compared to a sieved slag which can be in excess of 1 cm per sec . Now that all of the inputs are complete, we can run the program by clicking the Go button shown in Fig. 4.19.

Total P Removal (optional)

Mean Particle Size of Filter Media (mm)

Average Total Phosphorus Concentration (mg/L)

Average Sediment Concentration (mg/L)

Deposition Rate (grams of sediment/minute of flow)

Material Physical Characteristics

Bulk Density (g/cm³)

Hydraulic Conductivity (cm/sec)

Porosity (decimal)

Design Structure Existing Structure

Desired Retention Time (min)

Average Dissolved P Concentration (mg/L)

Annual Flow Volume (gallons)

Desired Removal Goal (%)

Desired Lifetime (years)

Drainage Pipe Diameter (inches)

Drainage Pipe Slope (decimal)

Estimate Design Curve Manually Input Design Curve (y=be^{mx})

Ammonium Oxalate Aluminum (mg/kg)

Ammonium Oxalate Iron (mg/kg)

Buffer Index (equivalents of acid per kg of material to reduce pH to 6)

Mean Particle Size (mm)

pH

Total Aluminum (mg/kg)

Total Calcium (mg/kg)

Total Iron (mg/kg)

Design Bed Size Existing Bed Size Design Ditch Size Existing Ditch Size

Maximum Width of Structure (feet)

Maximum Length of Structure (feet)

Minimum Flow Rate (gpm)

Hydraulic Head (inches)

Note: Hydraulic Head is equal to the elevation drop over the maximum length or the elevation difference between inlet and ultimate outlet.

Runs the Program

Figure 4.19. A screenshot of the interface of the PhROG software with the Go button highlighted in red.

The output of PhROG contains all of the information required to build a P removal structure and includes information about removal performance and how well the user's goals were met. The output for a ditch structure design is shown in Fig. 4.20 with the area containing structure design outlined in red.

How to Build Structure

| Ditch Output | |
|--|----------------------|
| Mass Required (tons) | 45.37 |
| Depth of Material (inches) | 6.3 |
| Length of Structure (ft) | 281.685 |
| Number of Subsurface Drainage Pipes Needed | 4 |
| Actual RT (min) | 11.8068 |
| Actual Maximum Flow Rate Through the PSM (gpm) | 295.945 Goal not met |
| Actual Decrease in Flow in Ditch (%) | 0. |
| Estimated lifetime to meet both minFR and RT | 1.3 |

| Years | Cumulative Dissolved P (%) | Cumulative Dissolved P (lbs) |
|-------|----------------------------|------------------------------|
| 1 | 35. | 2.921 |
| 1.733 | 21.5 | 3.11 |

Figure 4.20. A screenshot of a ditch structure design output produced using PhROG software.

The first line is the mass of PSM required, which in this case is 45.37 ton of gypsum; this amount of gypsum could be delivered in two tractor trailer loads. The depth of material is only 6.3 in deep

which is not surprising given the low hydraulic conductivity of this material. For a material with a low conductivity it has to be spread out thinly over a large area to be able to handle larger flow rates and also not exceed the maximum decrease in ditch flow capacity specified by the user. PhROG constrains the depth of material to be no less than the diameter of the subsurface drainage pipe, so that water has to flow through the material before entering the pipe. The output also specifies the length of the ditch structure to be 281.7 ft.

Lastly, the number of subsurface drainage pipes required for this ditch structure is shown to be 4 pipes, of the diameter specified by the user (4 inches). If the software calls for more pipes than the user wishes to use, simply increase the pipe diameter or reduce the minimum flow rate through the filter at the input, and rerun the program. The rest of the output shows how well this design meets the user's constraints and goals, which is highlighted in Fig. 4.21. The software calculates the retention time of the structure after designing it, which is then reported. If the

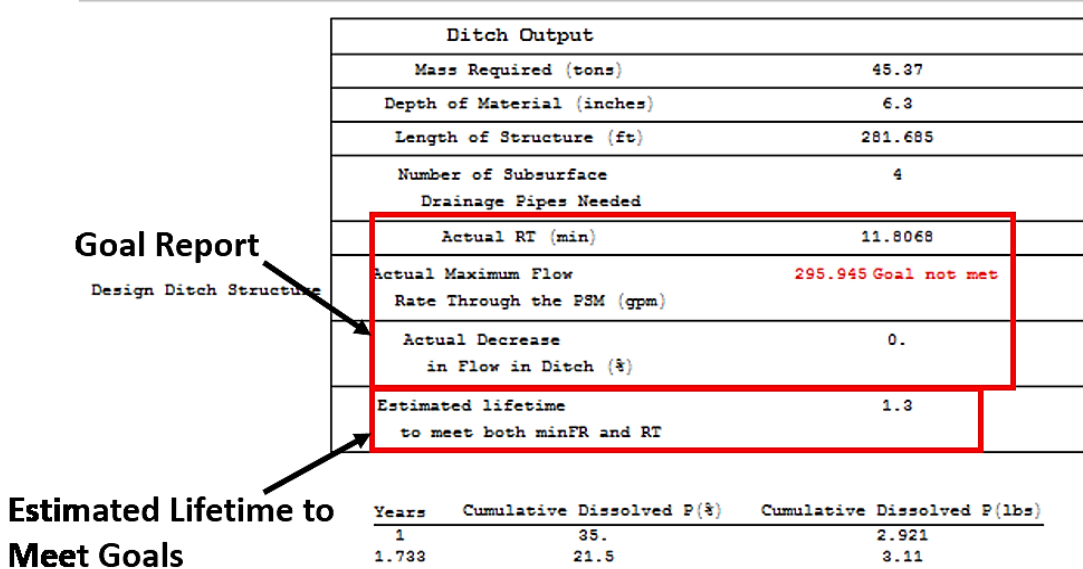


Figure 4.21. An example output from the PhROG software that highlights the goals and the estimated lifetime to meet minimum flow rate and retention time variable.

material is not retention time sensitive then the output will state “non-retention time sensitive”, and in some rare cases, if the retention time is not met for a sensitive material it will appear in red. In this case it was able to achieve the retention time desired, but was not able to meet the

minimum desired flow rate through the structure. It reports the actual flow rate that the structure can handle and highlights it in red if it is less than the user's specified goal. The actual decrease in ditch flow is also listed as a percentage of the original flow. In this example the material was shallow enough that there is no decrease in ditch flow with the addition of the P removal structure.

For designs that are unable to meet the flow requirements, there is an additional output variable calculated that estimates the lifetime required to meet both the retention time and minimum flow rate goals. As the lifetime is increased, the required mass of PSM increases, which increases the pore volume and surface area. The increased surface area increases the flow rate through the material, but does not sacrifice retention time because a proportional amount of pore space is also added with the increased mass. This in turn makes higher flow rates attainable without reducing the retention time, so both goals can be met. In some non-sensitive materials with very low hydraulic conductivity, the increase in mass and therefore surface area can help increase flow of the water down into the subsurface drainage layer allowing for greater flow rates through the filter. Regardless, the user simply needs to change the desired lifetime to the one suggested in red text and rerun the software.

The last portion of the output is a table that specifies P removal on an annual basis, expressed as both a percentage of the cumulative dissolved P removed and the cumulative mass (in lbs) removed (Fig. 4.22). In this example, the design meets the user goal of 35% cumulative P

Removal Performance

| | | |
|---|--|-----|
| Estimated lifetime to meet both minFR and RT | | 1.3 |
|---|--|-----|

| Years | Cumulative Dissolved P (%) | Cumulative Dissolved P (lbs) |
|-------|----------------------------|------------------------------|
| 1 | 35. | 2.921 |
| 1.733 | 21.5 | 3.11 |

Figure 4.22. An example output of the PhROG software that shows the removal performance of the ditch structure design highlighted in red.

removal in 1 y, but the table shows that the material will last 1.733 years, removing 21.5% of the

P that enters the structure during that time. The final listed time is essentially the predicted amount of time that the P removal structure will be able to remove any dissolved P at all. At that point, the concentration of dissolved P entering the structure is the same as the concentration exiting the structure (i.e. treated water), and therefore the material is “spent”. The year by year breakdown provides the complete performance of the structure and allows the user to make an informed decision on when to replace the PSM.

Since the design did not meet our minimum flow goal, and thus it called for increasing the lifetime in order to meet the goal, we will rerun the program with an increased lifetime of 3 yr instead of 1 yr. All of the other inputs were left unchanged before clicking “Go” to obtain the new output shown in Fig. 4.23.

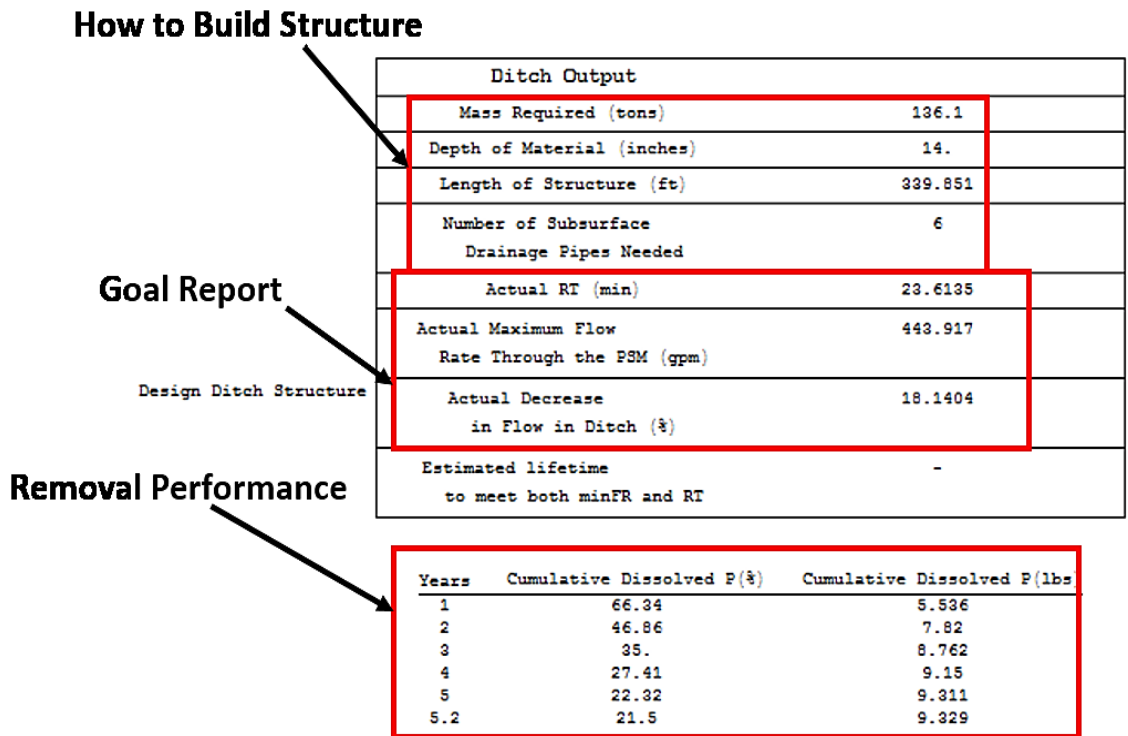


Figure 4.3. An example output for a ditch structure designed using PhROG software.

The mass increased from 45.33 ton to 136.1 ton or 3 times as much, which makes sense given the increase in lifetime from 1 to 3 yr. The depth of material increased from 6.3 to 14 inches, which allowed the length of the structure to only increase an additional 60 ft for a final length of 340 ft;

this was well within the maximum of 500 ft we chose for this example. The specified user goals were all achieved, as shown in the output; flow rate of 443 gpm and retention time of almost 24 min. A dramatic change in the output compared to the previous output is found in the table of annual performance; this structure is predicted to last a bit over 5 yr before it is spent, compared to the previous 1.733 yr in the last example. If this larger structure exceeded the available length, then another PSM with a greater P affinity would be required, or decreasing the acceptable minimum flow rate.

One benefit of this software is the ability to test out a variety of scenarios for a site, such as different PSMs or performance goals, without having to do the calculations by hand. Using the same inputs for site characteristics and goals, we change the PSM from the FGD gypsum used earlier to a medium quality steel slag that has been sieved to ¼ inch diameter. The output from the same scenario with the steel slag is shown below in Fig. 4.24. This is also a retention time sensitive material, so the retention time of 10 min was met at the cost of the minimum flow rate that we specified, 400 gpm. The structure is much smaller in length than the gypsum design due

Goal Report

Design Ditch Structure

| Ditch Output | |
|--|----------------------|
| Mass Required (tons) | 31.82 |
| Depth of Material (inches) | 19. |
| Length of Structure (ft) | 49.7739 |
| Number of Subsurface Drainage Pipes Needed | 3 |
| Actual RT (min) | 10.7356 |
| Actual Maximum Flow Rate Through the PSM (gpm) | 221.958 Goal not met |
| Actual Decrease in Flow in Ditch (%) | 34.6618 |
| Estimated lifetime to meet both minFR and RT | 1.9 |

| Years | Cumulative Dissolved P (%) | Cumulative Dissolved P (lbs) |
|-------|----------------------------|------------------------------|
| 1 | 35. | 2.921 |
| 1.733 | 21.5 | 3.11 |

Figure 4.24. An example output from PhROG software for a ditch structure that uses sieved steel slag as a PSM.

a greater depth of material, 19 inches versus 6.3 inches for the gypsum, which allows for a much shorter structure (only 153.6 ft long). Unfortunately, the minimum flow rate was not met, so we will increase the desired lifetime to 3 yr and rerun the program. The output shown in Fig. 4.25 shows that all of our goals, including removal percentage, retention time, minimum flow rate, and decrease in ditch flow, are all met. This slag structure uses less material and less space than the 3 yr design using gypsum, so it seems to be a better option assuming that the slag was locally available.

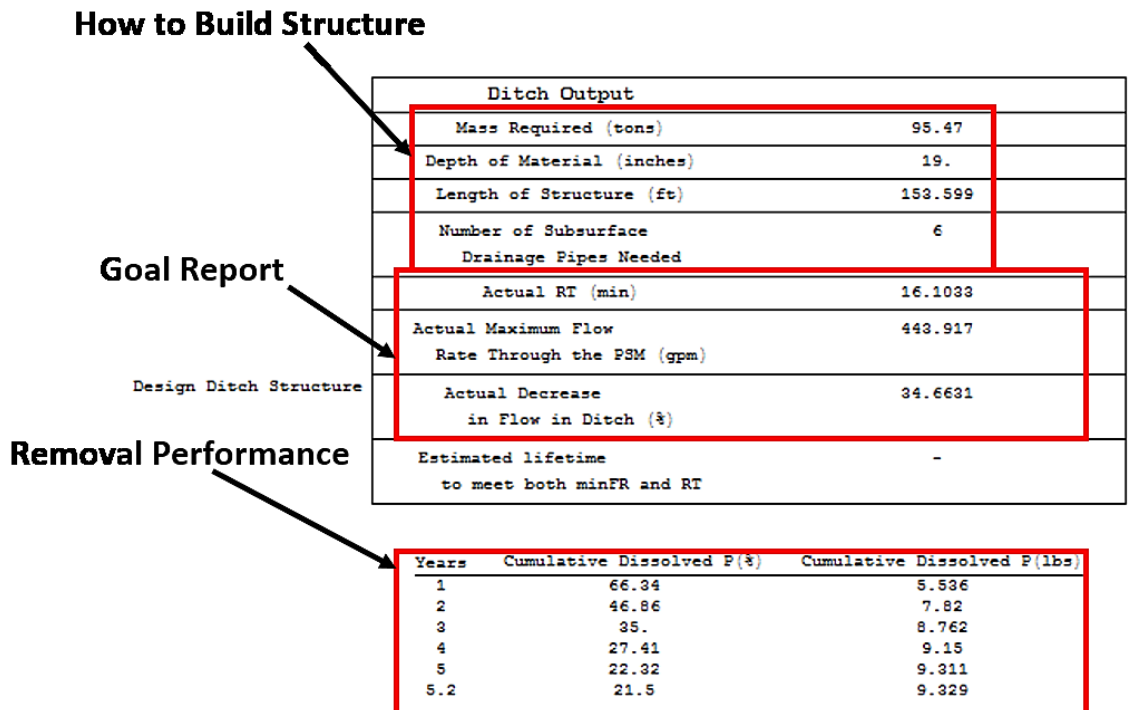


Figure 4.25. An example output from the PhROG software for a ditch structure that uses steel slag as a PSM.

The medium quality steel slag was an improvement over the gypsum with regard to space, but neither material was able to meet all of our goals with a desired lifetime of 1 yr. There is a treatment process that can, on average, increase the P affinity of the slag by 4 times that of an untreated slag of the same size. Developed at Oklahoma State University, it is patent pending and included with the license for the PhROG software. We will use all of the same inputs as the

previous examples and only change the chemical characteristics of PSM to reflect this “treated” slag material. The design output using this treated slag in the ditch with a desired lifetime of 1 yr is shown in Fig. 4.26.

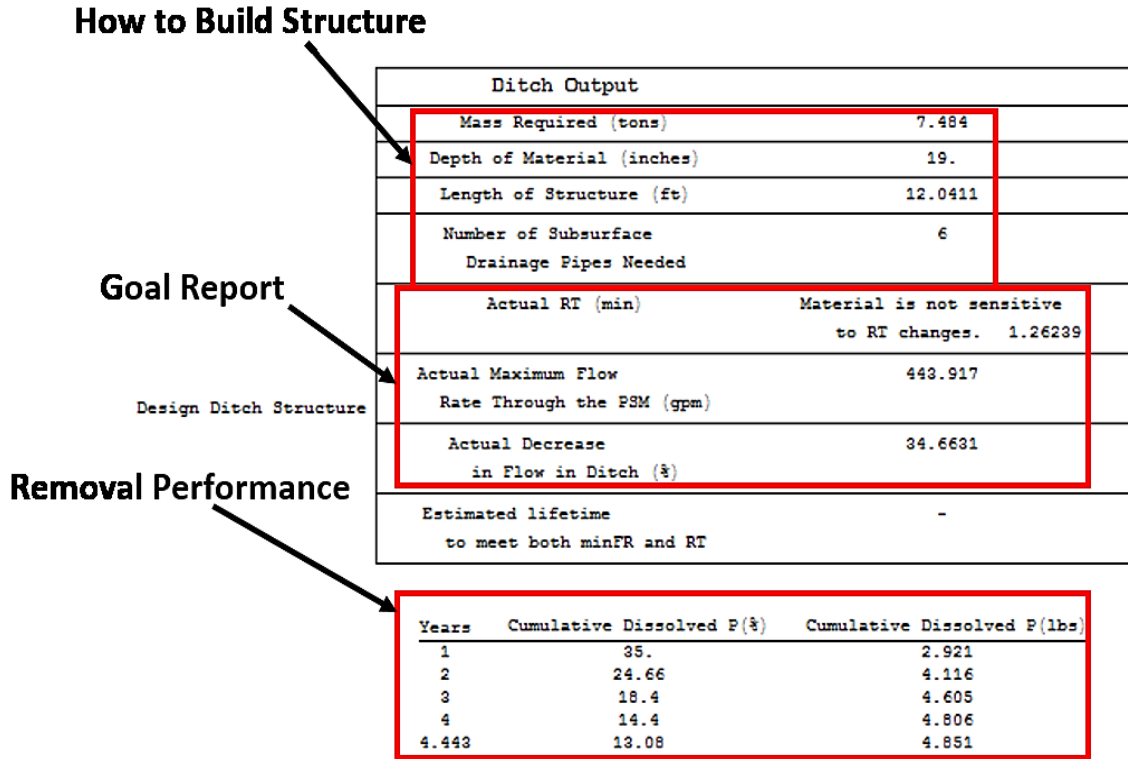


Figure 4.26. An example output from the PhROG software for a ditch structure designed using treated steel slag.

By using the treated slag we were able to meet all of the specified goals, including the minimum flow rate at a desired lifetime of 1 yr, while the other two materials required a lifetime increase to meet the goals. The most obvious difference between the treated slag, untreated slag, and FGD gypsum is their affinity for P which is evident by the mass required to meet the removal goal; 7.5, 31.8, and 45.4 tons, respectively. Both of the slag designs were much shorter in length than the gypsum structure due to their higher hydraulic conductivity which allows for the material to be deeper, yet maintain high flow rates. While the treated slag might seem like the obvious choice, there are other factors to consider: availability of PSM, size of the structure (i.e. length or area), ability to treat the slag, and the cost associated with all of these factors,

Existing Maryland Ditch

Not only does the PhROG software allow users to design a structure to meet certain goals, as shown in our previous example, but it can also be used to quantify the performance of an existing structure. The site characteristics used in the previous example were taken from actual data collected at a Maryland ditch structure, so we will use the same inputs to estimate the performance of a real ditch structure. Use of the software for predicting the performance of a structure requires input of PSMs characteristics as described in the previous example for designing a structure. The input tabs for “Existing Structure” shown in Fig. 4.27 require very similar information as the “Design Structure” tabs. The site characteristics include the average dissolved P concentration and annual flow volume, as illustrated in the previous examples for the design process.

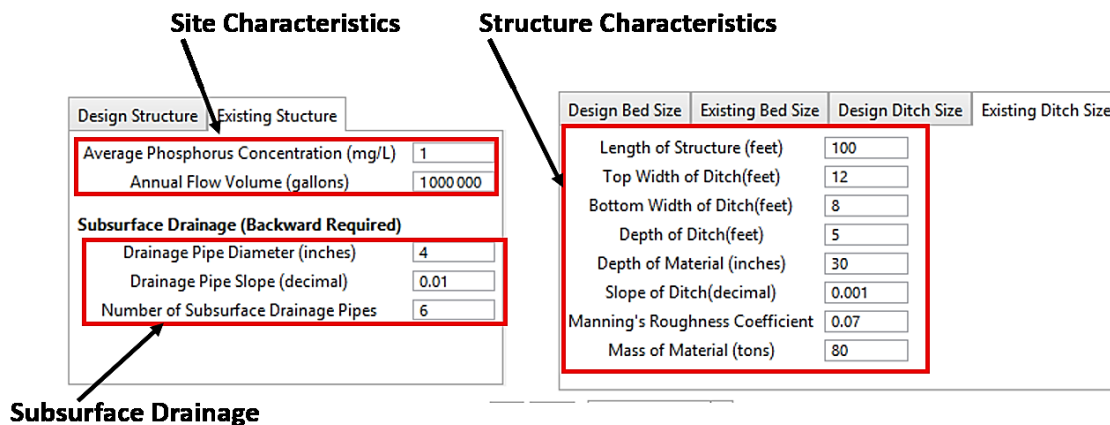


Figure 4.27. This screenshot of the PhROG software shows the input tabs for the characteristics of an existing ditch structure.

The size of the ditch and flow characteristics, such as the slope and Manning’s roughness coefficient, are used to calculate the peak flow rate of the ditch, as is, in order to estimate the decrease in flow rate due to the structure. The mass of PSM and its orientation, depth and length in this case, are each input into the software in order to predict performance. Finally, the diameter and number of subsurface drainage pipes utilized are input by the user, allowing for accurate calculation of the maximum flow through the structure. Many of the inputs are used to calculate what the retention time will be for the structure, and if the PSM is sensitive to retention time, then

this will be reflected in the design curve used to predict P removal. After running the program, the output quantifying the ditch structure will have three main parts as shown in Fig. 4.28. The first part reports the maximum flow through the structure (gpm) and the retention time of the structure (min). The next portion is the actual decrease in ditch flow capacity due to the addition of the structure, which was 60.7% in this case. Since this is an existing structure, there is nothing

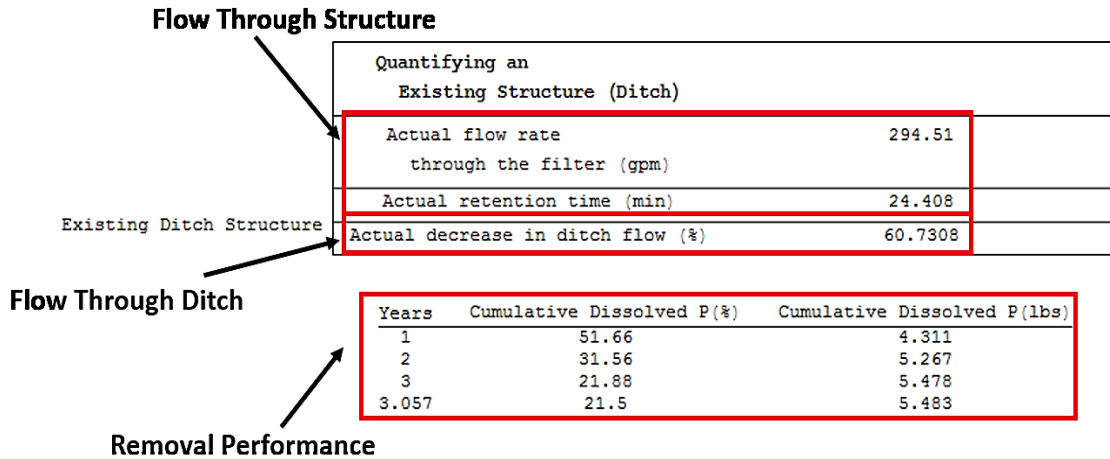


Figure 4.4. The PhROG output shown estimates the performance of an existing ditch structure. can be done to change this loss of flow capacity until the PSM is replaced. Considering that these drainage ditches were constructed to handle a certain amount of flow, a large loss in flow capacity such as this could lead to possible flooding. While it is useful to quantify an existing structure, if this structure had been initially designed using PhROG and then built accordingly, the large loss in ditch flow capacity could have been prevented by simply specifying a desired maximum. The last portion of the output is the year by year breakdown of the cumulative P removal both as a percentage and a load of dissolved P. The final entry in the table is when the PSM is no longer able to remove any more dissolved P.

Vermont Tile Drainage

Tile drained fields are common in the Midwest due to high water tables that interfere with agricultural operations. Water is drained from underneath the surface using a series of pipes which feed into drainage ditches. Unfortunately, the effluent from these drains can contain high concentrations of N and P which leads to eutrophication in surface water bodies that these ditches drain into. P removal structures can be implemented with other best management practices (BMPs) to help reduce nutrient loss from the site. There are several locations within these systems that a P removal structure could be built, including in the drainage ditches, as a blind inlet, or as a buried bed between the tile drain and the drainage ditch. For this example, we will focus on designing a structure that is a subsurface bed that is located between the end of a tile drain and a drainage ditch. This particular Vermont field produces 4,755,000 gal of drainage annually, a peak flow rate of 71.3 gpm, and an average dissolved P concentration of 0.28 mg L^{-1} . As shown in Fig. 4.29, the structure would be supplied by a trunk line and be located below the surface in order for water to flow through the structure freely. Ultimately, it is the elevation of the



Figure 4.5. An example P removal structure design that uses a subsurface bed to treat a tile drain is shown.

tile drain outlet in the ditch, and the distance between that outlet and the bottom of the ditch that provides the hydraulic head for drainage. Thus, the buried bed of PSMs cannot be deeper than the elevation of the bottom of the ditch in which it drains into. The black subsurface drainage pipes within the structure allow the treated water to exit the structure and enter the drainage ditch. For this first example we are designing a subsurface bed that is constrained to 10 ft by 10 ft with the site characteristics and removal goals shown in Fig. 4.30. While there is a relatively large volume

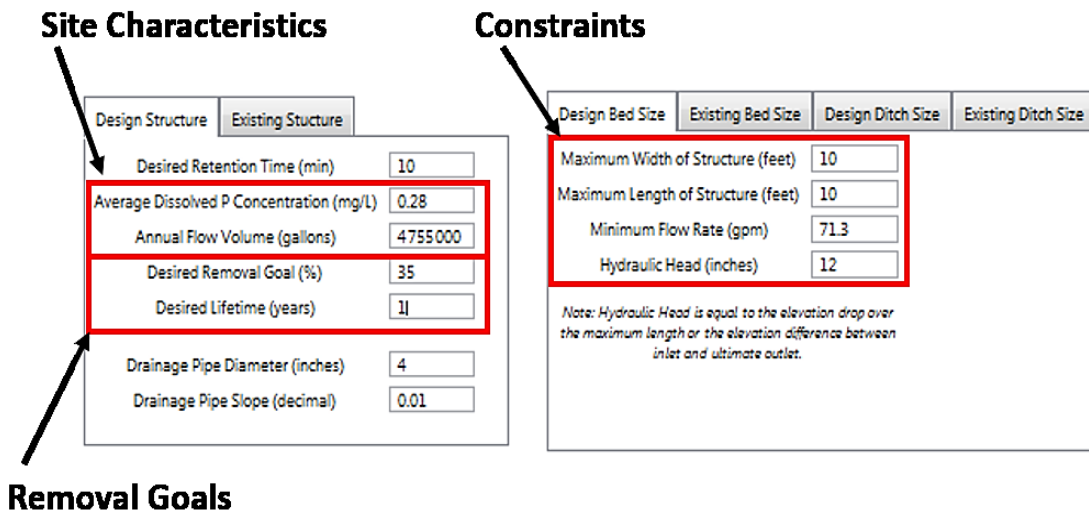


Figure 4.6. The site characteristics and bed design constraints are shown for an example structure in a tile drained field.

of annual runoff, almost 5 million gal, the P concentration of 0.28 mg L⁻¹ results in an annual P load that can be handled with a relatively small sized structure. We will set the size constraints to a 10 ft by 10 ft bed and aim to remove 35% of the load for 1 yr. For this potential structure, there were several PSMs that were locally available, which we characterized. Thus we will design this structure using two of those PSMs: a by-product from limestone mining and wollastonite, a calcium silicate mineral. We will start with the limestone material which is a relatively fine material with a mean particle size of 1.84 mm, but has a hydraulic conductivity of 0.7 cm sec⁻¹ which is similar to a much coarser material. Shown in Fig. 4.31, the design output for limestone meets all of our goals with a little over 1 ton of PSM in a structure that is 2.5 ft by 10 ft. The

structure design will meet our 1 yr goal of 35% and it will last almost 2 yr before it is completely

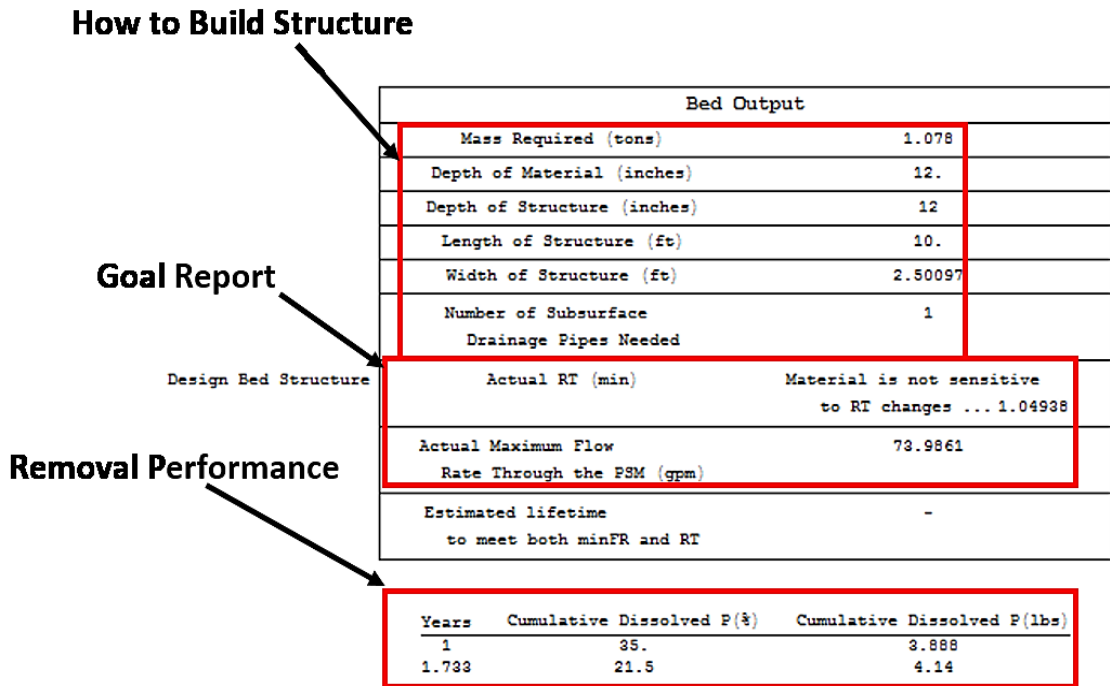


Figure 4.7. An example design for a P removal structure that uses fine limestone to treat tile drain effluent.

spent, but what if we wanted to remove more? Using all of the same site characteristics and the same PSM, let's change the desired removal from 35% to 70% and observe how that changes the design. The 70% removal design shown in Fig. 4.32 is more than twice the size of the structure that removed 35%, but still fits within our constraints of a 10 ft by 10 ft bed. The flow through the structure is the same since both designs had a desired minimum flow rate through the structure of 71.3 gpm. The PSM used in both of these designs has a relatively high hydraulic conductivity and the depth of material is set equal to the hydraulic head present at the site. In this case, our minimum flow rate was rather low due to the need for only a single 4 inch pipe that was required to drain this structure. The predicted performance of this structure was much better than the previous scenario even though it was only about 3.5 times wider than the original design. Instead of being spent after 1.733 yr this structure will last just over 6 yr and remove over 14 lb of P compared to the 4.14 lb for the previous design. The PhROG software makes it easy to compare a

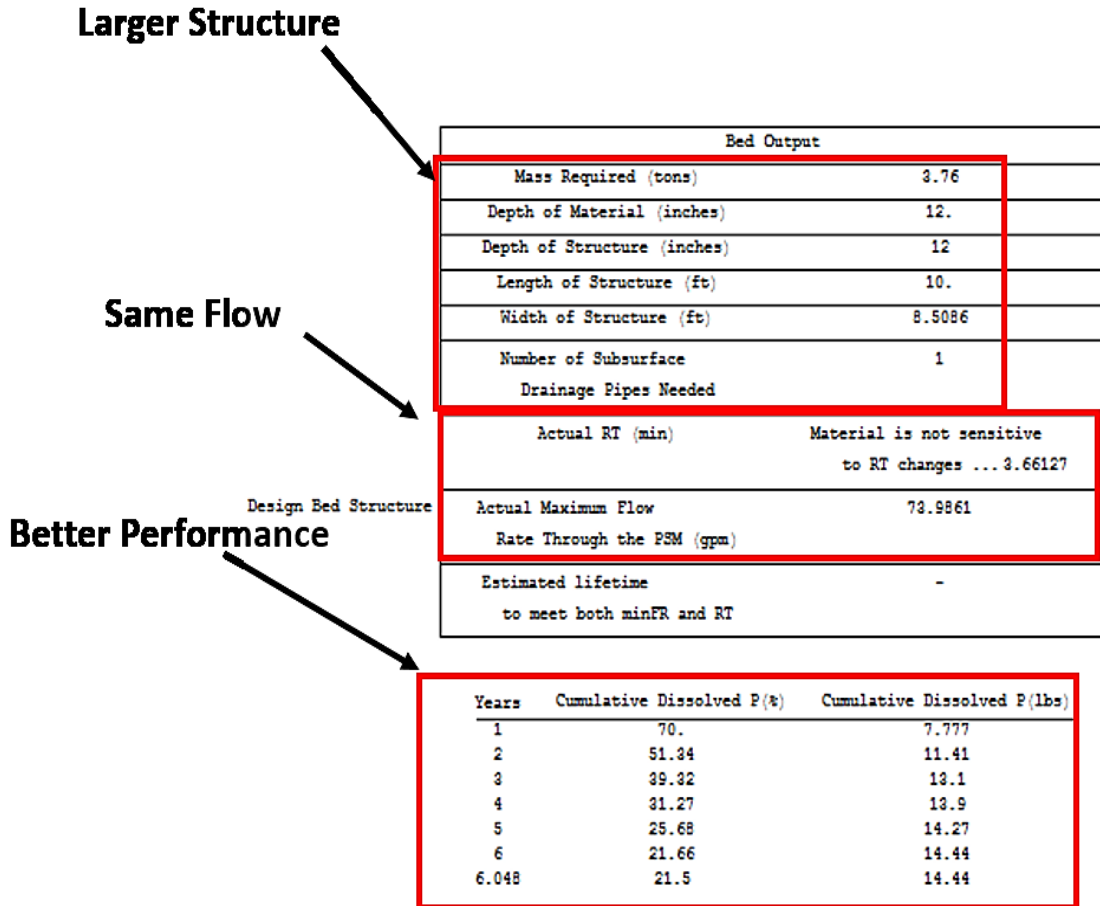


Figure 4.8. An example design for a P removal structure using a fine limestone material to remove 70% of the P load in tile drain effluent.

variety of situations which allows the user an opportunity to choose a design that meets their needs with the least inputs. The table output provided shows a breakdown of the annual cumulative P removal which allows the user to decide the perfect time to replace the PSM in the structure. For this example, the structure removed almost 8 lb in the first year, but that dropped off quickly with only an additional 3.63 lb, 1.69 lb, and 0.8 lb for years 2, 3, and 4, respectively. For the final example with this material, we will use the same inputs and change the removal goal to 70% for 5 y. The structure does not fit in our maximum allowable area being roughly 6 times the size of the previous structure (Fig. 4.33). It does meet our removal goal and will continue to remove P for just over 30 y. If the PSM is left until spent this structure will remove 72.22 lb of

| Bed Output | |
|--|---|
| Mass Required (tons) | 18.8 |
| Depth of Material (inches) | 12. |
| Depth of Structure (inches) | 12 |
| Length of Structure (ft) | 42.1939 Max Length Exceeded |
| Width of Structure (ft) | 10. |
| Number of Subsurface Drainage Pipes Needed | 1 |
| Actual RT (min) | Material is not sensitive to RT changes ... 18.3064 |
| Actual Maximum Flow Rate Through the PSM (gpm) | 73.9861 |
| Estimated lifetime to meet both minFR and RT | - |

Area is exceeded

Flow is met

Removal goal is met

Design Bed Structure

Lasts over 30 years

| Years | Cumulative Dissolved P (%) | Cumulative Dissolved P (lbs) |
|-------|----------------------------|------------------------------|
| 1 | 92.76 | 10.31 |
| 2 | 86.21 | 19.15 |
| 3 | 80.27 | 26.75 |
| 4 | 74.89 | 33.28 |
| 5 | 70. | 38.88 |
| 6 | 65.55 | 43.7 |
| 7 | 61.5 | 47.83 |
| 8 | 57.81 | 51.38 |
| 9 | 54.43 | 54.43 |
| 10 | 51.34 | 57.04 |
| 11 | 48.52 | 59.29 |
| 12 | 45.92 | 61.22 |
| 13 | 43.54 | 62.88 |
| 14 | 41.34 | 64.3 |
| 15 | 39.32 | 65.52 |
| 16 | 37.45 | 66.57 |
| 17 | 35.73 | 67.47 |
| 18 | 34.13 | 68.25 |
| 19 | 32.65 | 68.91 |
| 20 | 31.27 | 69.48 |
| 21 | 29.99 | 69.97 |
| 22 | 28.8 | 70.4 |
| 23 | 27.69 | 70.76 |
| 24 | 26.65 | 71.07 |
| 25 | 25.68 | 71.33 |
| 26 | 24.77 | 71.56 |
| 27 | 23.92 | 71.76 |
| 28 | 23.12 | 71.93 |
| 29 | 22.37 | 72.07 |
| 30 | 21.66 | 72.2 |
| 30.24 | 21.5 | 72.22 |

Figure 4.9. The PhROG design output for a subsurface bed structure using a fine limestone material is shown. This design will remove 70% of the cumulative dissolved P load for 5 y.

dissolved P, but should it be replaced sooner? There is a tradeoff between the cost of replacing the PSM in the structure and the amount of P being removed by the structure that will dictate when it should be cleaned out. The cleanout schedule will depend on a variety of factors, including removal goals and availability of funds. It is important to remember that the software makes all calculations based on the user inputs, so the design is for an average year. If the site is

located in an area that is experiencing drought, and does not produce runoff, then the structure will not remove the estimated amount of P and will last longer than predicted.

For the next example we will use the same inputs as the first scenario with two changes: the PSM used will be wollastonite, and the maximum size of the structure will be 30 ft by 30 ft due to the lesser quality of this material compared to the limestone. Wollastonite is a Ca silicate mineral that contains some Fe, Al, and magnesium (Mg), so it will be in the Ca-based group of materials. Since it relies on Ca phosphate precipitation, the pH must be above neutral and the material must be able to maintain that elevated pH in order for the PSM to be effective at removing P. The output for a structure that will remove 35% of the load over 1 yr is shown in Fig. 4.34, which is in sharp contrast to the structure design for limestone. The mass of wollastonite

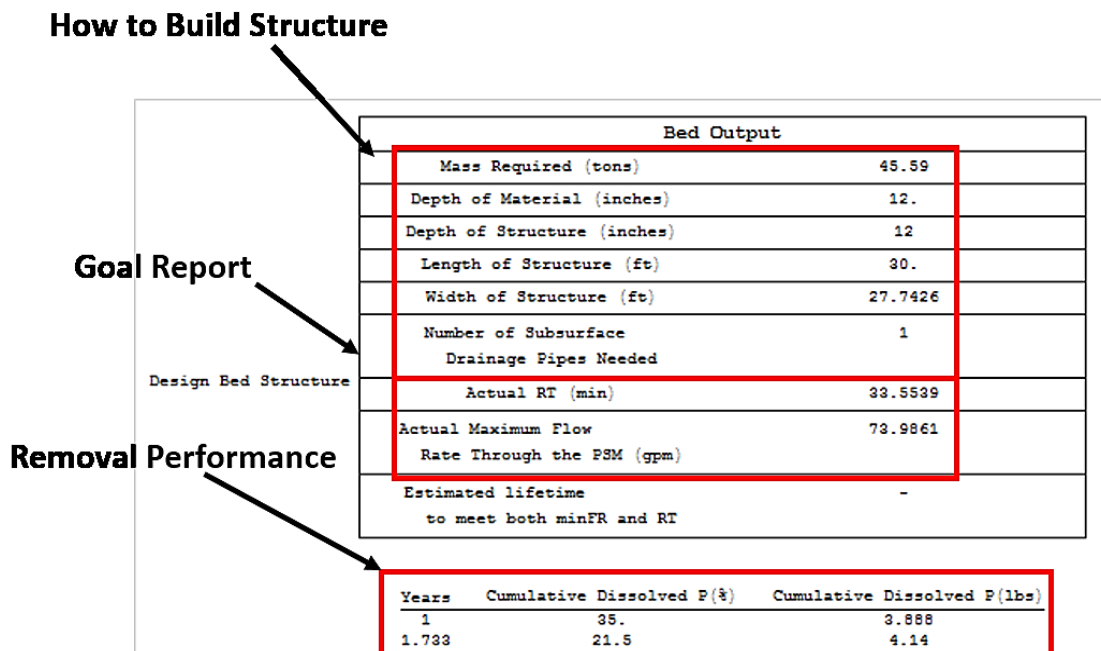


Figure 4.10. An example structure design that uses wollastonite to remove 35% of the annual load for 1 yr.

required to meet the goals is 45.59 tons and covers an area of 832 ft² compared to just over 1 ton of limestone that fit in 25 ft². The two materials have one distinct chemical difference: their buffer index which is 0.09 for wollastonite and 1.38 for the fine limestone. This buffering has a dramatic impact on the ability of a Ca-based material to sorb P, which is highlighted in the

difference in the mass required for wollastonite and limestone in meeting the same P removal goals. This difference is even more dramatic when we try to remove 70% of the load using the poorly buffered wollastonite. The design output shown in Fig. 4.35 calls for a structure that is almost 2,900 ft² and contains 159 tons of the wollastonite in order to meet the same 70% removal goal that 3.76 ton of limestone could achieve. If the user only has a small area available for the P removal structure, then the wollastonite would not be feasible with the current goals, so another PSM would have to be used or the goals would need to be reduced. The ability to work through these different scenarios easily using PhROG allows the user to find the appropriate design for their needs.

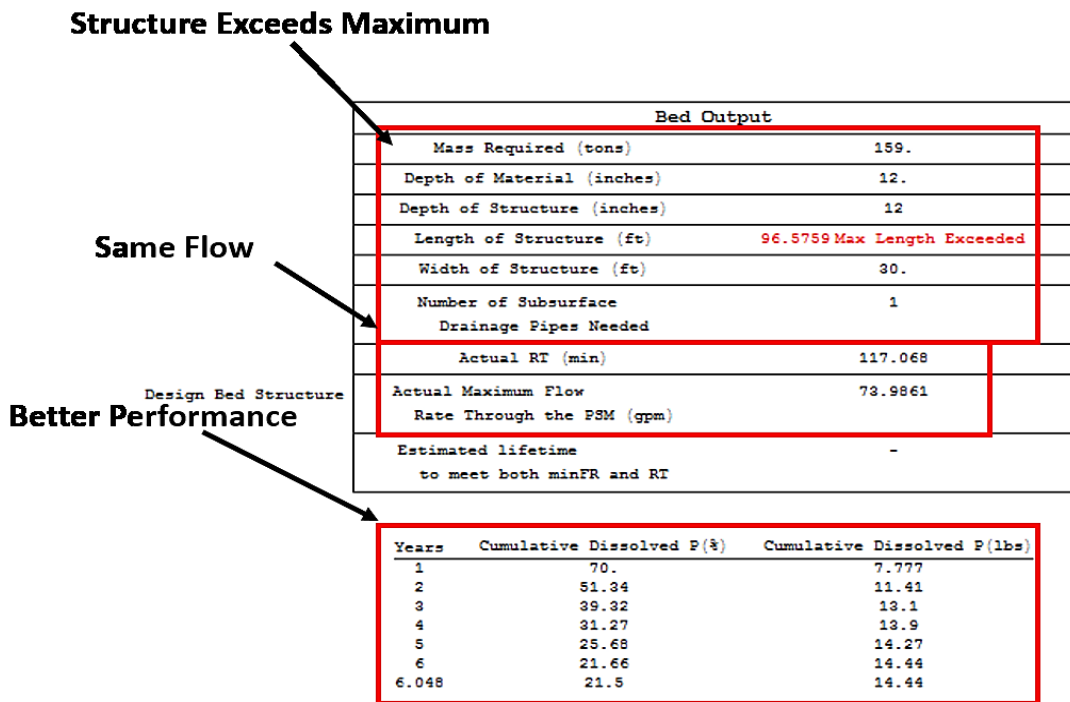


Figure 4.11. The example output from PhROG for a subsurface bed treating tile drainage using wollastonite material.

Surface and Blind Inlets

In tile drained fields there are small depressions where water collects that were originally drained using tile risers. This riser would connect the surface to the tile drain below, but these circumvent the soil allowing sediment and nutrients to reach the tile drain without coming into contact with the soil. In order to help reduce nutrient and sediment loss these tile risers have been replaced with inlets that consist of a gravel or sand bed that connects to the tile drain. If the inlet is buried with soil then it is considered a blind inlet like the one shown in Fig. 4.36 (Feyereisen et al., 2015; USDA, 2001). Water filters through the porous media before entering the tile drain which allows for sediment deposition and sorption of nutrients. The media used for these inlets is

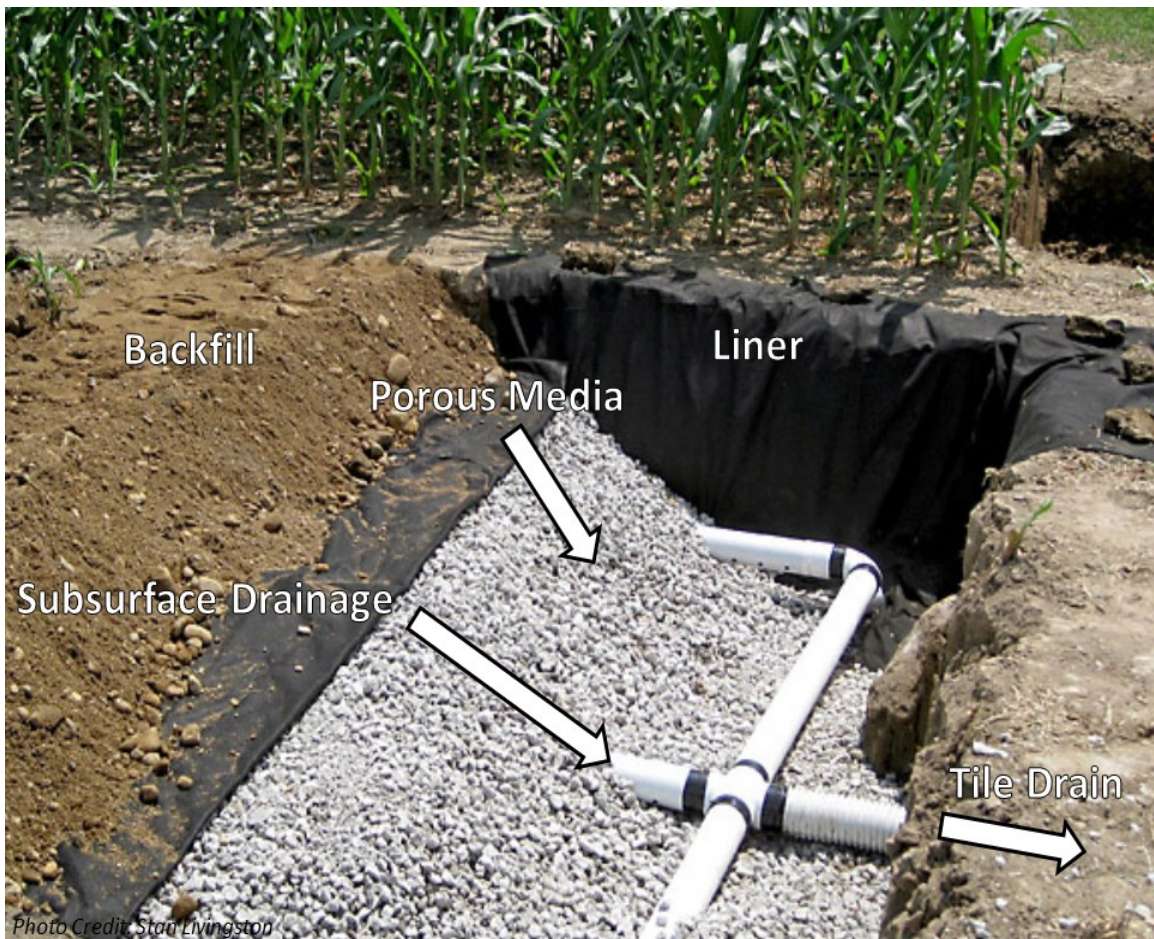


Figure 4.12. A blind inlet is pictured that is partially exposed to show the drainage layer and media.

usually a gravel or sand which work well for physical filtration. If the gravel used is a limestone material then precipitation of Ca phosphates is possible depending on the pH and buffering capacity of the material. If the media of an inlet is a PSM then these inlets can be considered a P removal structure since it encompasses all of the characteristics of a structure, and therefore can be designed or estimated using the PhROG software. For this example we will examine a blind inlet for an Indiana field that drains about 12 acres with an average dissolved P concentration of 0.25 mg L⁻¹, total P concentration of 0.75 mg L⁻¹, and produces an annual flow volume of 2,830,000 gal.

Existing Blind Inlet

For the next example, we will use PhROG to estimate the removal performance of an existing inlet. We will use the site characteristics previously listed. The blind inlet we are going to use for this is 14 ft wide by 14 ft long, 2 ft deep, and filled with 16 ton of limestone. We have flow data and P concentrations for this structure, as well as chemical characterizations of several limestone materials. Just like when we designed a structure, the software requires the user to input the annual flow volume and P concentration. In addition to this it requires the dimensions of the structure, mass of material used, and the size and number of drainage pipes as shown in Fig. 4.37. The software will use the dimensions of the filter and the number of drainage pipes in

Site Characteristics

| | |
|--|--------------------|
| Design Structure | Existing Structure |
| Average Phosphorus Concentration (mg/L) | 0.25 |
| Annual Flow Volume (gallons) | 2830 000 |
| Subsurface Drainage (Backward Required) | |
| Drainage Pipe Diameter (inches) | 4 |
| Drainage Pipe Slope (decimal) | 0.01 |
| Number of Subsurface Drainage Pipes | 1 |

Structure Characteristics

| Design Bed Size | Existing Bed Size | Design Ditch Size | Existing Ditch Size |
|----------------------------|-------------------|-------------------|---------------------|
| Length of Structure (feet) | 14 | | |
| Width of Structure (feet) | 14 | | |
| Depth of Material (inch) | 24 | | |
| Mass of Material (tons) | 16 | | |
| Hydraulic Head (inches) | 24 | | |

Note: Hydraulic Head is equal to the elevation drop over the maximum length or the elevation difference between inlet and ultimate outlet.

Figure 4.13. A screenshot from the PhROG software showing inputs used to quantify an existing bed structure.

conjunction with the physical characteristics of the PSM to calculate flow through the filter and the retention time. This information is reported along with removal performance. For the first material, it is a relatively large limestone gravel with a mean particle size of 8 mm and has a decent buffer index as shown in Fig. 4.38. The larger particle size would usually result in the material being less reactive therefore less able to buffer the pH. The chemical characteristics of

Sieved limestone

Estimate Design Curve Manually Input Design Curve (y=be^{mx})

Ammonium Oxalate Aluminum (mg/kg)

Ammonium Oxalate Iron (mg/kg)

Buffer Index (equivalents of acid per kg of material to reduce pH to 6)

Mean Particle Size (mm)

pH

Total Aluminum (mg/kg)

Total Calcium (mg/kg)

Total Iron (mg/kg)

Total P Removal (optional)

Mean Particle Size of Filter Media (mm)

Average Total Phosphorus Concentration (mg/L)

Average Sediment Concentration (mg/L)

Deposition Rate (grams of sediment/minute of flow)

Material Physical Characteristics

Bulk Density (g/cm³)

Hydraulic Conductivity (cm/sec)

Porosity (decimal)

Figure 4.14. A screenshot of the PhROG software showing the chemical and physical characteristics of a sieved limestone being used in a blind inlet.

gravel can vary with the source, so it is important to characterize prospective PSMs in order to accurately estimate P removal. The output when quantifying an existing structure is different from the design output since the structure is already built only the performance is reported as shown in Fig. 4.39. The first thing reported is the actual flow rate through the structure which is

Flow through structure

| Quantifying an Existing Structure (Bed) | |
|---|---------|
| Actual flow rate through the filter (gpm) | 73.9861 |
| Actual retention time (min) | 17.8682 |

Existing Bed Structure

Removal performance

| Years | DP (%) | DP (lbs) | PP (%) | PP (lbs) | TP (%) | TP (lbs) |
|-------|--------|----------|--------|----------|--------|----------|
| 1 | 74.02 | 4.37 | 95.98 | 2.994 | 88.66 | 7.364 |
| 2 | 56.63 | 6.686 | 95.98 | 5.988 | 82.86 | 12.67 |
| 3 | 44.68 | 7.913 | 95.98 | 8.982 | 78.88 | 16.9 |
| 4 | 36.26 | 8.564 | 95.98 | 11.98 | 76.07 | 20.54 |
| 5 | 30.18 | 8.908 | 95.98 | 14.97 | 74.05 | 23.88 |
| 6 | 25.66 | 9.091 | 95.98 | 17.96 | 72.54 | 27.06 |
| 7 | 22.23 | 9.188 | 95.98 | 20.96 | 71.4 | 30.15 |
| 7.252 | 21.5 | 9.204 | 95.98 | 21.71 | 71.15 | 30.92 |

Figure 4.15. The PhROG output quantifying the performance of a blind inlet is shown.

the maximum flow rate without overtopping and the retention time of the structure. The other portion of the output is the same removal performance table that is produced during the design of a structure. This P removal structure will remove a little over 30.92 lb of total P over the course of 7.252 yr which is very good for a material of this size fraction. In Fig. 4.40, we entered the characteristics of a steel slag that has a smaller particle size and buffer index, so it will reduce the removal of the structure. The hydraulic conductivity of this material is little less than the larger

Steel slag

Total P Removal (optional)

Mean Particle Size of Filter Media (mm)

Average Total Phosphorus Concentration (mg/L)

Average Sediment Concentration (mg/L)

Deposition Rate (grams of sediment/minute of flow)

Material Physical Characteristics

Bulk Density (g/cm³)

Hydraulic Conductivity (cm/sec)

Porosity (decimal)

Estimate Design Curve Manually Input Design Curve (y=be^{mx})

| | |
|---|-------------------------------------|
| Ammonium Oxalate Aluminum (mg/kg) | <input type="text" value="0"/> |
| Ammonium Oxalate Iron (mg/kg) | <input type="text" value="0"/> |
| Buffer Index (equivalents of acid per kg of material to reduce pH to 6) | <input type="text" value="0.375"/> |
| Mean Particle Size (mm) | <input type="text" value="5"/> |
| pH | <input type="text" value="10.2"/> |
| Total Aluminum (mg/kg) | <input type="text" value="0"/> |
| Total Calcium (mg/kg) | <input type="text" value="155000"/> |
| Total Iron (mg/kg) | <input type="text" value="0"/> |

Figure 4.16. The chemical and physical characteristics are shown for a steel slag used in a blind inlet.

one, 0.5 cm sec⁻¹ versus 0.7 cm sec⁻¹, but the flow through the structure will be limited by the single 4 in drainage pipe and not the material's conductivity. The output for this steel slag, shown in Fig. 4.41, highlights the impact of buffer index on removal. The flow through the structure and

Same flow

| Quantifying an Existing Structure (Bed) | |
|---|---------|
| Actual flow rate through the filter (gpm) | 73.9861 |
| Actual retention time (min) | 16.0814 |

Existing Bed Structure

Reduced performance

| Years | DP (%) | DP (lbs) | PP (%) | PP (lbs) | TP (%) | TP (lbs) |
|-------|--------|----------|--------|----------|--------|----------|
| 1 | 49.86 | 2.944 | 99.38 | 3.1 | 82.88 | 6.044 |
| 2 | 29.96 | 3.537 | 99.38 | 6.201 | 76.24 | 9.738 |
| 2.876 | 21.5 | 3.651 | 99.38 | 8.918 | 73.42 | 12.57 |

Figure 4.17. The PhROG output quantifying the P removal performance of a blind inlet is shown. retention time are the same, but the less well buffered steel slag it is only able to remove 12.57 lb of P over 2.876 y compared with 30.92 lb of P over 7.252 y. The final material we are going to

examine is a limestone sand that has a particle size of 2 mm, but has the lowest buffer index of the three at 0.09. The pH, Ca content, and physical characteristics are similar to the previous materials as shown in Fig. 4.42, so buffer index is the only factor affecting removal performance.

Limestone sand

Total P Removal (optional)

Mean Particle Size of Filter Media (mm)

Average Total Phosphorus Concentration (mg/L)

Average Sediment Concentration (mg/L)

Deposition Rate (grams of sediment/minute of flow)

Material Physical Characteristics

Bulk Density (g/cm³)

Hydraulic Conductivity (cm/sec)

Porosity (decimal)

| Estimate Design Curve | | Manually Input Design Curve (y=be ^{mx}) | |
|---|-------------------------------------|---|--|
| Ammonium Oxalate Aluminum (mg/kg) | <input type="text" value="0"/> | | |
| Ammonium Oxalate Iron (mg/kg) | <input type="text" value="0"/> | | |
| Buffer Index (equivalents of acid per kg of material to reduce pH to 6) | <input type="text" value="0.09"/> | | |
| Mean Particle Size (mm) | <input type="text" value="2"/> | | |
| pH | <input type="text" value="9.3"/> | | |
| Total Aluminum (mg/kg) | <input type="text" value="0"/> | | |
| Total Calcium (mg/kg) | <input type="text" value="165000"/> | | |
| Total Iron (mg/kg) | <input type="text" value="0"/> | | |

Figure 4.42. The PhROG input screen is shown with the characteristics of a limestone sand PSM.

All of the other inputs remain the same as the last two examples. The blind inlet utilizing limestone sand would only remove 4.855 lb of total P in just over a year (Fig. 4.43). Compared to

Same flow

| Quantifying an Existing Structure (Bed) | |
|---|---------|
| Actual flow rate through the filter (gpm) | 73.9861 |
| Actual retention time (min) | 16.0814 |

Existing Bed Structure

Reduced performance

| Years | DP (%) | DP (lbs) | PP (%) | PP (lbs) | TP (%) | TP (lbs) |
|-------|--------|----------|--------|----------|--------|----------|
| 1 | 23.65 | 1.396 | 100. | 3.12 | 74.55 | 4.516 |
| 1.106 | 21.5 | 1.404 | 100. | 3.451 | 73.83 | 4.855 |

Figure 4.18 The PhROG output for an existing blind inlet that utilizes a limestone sand is shown.

the previous examples which removed 2.5 and over 6 times the amount of P. The quality of material has a dramatic impact on removal, so it is vital that PSMs used have been adequately characterized both chemically and physically. Using the chemical characterization and PhROG, a user can explore a variety of scenarios, including different PSMs and goals, all at the touch of a button.

Bioretention Cell

Runoff from urban areas is an issue due to large impervious areas, such as parking lots, where water cannot infiltrate, so there is a larger volume of runoff produced in a short time period. Low impact development reduces the change in a site's hydrology due to urban development by utilizing green roofs, permeable pavement, bioretention cells, and other BMPs that increase infiltration or buffer runoff. The bioretention cell, or "rain garden", is constructed by removal of native soil which is replaced by a media layer like the one shown in Fig. 4.44. The surface of the bioretention cell is covered with a thin layer of soil or rocks which serve as

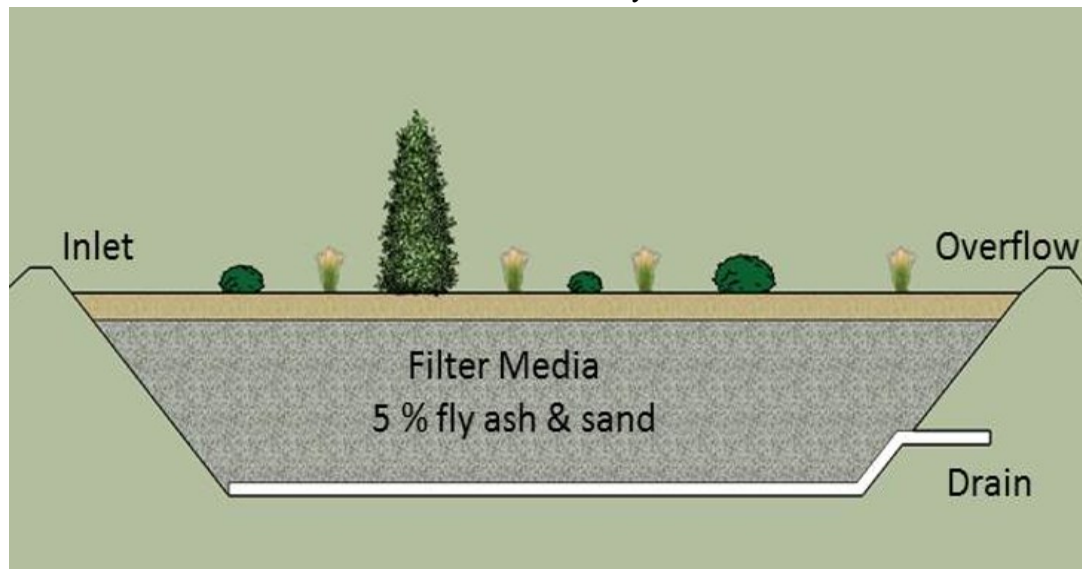


Figure 4.44. A cut away side view of a bioretention cell is shown with the inlet, outlet, and media layer labelled. The media layer is buried beneath a small layer of soil that is pictured as the thin brown layer.

growth media for plants, such as bushes or grass. The subsurface drainage and the porous media covering it make an easy path for water to flow through after it passes through the initial soil or rock layer. The size of the bioretention cell is a product of the runoff volume produced in a specific sized storm that the designer wishes the structure to handle (County, 1993). A completed bioretention cell, such as the one shown in Fig. 4.45, can make an attractive addition to the

landscape while also aiding in storm water retention and treatment of runoff water depending on



Figure 4.45. A completed bioretention cell is pictured in the foreground with a surface layer of rock with several small bushes planted in it.

the type of filter media used. If a PSM is used as the filter media and the area has elevated P, then the bioretention cell meets all of the characteristics of a P removal structure since runoff enters the structure and flows through a PSM, and the PSM can be cleaned out after it is spent. Since the bioretention cell is a bed of material with a drainage layer, it is no different than any other PSM bed we have designed using PhROG, and thus requires the same inputs. The inputs and desired removal goals are shown in Fig. 4.46. We will use a 5% fly ash 95% sand mixture for the PSM and aim to remove 50% of the annual P load for 25 yr. The site produces almost 200,000 gal of runoff annually that has an average dissolved P concentration of 0.5 mg L^{-1} . The maximum size of the bioretention cell will be 35 ft wide, 35 ft long, and 2 ft deep and must be able to handle 40 gpm. This is a relatively small flow rate to handle and the annual load of 0.2 lb of P would normally not require a large structure, but the desired lifetime of 25 y will result in a large structure.

Total P Removal

Total P Removal (Optional)

| | |
|--|-------|
| Mean Particle Size of Filter Media (mm) | 1.786 |
| Average Total Phosphorus Concentration (mg/L) | 0.8 |
| Average Sediment Concentration (mg/L) | 1.5 |
| Deposition Rate (grams of sediment/minute of flow) | 0.05 |

Chemical Characteristics

Estimate Design Curve | Manually Input Design Curve (y=be^{mx})

| | |
|---|-------|
| Ammonium Oxalate Aluminum (mg/kg) | 0 |
| Ammonium Oxalate Iron (mg/kg) | 0 |
| Buffer Index (equivalents of acid per kg of material to reduce pH to 6) | 0.22 |
| Mean Particle Size (mm) | 1.786 |
| pH | 8.479 |
| Total Aluminum (mg/kg) | 0 |
| Total Calcium (mg/kg) | 9957 |
| Total Iron (mg/kg) | 0 |

Physical Characteristics

Material Physical Characteristics

| | |
|-----------------------------------|-------|
| Bulk Density (g/cm ³) | 1.55 |
| Hydraulic Conductivity (cm/sec) | 0.36 |
| Porosity (decimal) | 0.312 |

Constraints

| Design Bed Size | Existing Bed Size | Design Ditch Size | Existing Ditch Size |
|------------------------------------|-------------------|-------------------|---------------------|
| Maximum Width of Structure (feet) | | 35 | |
| Maximum Length of Structure (feet) | | 35 | |
| Minimum Flow Rate (gpm) | | 40 | |
| Hydraulic Head (inches) | | 24 | |

Note: Hydraulic Head is equal to the elevation drop over the maximum length or the elevation difference between inlet and ultimate outlet.

Site Characteristics

Design Structure | Existing Structure

| | |
|--|--------|
| Desired Retention Time (min) | 10 |
| Average Dissolved P Concentration (mg/L) | 0.5 |
| Annual Flow Volume (gallons) | 196258 |
| Desired Removal Goal (%) | 50 |
| Desired Lifetime (years) | 25 |

Removal Goals

| | |
|---------------------------------|------|
| Drainage Pipe Diameter (inches) | 2 |
| Drainage Pipe Slope (decimal) | 0.01 |

Subsurface Drainage

Figure 4.46. The PhROG input screen is shown with the various sections highlighted in red. This is an example design of a bioretention cell.

For this initial design shown in Fig. 4.47, this structure will require four 2 inch diameter pipes to achieve 46.6 gpm of flow. All of our goals and constraints are achieved with 108.7 ton of PSM that is placed in a structure that is 35 ft long, 32.14 ft wide, and 2 ft deep. The design meets our flow and dissolved P removal goals while fitting within the maximum area. This structure will remove 13.48 lb of total P during 25 y and last 72.24 y removing 50.94% of the total P load before the material is spent.

| Bed Output | |
|--|---|
| Mass Required (tons) | 108.7 |
| Depth of Material (inches) | 24. |
| Depth of Structure (inches) | 24 |
| Length of Structure (ft) | 35. |
| Width of Structure (ft) | 32.1358 |
| Number of Subsurface Drainage Pipes Needed | 4 |
| Actual RT (min) | Material is not sensitive to RT changes ... 112.492 |
| Actual Maximum Flow Rate Through the PSM (gpm) | 46.6083 |
| Estimated lifetime to meet both minFR and RT | - |

Mass of PSM →

Structure Size →

Meets flow goal →

Design Bed Structure

Meets removal goal →

| Years | DP(%) | DP(lbs) | PP(%) | PP(lbs) | TP(%) | TP(lbs) |
|-------|-------|---------|-------|---------|-------|---------|
| 1 | 96.88 | 0.7933 | 100. | 0.1298 | 98.05 | 0.9231 |
| 2 | 93.89 | 1.538 | 100. | 0.2596 | 96.18 | 1.797 |
| 3 | 91.02 | 2.236 | 100. | 0.3894 | 94.39 | 2.625 |
| 4 | 88.27 | 2.891 | 100. | 0.5192 | 92.67 | 3.41 |
| 5 | 85.63 | 3.506 | 100. | 0.649 | 91.02 | 4.155 |
| 6 | 83.1 | 4.083 | 100. | 0.7788 | 89.44 | 4.861 |
| 7 | 80.67 | 4.624 | 100. | 0.9086 | 87.92 | 5.532 |
| 8 | 78.34 | 5.132 | 100. | 1.038 | 86.46 | 6.17 |
| 9 | 76.1 | 5.608 | 100. | 1.168 | 85.06 | 6.776 |
| 10 | 73.94 | 6.055 | 100. | 1.298 | 83.72 | 7.353 |
| 11 | 71.88 | 6.474 | 100. | 1.428 | 82.42 | 7.902 |
| 12 | 69.89 | 6.868 | 100. | 1.558 | 81.18 | 8.425 |
| 13 | 67.98 | 7.237 | 100. | 1.687 | 79.99 | 8.924 |
| 14 | 66.15 | 7.583 | 100. | 1.817 | 78.84 | 9.4 |
| 15 | 64.39 | 7.908 | 100. | 1.947 | 77.74 | 9.855 |
| 16 | 62.69 | 8.213 | 100. | 2.077 | 76.68 | 10.29 |
| 17 | 61.06 | 8.499 | 100. | 2.207 | 75.66 | 10.71 |
| 18 | 59.49 | 8.768 | 100. | 2.336 | 74.68 | 11.1 |
| 19 | 57.97 | 9.019 | 100. | 2.466 | 73.73 | 11.49 |
| 20 | 56.52 | 9.256 | 100. | 2.596 | 72.82 | 11.85 |
| 21 | 55.12 | 9.477 | 100. | 2.726 | 71.95 | 12.2 |
| 22 | 53.76 | 9.685 | 100. | 2.856 | 71.1 | 12.54 |
| 23 | 52.46 | 9.881 | 100. | 2.985 | 70.29 | 12.87 |
| 24 | 51.21 | 10.06 | 100. | 3.115 | 69.51 | 13.18 |
| 25 | 50. | 10.24 | 100. | 3.245 | 68.75 | 13.48 |
| - | - | - | - | - | - | - |
| 72.24 | 21.5 | 12.72 | 100. | 9.377 | 50.94 | 22.09 |

Figure 4.47. The PhROG output screen is shown with the different sections highlighted in red. This design is for a bioretention cell that will remove 50% of the annual P load for 20 y and is drained by 2 in pipes.

The diameter and slope of the pipes used in the subsurface drainage layer have a dramatic effect on the maximum flow rate a structure can handle. The choice of pipe diameter can impact the cost of materials and installation, so we will look at a couple of alternatives to this design. We will use all of the same site characteristics, goals, constraints, and PSM, but use a different diameter pipe. The design output shown in Fig. 4.48 uses 4 in pipes for subsurface drainage. The PSM mass,

Same Mass of PSM

Same Size Structure

Fewer Pipes

| Bed Output | |
|--|---|
| Mass Required (tons) | 108.7 |
| Depth of Material (inches) | 24. |
| Depth of Structure (inches) | 24 |
| Length of Structure (ft) | 35. |
| Width of Structure (ft) | 32.1358 |
| Number of Subsurface Drainage Pipes Needed | 1 |
| Actual RT (min) | Material is not sensitive to RT changes ... 70.8655 |
| Actual Maximum Flow Rate Through the PSM (gpm) | 73.9861 |
| Estimated lifetime to meet both minFR and RT | - |

Figure 4.48. The PhROG output screen is shown with the different sections highlighted in red. This design is for a bioretention cell that will remove 50% of the annual P load for 25 y and is drained by a 4 in pipe.

removal performance, and the structure size are all the same as the design that used 2 in pipes, but the pipe number is reduced. Instead of the 4 pipes required in the previous design this one only requires 1 pipe to handle all of the flow produced by the structure. The maximum flow of the structure increased from 46.6 gpm in the original design to 74 gpm in this one with no change in the structure size. The limiting factor in flow through the structure is due to the subsurface drainage, so the increase in flow is due solely to the increased pipe diameter. The number of pipes was reduced from 4 to 1, but what if we could not find any 4 in pipe locally? Fig. 4.49 shows the design output for a structure that has identical inputs as the previous two except for the drainage pipe which we changed to 6 in diameter. Just like the previous two structure designs the mass of PSM is 108.7 ton that removes 50% of the annual P load for 25 yr, but the structure size increased by 0.05 ft in width.

| Bed Output | |
|---|--|
| Mass Required (tons) | 108.7 |
| Depth of Material (inches) | 24. |
| Depth of Structure (inches) | 24 |
| Length of Structure (ft) | 35. |
| Width of Structure (ft) | 32.1904 |
| Number of Subsurface Drainage Pipes Needed | 1 |
| Actual RT (min) | Material is not sensitive to RT changes ... 24.0358 |
| Actual Maximum Flow Rate Through the PSM (gpm) | 218.136 |
| Estimated lifetime to meet both minFR and RT | - |

Figure 4.49. The PhROG output screen is shown with the different sections highlighted in red. This design is for a bioretention cell that will remove 50% of the annual P load for 25 y and is drained by a 6 in pipe.

PhROG will automatically increase the size of the structure to compensate for the volume displaced by the subsurface drainage pipes. The volume displaced by the drainage pipes used in the first two designs is equal, so the structure size was the same. The third design had the same mass of PSM with a larger volume displaced by the drainage pipe, so the structure size had to increase to allow room for the PSM and the drainage pipe. PhROG allows the user to try out a variety of pipe sizes and slopes for each design by changing one or two values which could potentially save money and time during construction.

Existing Bioretention Cell

For the final example, we will use PhROG to estimate the removal performance of an existing bioretention cell. The structure was filled with 293.3 ton of a 5% fly ash 95% sand mixture that less buffered than the mixture used in the previous design examples. It was a relatively large structure at 70 ft long by 29.3 ft wide and 3 ft deep (Fig. 4.50). The site produced an

annual runoff volume of 472,743 gal with an average dissolved P concentration of 0.5 mg L⁻¹.

Total P Removal

Total P Removal (optional)

| | |
|--|------|
| Mean Particle Size of Filter Media (mm) | 2.27 |
| Average Total Phosphorus Concentration (mg/L) | 0.75 |
| Average Sediment Concentration (mg/L) | 1.15 |
| Deposition Rate (grams of sediment/minute of flow) | 0.05 |

Chemical Characteristics

Estimate Design Curve | Manually Input Design Curve ($y=be^{mx}$)

| | |
|---|--------|
| Ammonium Oxalate Aluminum (mg/kg) | 0 |
| Ammonium Oxalate Iron (mg/kg) | 0 |
| Buffer Index (equivalents of acid per kg of material to reduce pH to 6) | 0.076 |
| Mean Particle Size (mm) | 2.27 |
| pH | 8.006 |
| Total Aluminum (mg/kg) | 0 |
| Total Calcium (mg/kg) | 4938.1 |
| Total Iron (mg/kg) | 0 |

Physical Characteristics

Material Physical Characteristics

| | |
|-----------------------------------|-------|
| Bulk Density (g/cm ³) | 1.55 |
| Hydraulic Conductivity (cm/sec) | 0.36 |
| Porosity (decimal) | 0.312 |

Subsurface Drainage

Design Structure | Existing Structure

| | |
|---|--------|
| Average Phosphorus Concentration (mg/L) | 0.5 |
| Annual Flow Volume (gallons) | 472743 |

Subsurface Drainage (Backward Required)

| | |
|-------------------------------------|------|
| Drainage Pipe Diameter (inches) | 2 |
| Drainage Pipe Slope (decimal) | 0.01 |
| Number of Subsurface Drainage Pipes | 2 |

Site Characteristics

Design Bed Size | Existing Bed Size | Design Ditch Size | Existing Ditch Size

| | |
|----------------------------|-------|
| Length of Structure (feet) | 70 |
| Width of Structure (feet) | 29.3 |
| Depth of Material (inch) | 33 |
| Mass of Material (tons) | 293.3 |
| Hydraulic Head (inches) | 36 |

Note: Hydraulic Head is equal to the elevation drop over the maximum length or the elevation difference between inlet and ultimate outlet.

Figure 4.50. The PINKOG software input screen for an existing bioretention cell that utilizes a 50% fly ash 95% sand mixture is shown with various tabs highlighted.

The total P removal of the structure can be estimated, but it requires input of total P concentration, sediment concentration, and the deposition rate which was estimated for this structure. The structure performance output shown in Fig. 4.51 estimates the lifetime of the PSM at almost 50 y with a cumulative removal of 21.5% dissolved P and 47.67% of total P. The flow rate through the structure, 23.3 gpm, is limited by the subsurface drainage, so an increase in the diameter or number of pipes would increase this flow rate. For this structure, 20 lb of dissolved P is removed in 30 y, but over the next 20 y only another 1.12 lb is removed which must be considered when deciding on a cleanout schedule. The reporting of annual removal allows for informed decisions to be made concerning the maintenance of these structures that is based on removal performance.

| Quantifying an Existing Structure (Bed) | |
|---|---------|
| Actual flow rate through the filter (gpm) | 23.3042 |
| Actual retention time (min) | 607.031 |

Flow through the structure

| Years | DP (%) | DP (lbs) | PP (%) | PP (lbs) | TP (%) | TP (lbs) |
|-------|--------|----------|--------|----------|--------|----------|
| 1 | 95.52 | 1.884 | 100. | 0.2606 | 97.01 | 2.145 |
| 2 | 91.3 | 3.602 | 100. | 0.5211 | 94.2 | 4.123 |
| 3 | 87.33 | 5.167 | 100. | 0.7817 | 91.55 | 5.949 |
| 4 | 83.59 | 6.595 | 100. | 1.042 | 89.06 | 7.637 |
| 5 | 80.07 | 7.896 | 100. | 1.303 | 86.71 | 9.199 |
| 6 | 76.75 | 9.083 | 100. | 1.563 | 84.5 | 10.65 |
| 7 | 73.62 | 10.16 | 100. | 1.824 | 82.41 | 11.99 |
| 8 | 70.67 | 11.15 | 100. | 2.084 | 80.44 | 13.24 |
| 9 | 67.88 | 12.05 | 100. | 2.345 | 78.59 | 14.39 |
| 10 | 65.25 | 12.87 | 100. | 2.606 | 76.83 | 15.48 |
| 11 | 62.76 | 13.62 | 100. | 2.866 | 75.17 | 16.48 |
| 12 | 60.41 | 14.3 | 100. | 3.127 | 73.61 | 17.42 |
| 13 | 58.18 | 14.92 | 100. | 3.387 | 72.12 | 18.31 |
| 14 | 56.08 | 15.49 | 100. | 3.648 | 70.72 | 19.13 |
| 15 | 54.08 | 16. | 100. | 3.908 | 69.39 | 19.91 |
| 16 | 52.2 | 16.47 | 100. | 4.169 | 68.13 | 20.64 |
| 17 | 50.4 | 16.9 | 100. | 4.429 | 66.94 | 21.33 |
| 18 | 48.71 | 17.29 | 100. | 4.69 | 65.8 | 21.98 |
| 19 | 47.09 | 17.65 | 100. | 4.951 | 64.73 | 22.6 |
| 20 | 45.56 | 17.97 | 100. | 5.211 | 63.71 | 23.19 |
| 21 | 44.11 | 18.27 | 100. | 5.472 | 62.74 | 23.74 |
| 22 | 42.73 | 18.54 | 100. | 5.732 | 61.82 | 24.27 |
| 23 | 41.41 | 18.79 | 100. | 5.993 | 60.94 | 24.78 |
| 24 | 40.16 | 19.01 | 100. | 6.253 | 60.11 | 25.26 |
| 25 | 38.97 | 19.22 | 100. | 6.514 | 59.31 | 25.73 |
| 26 | 37.84 | 19.4 | 100. | 6.774 | 58.56 | 26.18 |
| 27 | 36.75 | 19.57 | 100. | 7.035 | 57.84 | 26.61 |
| 28 | 35.72 | 19.73 | 100. | 7.296 | 57.15 | 27.02 |
| 29 | 34.74 | 19.87 | 100. | 7.556 | 56.49 | 27.43 |
| 30 | 33.8 | 20. | 100. | 7.817 | 55.87 | 27.82 |
| 31 | 32.9 | 20.12 | 100. | 8.077 | 55.27 | 28.19 |
| 32 | 32.04 | 20.22 | 100. | 8.338 | 54.69 | 28.56 |
| 33 | 31.22 | 20.32 | 100. | 8.598 | 54.15 | 28.92 |
| 34 | 30.44 | 20.41 | 100. | 8.859 | 53.62 | 29.27 |
| 35 | 29.68 | 20.49 | 100. | 9.119 | 53.12 | 29.61 |
| 36 | 28.96 | 20.57 | 100. | 9.38 | 52.64 | 29.95 |
| 37 | 28.27 | 20.63 | 100. | 9.641 | 52.18 | 30.27 |
| 38 | 27.61 | 20.69 | 100. | 9.901 | 51.74 | 30.6 |
| 39 | 26.98 | 20.75 | 100. | 10.16 | 51.32 | 30.91 |
| 40 | 26.37 | 20.8 | 100. | 10.42 | 50.91 | 31.22 |
| 41 | 25.78 | 20.85 | 100. | 10.68 | 50.52 | 31.53 |
| 42 | 25.22 | 20.89 | 100. | 10.94 | 50.15 | 31.83 |
| 43 | 24.68 | 20.93 | 100. | 11.2 | 49.78 | 32.13 |
| 44 | 24.16 | 20.97 | 100. | 11.46 | 49.44 | 32.43 |
| 45 | 23.66 | 21. | 100. | 11.72 | 49.1 | 32.72 |
| 46 | 23.17 | 21.03 | 100. | 11.99 | 48.78 | 33.01 |
| 47 | 22.71 | 21.05 | 100. | 12.25 | 48.47 | 33.3 |
| 48 | 22.26 | 21.08 | 100. | 12.51 | 48.18 | 33.58 |
| 49 | 21.83 | 21.1 | 100. | 12.77 | 47.89 | 33.87 |
| 49.8 | 21.5 | 21.12 | 100. | 12.98 | 47.67 | 34.09 |

Lifetime of PSM

Figure 4.51. The output from PhROG from quantifying the performance of an existing bioretention cell is shown with the flow results and lifetime of the filter highlighted.

Conclusion

Eutrophication due to nutrient loss from agricultural and urban areas is a serious threat to the quality of surface water bodies. Conventional BMPs target particulate P, but are not designed to reduce transport of dissolved P. Very small amounts of dissolved P can leak from sites with a history of mismanagement, so something must be done to prevent this. Large landscape filters filled with PSMs can be placed in areas that produce runoff with elevated levels of dissolved P.

These P removal structures are a viable means of reducing dissolved P transport, but they must be custom designed for each site which can be difficult without help or training. Years of research investigating the chemical basis for P sorption that occurs with different PSM has resulted in development of a model that can accurately predict the ability of both Ca materials and Fe and Al materials to sorb P. Using this model as the foundation, software was developed that allows users to design a structure that meets certain goals or to quantify performance of an existing structure. PhROG, the software, requires input of performance goals, constraints on size and flow, site characteristics, and certain characteristics of their desired PSM. The software can be used to design a variety of P removal structures, including a surface bed filter, a ditch filter, a buried bed filter attached to tile drainage, and a bioretention cell. Any structure that can fit into a square or a trapezoid can be designed using this software to meet removal and flow goals. By using PhROG, the user can investigate a variety of goals, constraints, PSMs, and drainage all with the touch of a button. There is no need to complete cumbersome calculations or multiple flow-through experiments. Years of experience building structures and research have been condensed into PhROG resulting in a straight forward tool that makes designing and quantifying P removal structures easy.

REFERENCES

- Antelo J., Avena M., Fiol S., López R., Arce F. (2005) Effects of pH and ionic strength on the adsorption of phosphate and arsenate at the goethite–water interface. *Journal of Colloid and Interface Science* 285:476-486.
- Arnold J.G., Srinivasan R., Muttiah R.S., Williams J.R. (1998) Large area hydrologic modeling and assessment part I: Model development I, Wiley Online Library.
- Canga E., Iversen B., Kjaergaard C. (2013) A Simplified Transfer Function for Estimating Saturated Hydraulic Conductivity of Porous Drainage Filters. *Water, Air, & Soil Pollution* 225:1-13. DOI: 10.1007/s11270-013-1794-8.
- Carpenter S.R., Caraco N.F., Correll D.L., Howarth R.W., Sharpley A.N., Smith V.H. (1998) Nonpoint Pollution of Surface Waters with Phosphorus and Nitrogen. *Ecological Applications* 8:559-568. DOI: 10.2307/2641247.
- Claveau-Mallet D., Wallace S., Comeau Y. (2011) Model of Phosphorus Precipitation and Crystal Formation in Electric Arc Furnace Steel Slag Filters. *Environmental Science & Technology* 46:1465-1470. DOI: 10.1021/es2024884.
- Codd G.A. (2000) Cyanobacterial toxins, the perception of water quality, and the prioritisation of eutrophication control. *Ecological Engineering* 16:51-60. DOI: [http://dx.doi.org/10.1016/S0925-8574\(00\)00089-6](http://dx.doi.org/10.1016/S0925-8574(00)00089-6).

- County P.G.s. (1993) Design manual for use of bioretention in stormwater management. Prince George's County (MD) Government, Department of Environmental Protection. Watershed Protection Branch, Landover, MD.
- Delorme T.A., Angle J.S., Coale F.J., Chaney R.L. (2000) Phytoremediation of Phosphorus-Enriched Soils. *International Journal of Phytoremediation* 2:173-181. DOI: 10.1080/15226510008500038.
- DeSutter T.M., Pierzynski G.M., Baker L.R. (2006) Flow-Through and Batch Methods for Determining Calcium-Magnesium and Magnesium-Calcium Selectivity. *Soil Science Society of America Journal* 70:550-554.
- Dodds W.K. (2002) *Freshwater Ecology: Concepts and Environmental Applications* Academic Press, San Diego, California.
- Essington M.E. (2004) *Soil and Water Chemistry: An Integrative Approach*. 1st ed. CRC Press, Boca Raton, Florida.
- Fenton O., Kirwan L., Ó Huallacháin D., Healy M.G. (2012) The Effectiveness and Feasibility of Using Ochre as a Soil Amendment to Sequester Dissolved Reactive Phosphorus in Runoff. *Water, Air and Soil Pollution* 223:1249-1261. DOI: <http://dx.doi.org/10.1007/s11270-011-0941-3>.
- Feyereisen G.W., Francesconi W., Smith D.R., Papiernik S.K., Krueger E.S., Wentz C.D. (2015) Effect of Replacing Surface Inlets with Blind or Gravel Inlets on Sediment and Phosphorus Subsurface Drainage Losses. *Journal of Environmental Quality* 44:594-604. DOI: 10.2134/jeq2014.05.0219.
- Froelich P.N. (1988) Kinetic control of dissolved phosphate in natural rivers and estuaries: A primer on the phosphate buffer mechanism. *Limnology and oceanography* 33:649-668.

- Gallimore L.E., Basta N.T., Storm D.E., Payton M.E., Huhnke R.H., Smolen M.D. (1999) Water Treatment Residual to Reduce Nutrients in Surface Runoff from Agricultural Land. *J. Environ. Qual.* 28:1474-1478. DOI: 10.2134/jeq1999.00472425002800050012x.
- Gotcher M.J., Zhang H., Schroder J.L., Payton M.E. (2014) Phytoremediation of Soil Phosphorus with Crabgrass. *Agronomy Journal* 106:528-536.
- Grubb K.L., McGrath J.M., Penn C.J., Bryant R.B. (2011) Land application of spent gypsum from ditch filters: Phosphorus source or sink? *Agricultural Sciences* 2:364-374.
- Hillel D. (2004) *Introduction to Environmental Soil Physics* Elsevier, San Diego, California.
- Hsu P.H. (1964) Adsorption of Phosphate by Aluminum and Iron in Soils. *Soil Sci. Soc. Am. J.* 28:474-478. DOI: 10.2136/sssaj1964.03615995002800040009x.
- Jarrett A.R. (1997) *Water management* Kendall/Hunt Publishing Company.
- Johansson L., Gustafsson J.P. (2000) Phosphate removal using blast furnace slags and opoka-mechanisms. *Water Research* 34:259-265.
- Kratochvil R., Coale F., Momen B., Harrison Jr M., Pearce J., Schlosnagle S. (2006) Cropping systems for phytoremediation of phosphorus-enriched soils. *International journal of phytoremediation* 8:117-130.
- Lyngsie G., Penn C.J., Pedersen H.L., Borggaard O.K., Hansen H.C. (2015) Modelling of phosphate retention by Ca-and Fe-rich filter materials under flow-through conditions. *Ecological Engineering* 75:93-102.
- McKeague J., Day J.H. (1966) Dithionite-and oxalate-extractable Fe and Al as aids in differentiating various classes of soils. *Canadian Journal of Soil Science* 46:13-22.
- NRCS U. (2004) *National Engineering Handbook: Part 630—Hydrology*.

- Penn C., McGrath J., Bowen J., Wilson S. (2014) Phosphorus removal structures: A management option for legacy phosphorus. *Journal of Soil and Water Conservation* 69:51A-56A.
- Penn C.J., Bryant R.B. (2006) Application of phosphorus sorbing materials to streamside cattle loafing areas. *Journal of Soil and Water Conservation* 61:303-310.
- Penn C.J., Bryant R.B., Kleinman P.J.A., Allen A.L. (2007) Removing dissolved phosphorus from drainage ditch water with phosphorus sorbing materials. *Journal of Soil and Water Conservation* 62:269-276.
- Penn C.J., McGrath J.M. (2011) Predicting Phosphorus Sorption onto Steel Slag Using a Flow-through approach with Application to a Pilot Scale System. *Journal of Water Resource and Protection* 03:235-244.
- Penn C.J., McGrath J.M., Rounds E., Fox G., Heeren D. (2012) Trapping Phosphorus in Runoff with a Phosphorus Removal Structure. *J. Environ. Qual.* 41:672-679. DOI: 10.2134/jeq2011.0045.
- Pionke H., Gburek W., Schnabel R., Sharpley A., Elwinger G. (1999) Seasonal flow, nutrient concentrations and loading patterns in stream flow draining an agricultural hill-land watershed. *Journal of Hydrology* 220:62-73.
- Pratt C., Shilton A., Pratt S., Haverkamp R.G., Elmetri I. (2007) Effects of Redox Potential and pH Changes on Phosphorus Retention by Melter Slag Filters Treating Wastewater. *Environmental Science & Technology* 41:6585-6590. DOI: 10.1021/es070914m.
- Salarashayeri A., Siosemarde M. (2012) Prediction of soil hydraulic conductivity from particle-size distribution. *World Acad. Sci. Eng. Technol* 61:454-458.

- Schewe J., Heinke J., Gerten D., Haddeland I., Arnell N.W., Clark D.B., Dankers R., Eisner S., Fekete B.M., Colón-González F.J., Gosling S.N., Kim H., Liu X., Masaki Y., Portmann F.T., Satoh Y., Stacke T., Tang Q., Wada Y., Wisser D., Albrecht T., Frieler K., Piontek F., Warszawski L., Kabat P. (2014) Multimodel assessment of water scarcity under climate change. *Proceedings of the National Academy of Sciences* 111:3245-3250. DOI: 10.1073/pnas.1222460110.
- Sharpley A., Foy B., Withers P. (2000) Practical and Innovative Measures for the Control of Agricultural Phosphorus Losses to Water: An Overview. *J. Environ. Qual.* 29:1-9. DOI: 10.2134/jeq2000.00472425002900010001x.
- Sharpley A., Jarvie H.P., Buda A., May L., Spears B., Kleinman P. (2013) Phosphorus Legacy: Overcoming the Effects of Past Management Practices to Mitigate Future Water Quality Impairment. *J. Environ. Qual.* 42:1308-1326. DOI: 10.2134/jeq2013.03.0098.
- Sharpley A.N., Kleinman P.J.A., Heathwaite A.L., Gburek W.J., Folmar G.J., Schmidt J.P. (2008a) Phosphorus Loss from an Agricultural Watershed as a Function of Storm Size *J. Environ. Qual.* 37:362-368. DOI: 10.2134/jeq2007.0366.
- Sharpley A.N., Kleinman P.J.A., Heathwaite A.L., Gburek W.J., Weld J.L., Folmar G.J. (2008b) Integrating Contributing Areas and Indexing Phosphorus Loss from Agricultural Watersheds. *Journal of Environmental Quality* 37:1488-96.
- Sigg L., Stumm W. (1981) The interaction of anions and weak acids with the hydrous goethite (α -FeOOH) surface. *Colloids and Surfaces* 2:101-117. DOI: [http://dx.doi.org/10.1016/0166-6622\(81\)80001-7](http://dx.doi.org/10.1016/0166-6622(81)80001-7).
- Standard A. (2007) D422–63 (2007) Standard test method for particle-size analysis of soils. ASTM International, West Conshohocken. doi 10:1520.

Stoner D., Penn C., McGrath J., Warren J. (2012) Phosphorus Removal with By-Products in a Flow-Through Setting. *J. Environ. Qual.* 41:654-663. DOI: 10.2134/jeq2011.0049.

Tisdale S.L., Nelson W.L., Beaton J.D., Havlin J.L. (1993) *Soil Fertility and Fertilizers*. 5th ed. Prentice Hall, Upper Saddle River, New Jersey.

USDA N. (2001) *National Engineering Handbook, Part 650, Engineering Field Handbook, Chapter 14. Water Management (Drainage) 4.*

USDA S. (1986) *Urban hydrology for small watersheds. Technical release 55:2-6.*

USEPA. (1996) *Method 3050B Acid Digestion of Sediments, Sludges, and Soils*, Environmental Protection Agency.

USEPA. (2011) *National Summary of Impaired Waterways and TMDL Information*, United States Environmental Protection Agency.

Vadas P.A., Kleinman P.J.A., Sharpley A.N., Turner B.L. (2005) Relating Soil Phosphorus to Dissolved Phosphorus in Runoff: A Single Extraction Coefficient for Water Quality Modeling. *Journal of Environmental Quality* 34:572-80.

VITA

James Michael Bowen

Candidate for the Degree of

Master of Science

Thesis: DESIGN, QUANTIFICATION, AND DEMONSTRATION OF LARGE SCALE PHOSPHORUS REMOVAL STRUCTURES IN OKLAHOMA

Major Field: Plant and Soil Sciences

Biographical:

Education:

Completed the requirements for the Master of Science in Plant and Soil Sciences at Oklahoma State University, Stillwater, Oklahoma in July, 2015.

Completed the requirements for the Bachelor of Science in Environmental Science at Oklahoma State University, Stillwater, Oklahoma in May, 2013.

Completed the requirements for the Associate of Science in Environmental Science at Tulsa Community College, Tulsa, Oklahoma in May, 2011.

Experience:

Graduate Research Assistant: Dept. of Plant and Soil Sciences, Oklahoma State University, May 2013-July 2015.

Graduate Teaching Assistant: Dept. of Plant and Soil Sciences, Oklahoma State University, January 2014-May 2014.

Undergraduate Research Assistant: Soil Chemistry, Dept. of Plant and Soil Sciences, Oklahoma State University, December 2012-May 2013.